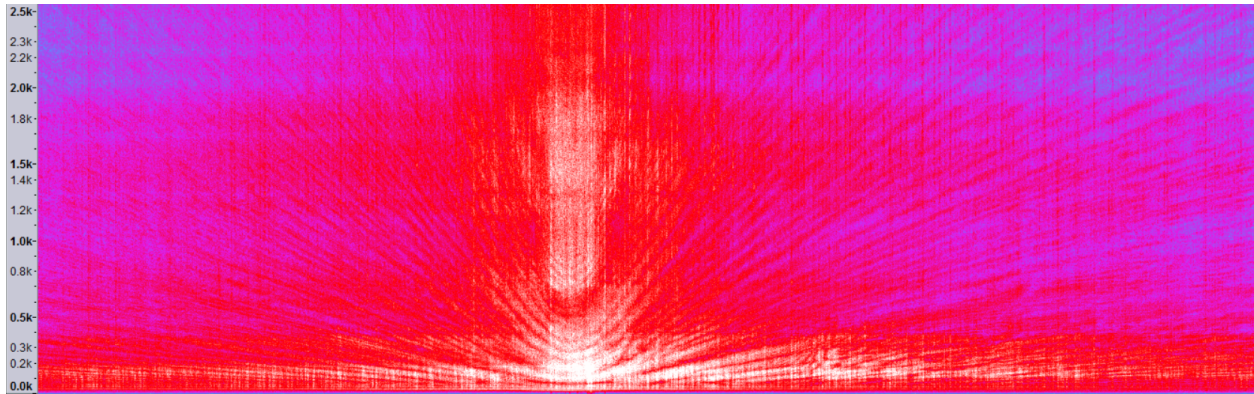




**CHALMERS**  
UNIVERSITY OF TECHNOLOGY

---



# Characterization of underwater noise in the Baltic Sea

Master's thesis in Sound and Vibration

Johan Portström



MASTER'S THESIS BOMX02-16-133

# Characterization of underwater noise in the Baltic Sea

Johan Portström



**CHALMERS**  
UNIVERSITY OF TECHNOLOGY

Department of Civil and Environmental Technology  
*Division of Applied Acoustics*  
CHALMERS UNIVERSITY OF TECHNOLOGY  
Gothenburg, Sweden 2016

Characterization of underwater noise in the Baltic Sea  
Johan Portström

© Johan Portström, 2016.

Supervisor: Prof. Peter Sigray, Totalförsvarets Forskningsinstitut  
Examiner: Prof. Mendel Kleiner, Chalmers University of Technology

Master's Thesis BOMX02-16-133  
Department of Civil and Environmental Engineering  
Division of Applied Acoustics  
Chalmers University of Technology  
SE-412 96 Gothenburg  
Telephone +46 31 772 1000

Cover: An example spectrogram of a ship passing in the near-field, generating strong propeller cavitation.

Typeset in L<sup>A</sup>T<sub>E</sub>X  
Printed by Chalmers Reproservice  
Gothenburg, Sweden 2016

Characterization of underwater noise in the Baltic Sea  
Johan Portström  
Department of Civil and Environmental Technology  
*Division of Applied Acoustics*

Chalmers University of Technology

## **Abstract**

Concern over the possibly harmful effects of increased levels of underwater ambient noise in the Baltic Sea has led to a number of large-scale EU projects investigating the current situation of the underwater soundscape. This thesis details an attempt at modelling the characteristics of the underwater noise at two positions in the Baltic Sea. Specifically spectral curves of the most common noise sources are described and presented in Wenz diagrams. The noise sources include: ships, piling, active sonar, wind and precipitation. The curves were created using available data for ship positions and weather together with audio data recorded using hydrophones laid out for the duration of 2014.

Keywords: underwater acoustics, environmental noise, SHEBA project, BIAS project, The Swedish Defense Research Agency, Baltic Sea, Wenz curves, shipping, infrastructure



## Acknowledgements

My warmest thanks to all those that have helped me, at FOI, Chalmers and more. This includes, but is not limited to:

Peter Sigray, Leif Persson, Emilia Erlander, Mathias Andersson, Alex Cederholm, Ilkka Karasalo, Johan Fridström, Ola Kärvell, Sven Ivansson, Jörgen Pihl, Mendel Kleiner, Anna Dimitrijevic, Robert Jungevi, Ulf Sonesson, Jukka Pajala, Andreas Nöjd, Line Hermannsen, Dayasagar V.S. and Rainer Matuschek. Special thanks to the coordinators of the SHEBA and BIAS projects.

Johan Portström, Gothenburg, August 2016



# Contents

<b>List of Figures</b>	<b>xi</b>
<b>1 Introduction</b>	<b>1</b>
1.1 List of abbreviations used in this report . . . . .	2
1.2 Positions studied . . . . .	3
1.2.1 Trelleborg . . . . .	3
1.2.2 Norra Midsjöbanken . . . . .	4
<b>2 Theory</b>	<b>5</b>
2.1 History of underwater acoustics . . . . .	5
2.2 Physics of sound in water . . . . .	6
2.2.1 Modes and rays . . . . .	6
2.2.2 Nearfield and farfield . . . . .	8
2.2.3 Speed of sound . . . . .	9
2.2.4 Reflections against the surface . . . . .	11
2.2.5 Reflections against the seabed . . . . .	12
2.2.6 Passive sonar . . . . .	12
2.3 Sounds in the sea . . . . .	12
2.3.1 Shallow seas . . . . .	13
2.3.2 The Baltic Sea . . . . .	13
2.3.3 Sound from ships . . . . .	13
2.3.4 Cavitation . . . . .	14
2.3.5 Active sonar . . . . .	15
2.3.6 Sound from precipitation . . . . .	16
2.3.7 Offshore piling . . . . .	18
2.3.8 Wenz curves . . . . .	19
2.3.9 Environmental impact of noise and regulation . . . . .	20
2.4 Statistics and signal processing . . . . .	23
2.4.1 Correlation, cross-correlation and autocorrelation . . . . .	23
2.4.2 Stationarity . . . . .	24
2.4.2.1 Ergodicity . . . . .	26
2.4.2.2 Grubbs' test . . . . .	26
2.4.3 The Fourier transform . . . . .	26
<b>3 Methods</b>	<b>29</b>
3.1 Equipment and recording of audio data . . . . .	29
3.2 Pre-processing of audio data . . . . .	30

3.2.1	Third-octave band frequency spectra . . . . .	30
3.2.2	RMS averaging frequencies . . . . .	31
3.2.3	Audio errors and abnormalities . . . . .	31
3.2.3.1	High-pass filter . . . . .	32
3.2.3.2	Digital glitches . . . . .	32
3.2.3.3	DC correction . . . . .	33
3.2.3.4	Time windowing over the files . . . . .	33
3.2.3.5	Self-noise . . . . .	34
3.2.3.6	Time drift . . . . .	34
3.3	Pre-processing of AIS data . . . . .	34
3.3.1	Defects with the AIS data set . . . . .	35
3.4	Quantification of stationarity . . . . .	35
3.5	Transient sources . . . . .	36
3.5.0.1	Detection of piling . . . . .	36
3.6	Correlating factors . . . . .	37
3.7	Time-related noise sources . . . . .	38
3.7.0.2	Dependance on time slot of recordings . . . . .	38
3.7.1	Dependance on time of day . . . . .	39
3.7.2	Dependance on day of the week . . . . .	40
3.7.3	Dependance on month . . . . .	41
3.7.4	Summary of time-related noise-sources . . . . .	44
3.8	Natural noise sources . . . . .	45
3.8.1	Influence of wind speed . . . . .	45
3.8.1.1	Method and Results for windspeed analysis . . . . .	47
3.8.2	Influence of rain . . . . .	49
3.8.3	Influence of temperature . . . . .	53
3.8.4	Influence of biological noise . . . . .	54
3.8.5	Summary of natural noise sources . . . . .	54
3.9	Anthropogenic noise sources . . . . .	54
3.9.1	Influence of shipping . . . . .	55
3.9.1.1	Influence of velocity of nearest ship . . . . .	56
3.9.1.2	Influence of the number of ships near to the hydrophone positions . . . . .	57
3.9.1.3	Influence of type of ship . . . . .	57
3.9.1.4	Spectrum of ship noise . . . . .	57
3.9.2	Influence of piling . . . . .	59
3.9.3	Influence of active sonar . . . . .	61
3.9.4	Summary of anthropogenic noise sources . . . . .	62
3.10	Baseline levels of ambience . . . . .	63
3.11	Distance dependence . . . . .	64
3.11.1	Methodology for determining transmission loss . . . . .	65
3.11.2	Example of the method . . . . .	65
3.11.3	Error estimation . . . . .	68
3.11.4	Comparison with FOI's empirical TL . . . . .	69
3.11.5	Comments on the method . . . . .	70

<b>4</b>	<b>Results and Conclusions</b>	<b>71</b>
4.0.6	Comparisons between Wenz diagrams . . . . .	72
4.0.7	Shipping . . . . .	73
4.0.8	Wind . . . . .	73
4.0.9	Rain . . . . .	74
4.0.10	Thunder . . . . .	74
4.0.11	Active sonar . . . . .	74
4.0.12	Piling . . . . .	74
4.0.13	Baseline ambience . . . . .	75
4.0.14	Overall comparison between Trelleborg and Norra Midsjöbanken	75
<b>5</b>	<b>Conclusion</b>	<b>77</b>
5.1	Evaluation of the methodology . . . . .	77
5.1.1	Future research . . . . .	77
	<b>Bibliography</b>	<b>79</b>



# List of Figures

1.1	Map of traffic density in the Baltic Sea. Red regions are the most dense and green areas are the least dense. (map from MarineTraffic.com) . . . . .	3
1.2	Location of hydrophone in Trelleborg is marked by the red arrow. (map from OpenStreepMap.org) . . . . .	4
1.3	Location of hydrophone in Norra Midsjöbanken is marked by the red arrow. (map from OpenStreepMap.org) . . . . .	4
2.1	Spectrogram of recording with large waves on the water surface. X-axis is time. Y-axis is frequency. Sound in the frequency range above 1 kHz is propagated as rays, making it modulated in frequency with the movement of the waves. Sound in the lower frequency range is unaffected by motions of the sea surface. . . . .	8
2.2	Examples from Finska viken in January, showing the knee shape of distance versus SPL plots [55]. . . . .	9
2.3	Spectrogram showing Lloyd’s mirror effect based on a ship passage at Trelleborg. X-axis is time, Y-axis is frequency. The minimum of the hyperbola is the closest point of approach. . . . .	11
2.4	Spectrogram showing Lloyd’s mirror effect based on a ship passage at Norra Midsjöbanken. X-axis is time, Y-axis is frequency. The minimum of the hyperbola is the closest point of approach. . . . .	11
2.5	Spectrogram showing the cavitation of a ship at Trelleborg. X-axis is time, Y-axis is frequency (kHz). SPL is the highest in the white areas. Cavitation starts being dominant at one-third into the spectrogram and is constant after the half-way point. . . . .	15
2.6	Spectrogram showing light rain on the surface. X-axis is time. Y-axis is frequency. There are two main bands of sound energy: 1 – 3 kHz and 4 – 6 kHz. . . . .	17
2.7	Spectrogram showing heavy rain with thunder. X-axis is time. Y-axis is frequency. There are the same two main bands of sound energy as in Figure 2.6 but they are amplified. A loud thunderstrike is present at 07:12:05 in the frequency range 0 to 0.5 kHz. . . . .	17
2.8	Rain spectra taken from Scrimger, 1985. Shown in the left panel is underwater noise spectra of rain, hail and snow for wind speeds less than 1.5 m/s. In the right panel is shown underwater noise spectra of rain for wind speeds greater than 1.5 m/s. SPL is expressed in dB re 1 $\mu$ Pa. . . . .	17

2.9	Sound Pressure Level (denoted $SLE$ ) spectra for different seabeds. Estimated for a site in the Netherlands by Ainslie <i>et al.</i> , 2012. Pile diameter was 4 m and hammer energy 800 kJ. . . . .	18
2.10	The Wenz curves, redrawn by Miller, 2010. . . . .	19
2.11	Curves of hearing thresholds for some common animals in the Baltic Sea, adapted from Nedwell <i>et al.</i> , 2004. The curves are gathered from various measurements of animals. Hence the large variations in levels. Note that hearing among fish is in general best at low to mid frequency range, whereas the harbor porpoise has excellent hearing in high frequency range but poorer at the lower frequency ranges. . .	22
3.1	Photograph showing a recording setup being retrieved. The buoy keeps the setup suspended. The yellow part is the recorder. The gray PVC pipe contains the release mechanism that responds to an acoustic signal containing a password by releasing the setup so that it floats up to the surface. . . . .	29
3.2	Example of a single audio file, divided into mean third-octave bands in four different ways . . . . .	31
3.3	Spectrogram showing time and frequency composition of a typical glitch. X-axis is time (minutes). Y-axis is frequency (Hz). . . . .	33
3.4	Broadband mean values of all files of the months for the Trelleborg position. Most months show decreasing levels over the first 13 minutes of the recordings. Recordings in July stand out as having a particularly clear pattern of decreasing levels over the first 13 minutes and then rising levels over the last 10 minutes. . . . .	39
3.5	Broadband mean values of all files of the months for the Norra Midsjöbanken position. The mean recordings are flat. Some months show slow glitches for the first 6 minutes of the recordings but those have subsequently been taken care of. . . . .	39
3.6	Mean SPL for different times of the day for Trelleborg. Windspeed was 0-10 m/s. . . . .	40
3.7	Mean SPL for different times of the day for Norra Midsjöbanken. Windspeed was 0-10 m/s. . . . .	40
3.8	Mean SPL at Trelleborg for different days of the week. Windspeed was 0-10 m/s . . . . .	41
3.9	Mean SPL at Norra Midsjöbanken for different days of the week. Windspeed was 0-10 m/s . . . . .	41
3.10	Mean SPL for different months for both positions as well as the total mean. Windspeed was 0-5 m/s . . . . .	41
3.11	Mean SPL for different months for both positions as well as the total mean. Windspeed was 5-10 m/s . . . . .	41
3.12	Trelleborg, CDF plot of all months, $f_c = 63$ Hz. The bar shows the median. Upper orange is 0.95 exceedance level, upper blue 0.90, upper yellow 0.70, lower yellow 0.25, lower blue 0.10 and lower orange 0.05. . . . .	42

3.13	Trelleborg, CDF plot of all months, $f_c = 1000$ Hz. The bar shows the median. Upper orange is 0.95 exceedance level, upper blue 0.90, upper yellow 0.70, lower yellow 0.25, lower blue 0.10 and lower orange 0.05.	42
3.14	Trelleborg, CDF plot of all months, $f_c = 8000$ Hz. The bar shows the median. Upper orange is 0.95 exceedance level, upper blue 0.90, upper yellow 0.70, lower yellow 0.25, lower blue 0.10 and lower orange 0.05.	43
3.15	Trelleborg, CDF plot of all months, $f_c = 16000$ Hz. The bar shows the median. Upper orange is 0.95 exceedance level, upper blue 0.90, upper yellow 0.70, lower yellow 0.25, lower blue 0.10 and lower orange 0.05.	43
3.16	Norra Midsjöbanken, CDF plot of all months, $f_c = 63$ Hz. The bar shows the median. Upper orange is 0.95 exceedance level, upper blue 0.90, upper yellow 0.70, lower yellow 0.25, lower blue 0.10 and lower orange 0.05.	43
3.17	Norra Midsjöbanken, CDF plot of all months, $f_c = 1000$ Hz. The bar shows the median. Upper orange is 0.95 exceedance level, upper blue 0.90, upper yellow 0.70, lower yellow 0.25, lower blue 0.10 and lower orange 0.05.	43
3.18	Norra Midsjöbanken, CDF plot of all months, $f_c = 8000$ Hz. The bar shows the median. Upper orange is 0.95 exceedance level, upper blue 0.90, upper yellow 0.70, lower yellow 0.25, lower blue 0.10 and lower orange 0.05.	44
3.19	Norra Midsjöbanken, CDF plot of all months, $f_c = 16000$ Hz. The bar shows the median. Upper orange is 0.95 exceedance level, upper blue 0.90, upper yellow 0.70, lower yellow 0.25, lower blue 0.10 and lower orange 0.05.	44
3.20	Correlation between windspeed and SPL at the Trelleborg position for different frequencies and minimum distances to the closest ship.	45
3.21	Correlation between windspeed and SPL at the Trelleborg position for different frequencies and minimum distances to the closest ship. Only correlations with absolute value above 0.5 is shown.	45
3.22	Correlation between windspeed and SPL at the Norra Midsjöbanken position for different distances to the closest ship	46
3.23	Correlation between windspeed and SPL at the Norra Midsjöbanken position for different distances to the closest ship. Only correlations with absolute value above 0.5 is shown.	46
3.24	Correlation between windspeed and SPL for full months at the Trelleborg position.	47
3.25	Correlation between windspeed and SPL for full months at the Norra Midsjöbanken position.	47
3.26	CDF of windspeed distributions at the two positions.	48
3.27	Curvefitted windspeed spectrum for 1 – 20 m/s at the Trelleborg position.	49
3.28	Curvefitted windspeed spectrum for 1 – 20 m/s at the Norra Midsjöbanken position.	49

3.29	Correlation between monthly rain and monthly SPL for the Trelleborg position for different frequencies and minimum distances to the closest ship. The sudden rise in correlation when ships are at above 15 km distance is likely due to a low number of data points. . . . .	50
3.30	Correlation between monthly rain and monthly SPL for the Norra Midsjöbanken position for different frequencies and minimum distances to the closest ship. The sudden rise in correlation when ships are at above 19 km distance is likely due to a low number of data points. . . . .	50
3.31	Spectrum of heavy rainfall with thunderstrikes at Norra Midsjöbanken. . . . .	51
3.32	Sequence of heavy rain in Trelleborg in August. Note the flat levels in bands lower than 1000 Hz. At ten minutes a heavy rainfall starts sweeping by and the levels in the frequency range above 1000 Hz rise smoothly, with a peak at 15 min. The spectra that stand out the most in low frequencies are of clearly audible thunderstrikes at 17 min.	51
3.33	All spectra during the increasing rain that was recorded at Trelleborg. Note the smooth increase of the frequency range above 1000 Hz. . . . .	52
3.34	The region in which rain noise was dominant at Trelleborg. . . . .	52
3.35	The spectra for the loudest thunderstrike of the year at Trelleborg is shown. Note that the frequency range is almost opposite that of rain noise. . . . .	52
3.36	The region in which thunderstrike noise is dominant at Trelleborg. . . . .	52
3.37	Correlation between SPL and temperature for the Trelleborg position for different frequencies and minimum distances to the closest ship. . . . .	53
3.38	Correlation between SPL and temperature for the Norra Midsjöbanken position for different frequencies and distances to the closest ship. . . . .	53
3.39	Correlation between sound speed gradient and SPL for the Trelleborg position for different frequencies and minimum distances to the closest ship. . . . .	54
3.40	Correlation between sound speed gradient and SPL for the Norra Midsjöbanken position for different frequencies and minimum distances to the closest ship. . . . .	54
3.41	CDF of the number of ships within 20 km distance to the hydrophones. Especially at the Trelleborg position there were at all times several ships within 20 km distance. At Norra Midsjöbanken the density was considerably lower but there were a few ships present most of the time.	55
3.42	CDF of the distance to the nearest ship from the hydrophones. At Trelleborg there was almost 90% of the time a ship within 10 km distance. At Norra Midsjöbanken there were 3% of the time no ships within a 25 km distance. . . . .	55
3.43	Spectrogram example of the sound of defect machinery. X axis is time and Y axis is frequency (Hz). . . . .	56
3.44	Spectrogram example of the sound of low tonals, as a cause of (possibly) an empty ship functioning as a resonance box. X axis is time and Y axis is frequency (Hz). . . . .	56

3.45	Mean spectra of ships at 1 km distance . . . . .	58
3.46	Decomposed wind and ship noise for a spectrum with a windspeed of 2 m/s at the Trelleborg position. $L_{\Sigma}$ is raw data, $L_{wind}$ is modelled and $L_{ship}$ is the result using Equation 3.10. . . . .	59
3.47	Decomposed wind and ship noise for a spectrum with a windspeed of 10 m/s at the Norra Midsjöbanken position. $L_{\Sigma}$ is raw data, $L_{wind}$ is modelled and $L_{ship}$ is the result using Equation 3.10. . . . .	59
3.48	Piling performed on land, at Trelleborg harbor (6.2 km distance) plotted in frequency, time and SPL. . . . .	60
3.49	Piling performed in the water, just outside the harbor (6.2 km distance) plotted in frequency, time and SPL. . . . .	60
3.50	Piling performed in the open sea, during the construction of off-shore wind farms (36 km distance) plotted in frequency, time and SPL. . . . .	60
3.51	An aggregation of the loudest individual spectra from the loudest recordings of piling observed at the Trelleborg position. The upper envelope is shown in a thick black line. The shaded area shows the approximate region that is influenced by piling. . . . .	61
3.52	The zone-spectrum of piling captured by the hydrophone at the Trelleborg position. The upper envelope is shown in a thick black line. The shaded area shows the approximate region that is influenced by piling. . . . .	61
3.53	Example of a recording with sonar pings obtained at Trelleborg. The pings are notable in the frequency range 6350 to 8000 Hz. Note the limited frequency range as well as the periodicity of the pings. . . . .	62
3.54	SPL of active sonar at the two positions. The peaks correspond to three main frequency ranges of transmitters. The lowest and most common consists mainly of sweeps centered around 3000 Hz. The higher frequency ranges are centered around 7000 and 9000 Hz. . . . .	62
3.55	Lowest 100000 seconds for Trelleborg for each third-octave frequency band. . . . .	63
3.56	Lowest 100000 seconds for Norra Midsjöbanken for each third-octave frequency band. . . . .	63
3.57	Baseline silence for both positions. . . . .	64
3.58	Example usage of the TL surface, part (1/8) . . . . .	66
3.59	Example usage of the TL surface, part (2/8) . . . . .	66
3.60	Example usage of the TL surface, part (3/8) . . . . .	66
3.61	Example usage of the TL surface, part (4/8) . . . . .	67
3.62	Example usage of the TL surface, part (5/8) . . . . .	67
3.63	Example usage of the TL surface, part (6/8) . . . . .	67
3.64	Example usage of the TL surface, part (7/8) . . . . .	68
3.65	Example usage of the TL surface, part (8/8) . . . . .	68
3.66	Mean mean errors of TL for individual third-octave bands at Trelleborg, calculated using Monte Carlo method. . . . .	69
3.67	Mean mean errors of TL for individual third-octave bands at Norra Midsjöbanken, calculated using Monte Carlo method. . . . .	69

3.68	Comparison between FOA's empirical TL and the ones found for the Trelleborg position. The results are shown as the mean of TL at the frequency range of modal propagation (below 1 kHz) and the one of ray propagation (above 1 kHz) . . . . .	70
3.69	Comparison between FOA's empirical TL and the ones found for the Norra Midsjöbanken position. The results are shown as the mean of TL at the frequency range of modal propagation (below 1 kHz) and the one of ray propagation (above 1 kHz) . . . . .	70
4.1	Wenz diagram for Trelleborg . . . . .	71
4.2	Wenz diagram for Norra Midsjöbanken . . . . .	72

# 1

## Introduction

Airborne community noise from traffic and heavy industry has been the subject of much study in recent decades, as prolonged noise exposure has been shown to have harmful effects on human health [72]. It is theorized that aquatic life are experiencing similar effects. Only in recent years has the potentially harmful effects of lower but more prolonged noise from anthropogenic activities started to be studied by researchers. Various commercial activities in the sea, such as shipping, piling, oil drilling and offshore wind farms cause prolonged low-to-mid-frequent noise that raises the overall levels in the oceans. For some of this noise there is the risk of anthropogenic noise masking the animals' own communication. For some there is the possibility of it displacing the animals from their preferred habitat or damaging the animals through prolonged stress.

The **S**ustainable **s**Hipping and **E**nvironment of the **B**altic Sea region (SHEBA) project is an international collaborative EU project studying the impact of shipping on the environment. On its website, the project is described as follows: *"The project will analyse the drivers for shipping, obtain the present and future traffic volumes and calculate a set of scenarios which will then feed into calculations of emissions to water, to air, and of underwater noise using and extending the currently most advanced emission model based on Automatic Identification System (AIS) ship movement data."* A noise budget will be derived by ascribing a source level (SL) to every ship and calculating the budget using AIS data. It is, thus, essential to evaluate the accuracy of the SL that are employed. The number of investigations of noise sources in the Baltic Sea is limited. The project includes, among others, FOI and Chalmers University as partners. For more information on the SHEBA project the reader is recommended to visit the website for the project at: [<http://www.sheba-project.eu/>]

The **B**altic Sea **I**nformation on the **A**coustic **S**oundscape (BIAS) project is an EU project between the countries surrounding the Baltic Sea with the aim of investigating the underwater noise environment of the Baltic Sea. The results will lay the knowledge base for upcoming regulations concerning the acoustic environment of the Baltic Sea. The project began in 2012 and ends officially in 2016 although the data set continues to be used in various other research areas. For more information on the BIAS project the reader is recommended to visit the website for the project at: [<https://bias-project.eu/>]

This thesis aims to shed some light on ship noise and especially to investigate the noise dependence on distance. It attempts to model the characteristics of noise at

two positions in the Baltic Sea using data from the BIAS project. The positions are to the southwest of Trelleborg harbor and to the southeast of the southern cape of Öland. Both of these positions have heavy ship traffic. Especially the Trelleborg position is in one of the noisiest regions of the Baltic Sea. Using underwater audio recordings from the duration of 2014 together with location data from ship traffic, a model for predicted sound pressure level third-octave band spectra from ship data was established.

The hypothesis of the thesis is that site-specific Wenz curves can be created from raw data that has been recorded by hydrophones, given that the data size is large enough. The aim and approach of this report is inspired by previous work done by Hamson [21], Knudsen [32], Wenz [68], Ross [54], Merchant [38] and by the Baltic Sea studies done at FOI [18, 10, 47] and by participants in the BIAS and SHEBA projects. The main focus is on the process of developing an all-encompassing method and the way in which interconnected variables can be extracted and their influence studied separately. The approach is tentative, influenced by the approach taken by Knudsen and Wenz with more of an emphasis on developing methodologies for disentangling the influence of different variables than on the actual end result. Each step of the methodology is made visible, in order to be as helpful as possible to those that will continue and expand on the work.

### 1.1 List of abbreviations used in this report

- **AIS:** *Automatic Identification System.* A system that keeps track of data on all large vessels at sea.
- **BIAS:** *Baltic Sea Information on the Acoustic Soundscape.* An EU project aimed recording and analyzing underwater noise in the Baltic Sea.
- **CFD:** *Computational Fluid Dynamics.*
- **CDF:** *Cumulative Distribution Function.* A function showing the distribution of elements of different sizes in an array.
- **CR:** *Critical Ratio.* The pressure ratio below which individual sounds become imperceptible in ambient noise.
- **dB:** *Decibel.*
- **FOI:** *Totalförsvarets Forskningsinstitut.* The Swedish Defense Research Agency.
- **Hz:** *Hertz.*
- **kHz:** *Kilohertz.*
- **MMSI:** *Maritime Mobile Service Identity.* An index number that is given to each vessel and is used to identify the individual in, for example, AIS.
- **NaN:** *Not a Number.* Non-valid value in an data entry.
- **$\mu\text{Pa}$ :** *Micropascal.*
- **PDF:** *Probability Density Function.* A function that describes how large a part of a given set being above a given value.
- **PSD:** *Power spectral density.*
- **RMS:** *Root-mean-square.* Refers to the integral of the root of the arithmetic average of the square of a signal.
- **SHEBA:** *Sustainable sHipping and Environment of the BAltic Sea region.* An EU project aimed at quantifying the various emissions from shipping, including

noise.

- **SMHI:** *Sveriges Meteorologiska och Hydrologiska Institut.* The Swedish Meteorological and Hydrological Institute.
- **SPL:** *Sound Pressure Level.* In this thesis always in the form of dB re 1  $\mu$ Pa in third-octave bands.

## 1.2 Positions studied

In the BIAS project 37 different sensors were deployed at different locations covering the full Baltic Sea. Ten of these were along the Swedish coasts and were handled by FOI. Two of these positions were used in this study. One of the positions was in an area with high density of ships and the other with less.

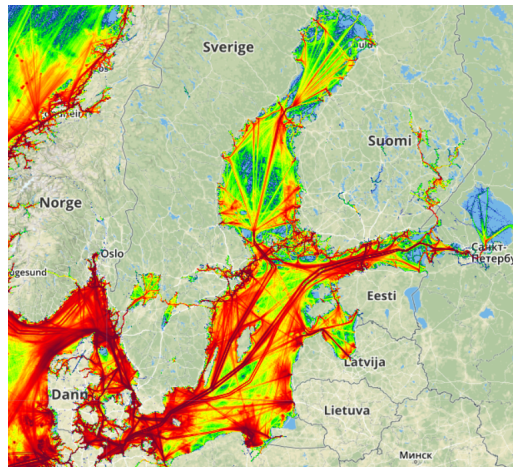


**Figure 1.1:** Map of traffic density in the Baltic Sea. Red regions are the most dense and green areas are the least dense. (map from MarineTraffic.com)

### 1.2.1 Trelleborg

One hydrophone was deployed southwest of Trelleborg harbor, about 6.2 km out from the harbor entrance. The seabed is sand and gravel. The depth is 23 m at the place of the hydrophone. The hydrophone itself was located 3 m from the bottom. The position was dense with shipping, with two shipping lanes crossing it and with activity in and around the harbor being clearly audible. There was almost always shipping activity going on at just a few kilometers distance away.

## 1. Introduction

---

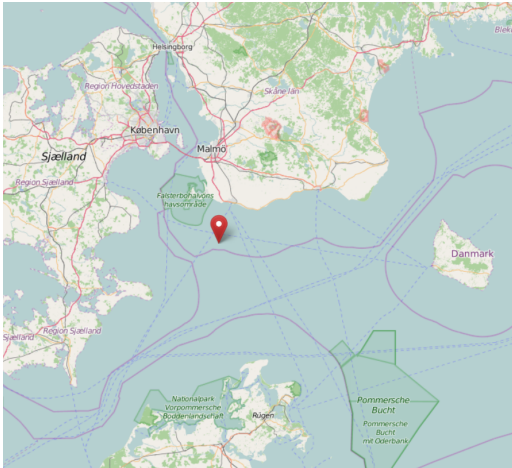


**Figure 1.2:** Location of hydrophone in Trelleborg is marked by the red arrow. (map from OpenStreepMap.org)

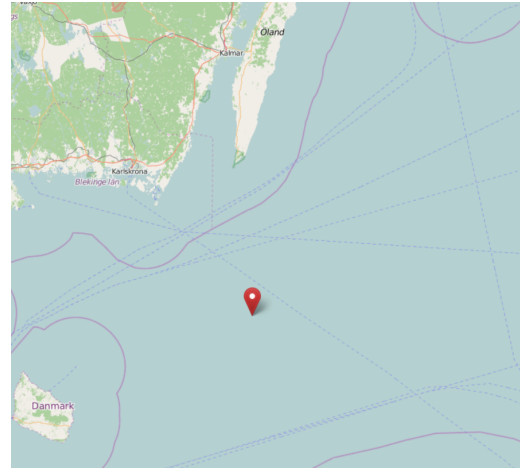


**Figure 1.3:** Location of hydrophone in Norra Midsjöbanken is marked by the red arrow. (map from OpenStreepMap.org)

### 1.2.2 Norra Midsjöbanken

The second hydrophone was located to the southeast of Öland, out in the open sea. The seabed around the hydrophone consists mostly of regions with sand and gravel, but there are also regions of hard ground such as bedrock and regions of soft ground such as silt, clay and mud.

The depth was 40 m at the place of the hydrophone which was about twice the depth of the Trelleborg position. The hydrophone itself was located 3 m from the bottom. The position was close to a shipping lane but with far less traffic than outside of Trelleborg.

# 2

## Theory

This chapter deals with the theory that is relevant for the subsequent chapters and is divided into four parts. The first part contains some historical background of the subject, the second part discusses the physics of sound in water, the third part deals with more specific facts pertaining to the characteristics of the region studied and the fourth part contains explanations of terms related to statistics.

### 2.1 History of underwater acoustics

Sound propagation in water has been a subset of the general study of acoustics since the 15th century. Early theoretical and experimental work was performed by scientists such as Leonardo da Vinci, Sir Isaac Newton and Lord Rayleigh. In modern days underwater acoustics started becoming a serious area of scientific focus after the sinking of the Titanic in 1912. At this time it was known that sending out an underwater sound signal and waiting for its echo was a possible way of detecting the distances to large objects such as icebergs. Together with beamforming techniques it was shown that the direction of these objects could be determined. At this time, however, not much was known about the effect of temperature, pressure and salinity on the sound propagation. The technology available at the time could only be used to perform very rudimentary estimates. This active sonar technology was soon extended to also detect fish and measure depth [26, 64].

During the two World Wars the subject underwater acoustics came to be largely related to Naval applications to the point that even scientific research papers were often classified. Much of the focus was on detecting enemy submarines and finding means of making the state's own submarines harder to detect. Up to World War II passive sonar, i.e. mere passive listening to the sounds in the water, was often sufficient to detect the submarines of the time, which could generate up to 135 dB re 1  $\mu$ Pa at 1000 Hz [64]. Most of the focus, however, was on detection through the use of active sonar.

This connection between underwater acoustics in general and submarines in particular continued for a long time, which is reflected in the published text books on underwater acoustics. Many of them use the detection of submarines as examples for many of the concepts, e.g. *The principles of Underwater Sound* by Urick (1983), or more implicitly cylinder-shaped objects, in e.g. *Marine acoustics* by Hovem (2010).

The more general categorization of ambient noise levels began with the paper *Underwater ambient noise* by Knudsen *et al.* [32]. In this paper the authors summarize

the, at the time, known sound spectra of individual contributors of ambient noise and suggest how background levels of noise can be predicted by known variables such as weather, season, types of animal life and shipping. As a fatalistic sign of the times, one of the reasons for the study is said in the introduction to be: "*Since atomic bombing may render obsolete most types of surface ships, the relative if not absolute importance of the submarine certainly has increased*" [32].

Knudsen's theories were further expanded by Gordon Wenz in the paper "Acoustic Ambient Noise in the Ocean: Spectra and Source" in 1962. Wenz refers to a type of curve that Knudsen made as "*Knudsen curves*". The same types of curves have subsequently come to be referred to as "*Wenz curves*". The paper by Wenz is still cited and used as a legacy paper [44].

## 2.2 Physics of sound in water

Anything that injects energy into or below the surface causes sound below the surface. Wind causes the surface to oscillate, which makes it radiate sound waves into the water column. Rain that falls on the surface excites the surface stochastically, which causes wideband noise. Ships are driven by propellers that push the ship forward. This inserts a lot of sound energy and non-laminar flow into the water. Another cause of noise is vibrations in the part of the hull that is inserted into the water.

Sound that is incident from above the sea surface is considerably attenuated due to the impedance mismatch, see section 2.2.4. Sound that is generated above the surface can normally be disregarded completely unless there is something solid connecting it below the surface. The exception to this is something that makes sound and also displaces enough air that the surface of the water is excited, such as a low-flying helicopter or explosions close to the surface.

Low-frequency waves can travel long distances without being attenuated. High frequencies are absorbed over short distances. The frequency ranges that fishing vessels use are often around 400 kHz which provides good resolution but the sound waves are attenuated by more than 1000 dB/km.

The frequency ranges normally studied in underwater acoustics range from 0.1 – 10 Hz, which is the frequency range of microseisms and backwash, up to several hundreds of kHz, which is the frequency range of fishing sonar and underwater modems.

### 2.2.1 Modes and rays

Propagation of soundwaves of high frequencies is often modelled using ray theory. High frequencies are defined as soundwaves with short wavelengths compared to the depth of the water column. This means that there is a lower limit of around 1 kHz for ray theory to be usable in shallow water. In the deepest oceans ray theory is almost always applicable.

It makes intuitive sense to think of propagating rays of sound as similar to optical rays. For example Snell's law applies to the propagation of sound rays as well, causing rays to bend towards layers with lower sound speed. In shallow waters such as the Baltic Sea, however, ray theory is only applicable when studying specifically high frequency sound sources such as sonar. For describing the soundwave propagation of most sound sources in shallow waters normal mode theory is used.

Normal mode theory is a way of describing the propagation of waves as eigenfunctions with sums of trigonometric functions of depth, width and time:

$$\Phi(z, x, t) = f(z)g(x, t)h(t). \quad (2.1)$$

Each vertical slice of the water column can be thought of as an axis. The  $f(z)$  is the shape of the function along the  $z$  axis as all other factors remain constant. The  $g(x, t)$  function is the one-dimensional wave function, which describes how the function changes as  $x$  and  $t$  are varied. The  $h(t)$  function describes the decay of the soundwave with time.

Consider a simple example: A single ray being sent out in a uniform medium in a downward angle by a source at the surface. The ray will travel downward and to the side until it hits the bottom after which it will travel upward and to the side. This can be described by modes as a scaled Gaussian distribution where the scaling represents the absolute pressure being translated along the  $z$  axis as  $x$  and  $t$  increases. The oscillations between positive and negative pressure are represented by the  $g(x, t)$  function oscillating between positive and negative value. The function  $g(x, t)$  also describes the translation of the ray. If  $t$  is held at the constant value  $t_c$ ,  $g(x, t_c)$  describes the path of the beam. If  $x$  is held at a constant value  $x_c$ ,  $g(x_c, t)$  describes the passing of the beam through a given slice of the  $x$  axis.

Just as Fourier series can describe the shape of any waveform, normal mode theory can describe any distribution of positive and negative pressure in the water with the exception of shapes that require mode shapes below the lowest order mode [26]. This sets the following lower bound for mode theory:

$$f_{lowest} = c/(4D), \quad (2.2)$$

where  $c$  is the sound speed (m/s) and  $D$  the depth (m).

The transition between mode and ray propagation is visible in Figure 2.1, which shows the entire soundscape modulated by interaction with waves on the sea surface. The periodic modulation gets stronger with increasing frequency. At higher frequencies, sound starts to propagate like rays and becomes increasingly sensitive to the direction of the surface it impinges on. The transition between the two types of propagation happens at around 1 kHz.

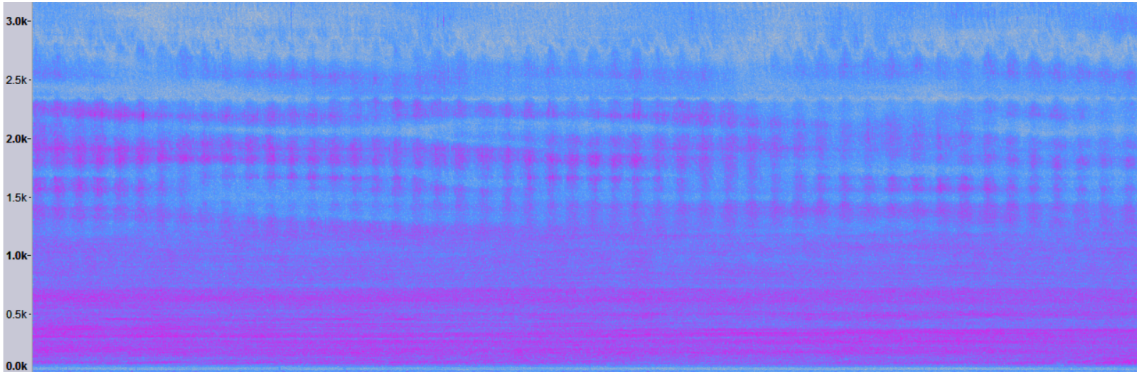


**Figure 2.1:** Spectrogram of recording with large waves on the water surface. X-axis is time. Y-axis is frequency. Sound in the frequency range above 1 kHz is propagated as rays, making it modulated in frequency with the movement of the waves. Sound in the lower frequency range is unaffected by motions of the sea surface.

## 2.2.2 Nearfield and farfield

Geometrical spreading is the main cause of transmission loss for sound propagation in water. An acoustic monopole is a sound source that is assumed to have point size and to emit sound equally in all directions. The sound intensity is proportional to the surface area of the expanding sphere of sound. The Sound Pressure Level (SPL) at a distance  $r$  meters from the source is thus:

$$L_p = SL - 10\log(\pi r^2) = SL - 10\log(\pi) - 20\log(r), \quad (2.3)$$

where  $SL$  is the source level of the source, at 1 m distance. For each doubling of the distance the  $20\log(r)$  term changes to  $20\log(2r)$  meaning that the SPL drops by  $20\log(2)$  or 6 dB. The assumption of monopole spreading from a source holds true provided that the source is small in comparison to the distance.

A source with cylindrical spreading is a source that spreads like a circle in one plane and like a plane wave in all orthogonal planes. The sound intensity is spread over a cylindrical surface and the SPL at a distance  $r$  meters from the source is:

$$L_p = SL - 10\log(\pi r) = SL - 10\log(\pi) - 10\log(r). \quad (2.4)$$

where  $SL$  is the Source Level [63].

In a shallow water the sphere of propagation from a monopole source will eventually impinge on the sea surface and the seabed. The shape of the spread starts to resemble cylindrical spreading the further the distance becomes. Over sufficiently large distances this will lead to any source approximately spreading as a cylindrical source. For short distances (near-field) the  $20\log(r)$  assumption is valid. For longer distances (far-field) the  $10\log(r)$  assumption is generally valid.

For even longer distances the shape of the sound wave spreading starts to approximate a plane wave spreading. For this type of spreading there is no geometrically based decline in sound intensity. Instead there is only the absorption that comes

from heat absorption by the water and salt, absorption into the seabed and collisions with bubbles [26]. This type of wave can travel long distances unimpeded. In waters with heavy shipping this leads to there constantly being a baseline level of ambient noise. There is no tangible way of identifying the noise contribution of individual ships to the baseline ambience. In shallow waters such as the Baltic Sea the level will be lower than in deep waters. This is because the channel in which the sound-wave can travel is smaller (which is relevant for low-frequent sound) and because the sound reflects more times against the seabed, which leads to the soundwaves being attenuated to a higher degree (which is relevant for mid-to-high-frequent sound).

Propagation loss is also dependent on the bathymetry of the sea. For the Baltic Sea, transmission loss measurements show that the geometrical transmission loss tends to be between  $14\log(r)$  to  $17\log(r)$  [47].

The distance at which spreading of sound goes from spherical spreading to cylindrical spreading is sometimes referred to as the knee distance. The shape of a distance versus SPL graph when a ship passes by can resemble the bending of a knee with a steep and approximately linear slope at first and a less steep slope after the knee distance. Previous research has shown the distance to usually be found around 5 – 7 km [18, 55]. Two examples are shown in Figure 2.2.

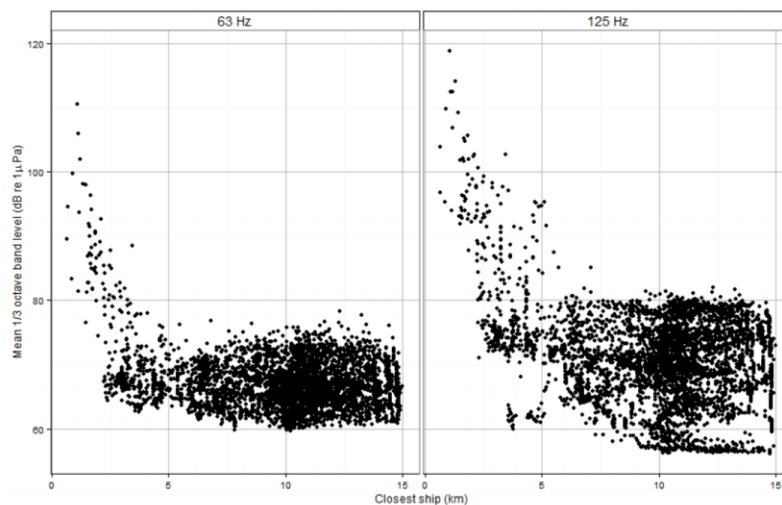


**Figure 2.2:** Examples from Finska viken in January, showing the knee shape of distance versus SPL plots [55].

### 2.2.3 Speed of sound

The general equation for speed of sound in fluids is:

$$c = \sqrt{\frac{K}{\rho}}, \quad (2.5)$$

where  $c$  is speed of sound,  $K$  stiffness and  $\rho$  density. In compressible fluids (such as air) stiffness is proportional to pressure but so is density. Although there is higher

pressure at ground level than high up in the air both stiffness and density scale linearly with pressure meaning that the speed of sound does not change as the pressure decreases. Stiffness, however, scales with temperature and usually there is some temperature difference with height, meaning that there is a difference in sound speed.

In water, which is an incompressible fluid, density remains constant even as pressure goes up. The stiffness, however, gets larger meaning that with all other variables remaining constant the sound speed increases with depth. There is usually a temperature-difference with depth because the surface part of the water will either get heated by the sun and the hot air or get cooled down by starry skies and cold air. This leads to a temperature gradient that affects the sound speed dependent on depths, times of the day and season. Salinity may also differ with depth, season and time of day. It causes the speed of sound to raise slightly.

There are several different equations for calculating speed of sound in water. The most common is the MacKenzie formula:

$$c = 1448.96 + 4.591T - 5.304 \times 10^{-2}T^2 + 2.374 \times 10^{-4}T^3 + 1.340(S - 35) + 1.630 \times 10^{-2}D + 1.675 \times 10^{-7}D^2 - 1.025 \times 10^{-2}T(S - 35) - 7.139 \times 10^{-13}TD^3 \text{ (m/s)},$$

where  $D$  is depth in metres,  $S$  is salinity in ppm and  $T$  is temperature in  $^{\circ}C$  [64].

Snell's law describes how the speed of sound in a medium will make a ray change angle when it passes between the media:

$$\frac{\Theta_1}{c_1} = \frac{\Theta_2}{c_2} = \frac{\Theta_3}{c_3} = \dots = \text{constant}, \quad (2.6)$$

where  $\Theta_i$  is an angle and  $c_i$  is the sound speed of that layer.

The difference in speed of sound at different depths can be thought of as discrete layers. As the ray passes from one layer to the next, it will bend slightly in the direction of the the layer of the slower sound speed. With infinitesimally thin layers the ray will continuously bend towards the slower sound speed. If the sound speed is faster near the surface the rays will bend downwards and if the sound speed is faster near the bottom the rays will bend upwards. A phenomenon that is commonly present in the deep oceans of the world is a temperature that is high near the surface and then decreases with depth, which results in a decrease of sound speed with temperature until the base temperature of  $4^{\circ}C$  is reached. At the same time pressure increases continuously which results in sound speed rising with depth. This results in a layer of the slowest sound speed at a depth of around 1 km near to the equator. Sound that is in this layer tends to get trapped since it gets bent towards the middle of the layer where the speed is the lowest. This leads to low transmission loss as the sound intensity is only geometrically spread out in a two-dimensional plane.

Even in the shallow Baltic Sea there can sometimes be local channels that cause

sound to be transmitted very effectively. Normally the sound speed gradient is either flat in warm seasons or negative (decreases with depth) in cold seasons. A negative gradient will cause rays to interact more with the seabed than the surface.

### 2.2.4 Reflections against the surface

In spectrograms a hyperbolic shape is often clearly visible when a sound source passes the hydrophone. This is a result of the interference between the direct sound and the sound reflected from the sea surface. The density of air can be assumed to be  $1.2 \text{ kg} \times \text{m}^{-3}$  and the speed of sound  $340 \text{ m} \times \text{s}^{-1}$ , whereas the density of water can be assumed to be  $1028 \text{ kg} \times \text{m}^{-3}$  and speed of sound  $1500 \text{ m} \times \text{s}^{-1}$ . The impedance of water is thus thousands of times larger than that of air, which leads to the reflection coefficient of sound from underwater being approximately  $r = -1$ , according to:

$$r = \frac{Z_2 - Z_1}{Z_2 + Z_1}, \quad (2.7)$$

where  $Z_i \approx \rho_i c_i$  is the impedance of medium  $i$  [31].

The reflected sound has the same amplitude (almost no sound breaks the surface) but with a change of phase [53]. If both the source and the receiver are close to the surface there will be negative interference. The phenomenon is known as Lloyd's mirror effect, after Humphrey Lloyd, who described it for optics in 1837. Two examples are shown in Figures 2.3 and 2.4.

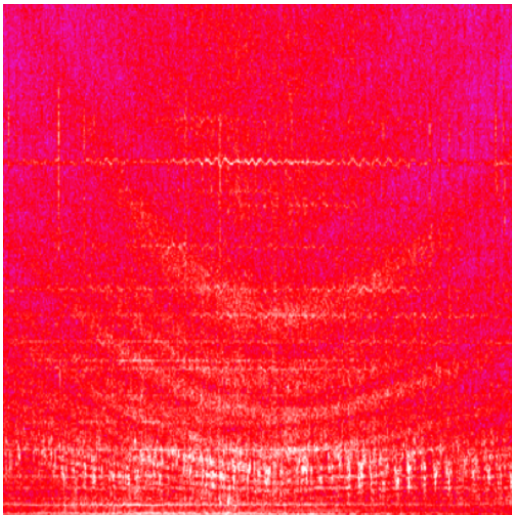


**Figure 2.3:** Spectrogram showing Lloyd's mirror effect based on a ship passage at Trelleborg. X-axis is time, Y-axis is frequency. The minimum of the hyperbola is the closest point of approach.

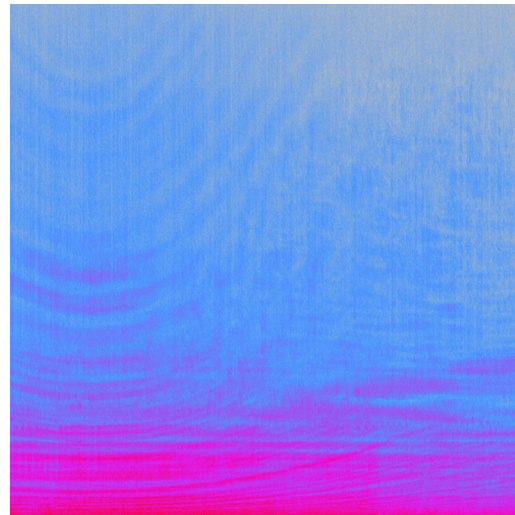


**Figure 2.4:** Spectrogram showing Lloyd's mirror effect based on a ship passage at Norra Midsjöbanken. X-axis is time, Y-axis is frequency. The minimum of the hyperbola is the closest point of approach.

If the receiver is at a known depth and the sound source is also at a known depth (e.g. a surface-going vessel with known displacement) then the bending of the hyperbolic

stripes can be used to determine the velocity of the vessel. If the velocity is known then they can be used to determine the depth of the vessel. The minimum of the hyperbolic shape gives the time of the closest position of the vessel.

### 2.2.5 Reflections against the seabed

The seabed can have varying properties depending on the type of substrate. There will always be some reflection from and some absorption into the seabed. The ratio between these will vary depending on the type and geometry of the seabed.

Absorption by the seabed leads to the sound being attenuated in the body of water. Some parts of the sound will travel through the ground and leak back into the water. There will always be some leakage back and forth between the ground and the body of water.

Reflections against the seabed will cause the sound energy to stay in the water. An uneven seabed leads to the sound being diffused and causes reverberation. An even seabed may lead to more predictable patterns of reflection, which will cause positive or negative interference at a given position.

If the substrate is hard rock the difference between water and sediment will be substantial and most sound will be reflected. For some types of soft material such as humus the density will gradually change from that of water to a higher density while at the same time speed of sound will be lower so that sound waves will bend downwards. In those cases the impedance can be almost perfectly matched, meaning that almost all the sound will be absorbed into the seabed [26].

### 2.2.6 Passive sonar

Hydrophones are passive sonar devices in that they only receive sound. This is in contrast to active sonars which send out wavefronts of sound and measure the timing, doppler-shifted frequency and direction of the returning sound that is reflected from objects in the water or from the bathymetry itself.

Modern hydrophones are transducers with built-in digital signal processing capability. They usually have highpass filters that attenuate the low frequencies which are induced by slow movement of the hydrophone in the waters. For this reason recording of frequencies much lower than 10 Hz requires seismological transducers that are mounted tightly to the sea bottom [14].

## 2.3 Sounds in the sea

There are a number of common underwater sound sources both natural and anthropogenic. In the Baltic Sea the most often audible natural sound sources are the ones that excite the surface itself (such as wind and rain) and the most audible anthropogenic sound sources are from machines that insert energy into the water (such as ships). In other oceans, biological sound sources might dominate but the Baltic Sea has very little such sound.

### 2.3.1 Shallow seas

In acoustics a deep sea can be regarded as a free field. It is a sea that is deep enough that sound can be assumed not to interact with the bottom. In contrast a shallow sea is a sea in which the sound can not spread out without coming in contact with both the seabed and the surface [63]. At every interaction with the seabed a certain portion of the sound will be absorbed into the ground or scattered. How this filters the sound over longer distances can vary quite a bit due to the lack of uniformity of the seabed. Looking at 4000 measurements of transmission loss Urick noted a spread of 40 dB transmission loss at 16 km distance (10 miles). This depends on factors such as frequency, bottom type, layer depth, wind speed and salinity [63]. As a consequence the contribution from long distance shipping is lower in shallow waters than in deep waters. This implies that the contribution from shipping in the near-field will influence the entire ecosystem relatively more in shallow waters than in deep waters.

From a community noise point of view this means that while shipping causes more noise pollution in the areas close to a shipping highway the total influence to the entire ecosystem is less than in deep waters. For this reason noise pollution can be decreased by restricting heavy traffic to well-defined shipping lanes [26, 63].

### 2.3.2 The Baltic Sea

The Baltic Sea is a sea surrounded by 10 countries. The average depth is 57 m [15]. The sea is in general shallow in the south. The deepest parts are in the regions to the southeast of Stockholm and east of Gotland [47]. The salinity is low, meaning that absorption of low-frequency sources is low [14].

The seabed for the two studied positions differ. The Trelleborg position is dominated by sand bottom (sand and gravel). At the Norra Midsjöbanken position several types of sediments occur: hard bottom (till and bedrock), sand bottom (sand and gravel) and soft bottom (silt, clay and mud) [47].

The Baltic Sea has heavy traffic in the southern parts and at specific shipping lanes. The parts north of Ålandshav have little shipping and the underwater noise levels are lower, see the shipping density map in Figure 1.1.

### 2.3.3 Sound from ships

Motorized ships are usually driven by propellers that rotate quickly and generate strong tones and overtones related to the rotational velocity. Due to the propellers moving the ship forward by oscillatory forcing the water, pressure changes in the water are produced. Some of these are small harmonic oscillations around the ambient pressure, which lead to tonal sounds at the rotational frequency of the propeller blades. Some of them are non-harmonic, non-linear oscillations where the oscillations start to become large compared to the ambient pressure, which lead to wideband noise.

Wittekind has studied the components of ship noise and developed a model for ship noise [71]. In the model three components dominate the noise: low frequencies

from propeller cavitation, medium to high frequencies from propeller cavitation and medium frequencies from four-stroke diesel engines.

Wagstaff and Aitkenhead mention that *"the noise in the frequency regime dominated by shipping was found to be extremely high with a spectrum level of 92dB re 1  $\mu$ Pa @ 50 Hz."* They also found that shipping dominates ambience below 200 Hz [65].

In the near-field individual ships tend to be the dominant sound source at all frequencies. Most diesel generators in ships turn at 720 rpm, which is related to the electric mains frequency at 60 Hz. This generates tonalities at 6 Hz and with overtones up to the several kHz. Because more total energy is pushed into the water when the propellers move faster, it might seem naively obvious that a higher rotational velocity would lead to a louder sound. In fact, however, some propellers are designed for optimal performance at the most common speeds at sea and start to become noisier at lower speeds [71].

In 1974 the oceanographer Donald Ross studied the increased anthropogenic underwater noise. At the time, noise from shipping had been steadily increasing by 0.55 dB/year, which was much faster than what was theorized from the increase in number and size of ships. The main reason turned out to be that ships needed less maintenance. This meant that ships could spend more time out at sea and less time in port. Further, the ships had become stronger. Older ships that were being phased out averaged 5000 horsepower, while the more modern ships averaged 40000 horsepower. The total horsepower at sea had doubled in a ten year period [54].

Large ships are more effective converters of mechanical power to acoustic power. Ships built in the very recent years, however, are designed using Finite Element and CFD simulations to be more energy effective meaning that it is possible that some types of resonances that could occur in large old ships can be expected to be less common in ships being built today. Vibrations, in general, are always bad for the long-term sustainability of ships so incentives are to reduce noise to decrease wear and tear.

As old ships are phased out and new ships built with different designs, different propulsion systems and different cargo capabilities, some parts of the sound signatures will change over time. Noise models that are established using data from previous generations of ships will be outdated and there will be a need of improvements.

### 2.3.4 Cavitation

In acoustics it is assumed that sound signals are small and quick pressure oscillations around ambient pressure. The word "small" in this sense refers to the pressure changes in comparison with the ambient pressure. If the pressure changes start being large in comparison with the ambient pressure non-linear phenomena start to occur. This can either be because the oscillations themselves have very high amplitude or because the ambient pressure starts being lower [14, 53].

Fast-moving propellers give rise to a phenomenon referred to as cavitation. This is when local variations in pressure in certain regions around the propeller become systematic so that the ambient pressure gets reduced. This can cause the threshold of boiling to be passed, even at normal temperatures. Many bubbles take shape and collapse, which causes local releases of energy and causes the centers of the bubbles to increase in temperature to the point of releasing clearly visible light. This release of energy causes the bubbles to oscillate back and forth. The frequency depends on the size of the bubbles. This leads to a loud and sharp noise that can clearly be distinguished from the rest of the noise from a ship. Each bubble acts like a spherical monopole source [53].

Cavitation usually starts and stops suddenly, causing a random pattern in the audio recording, see Figure 2.5.

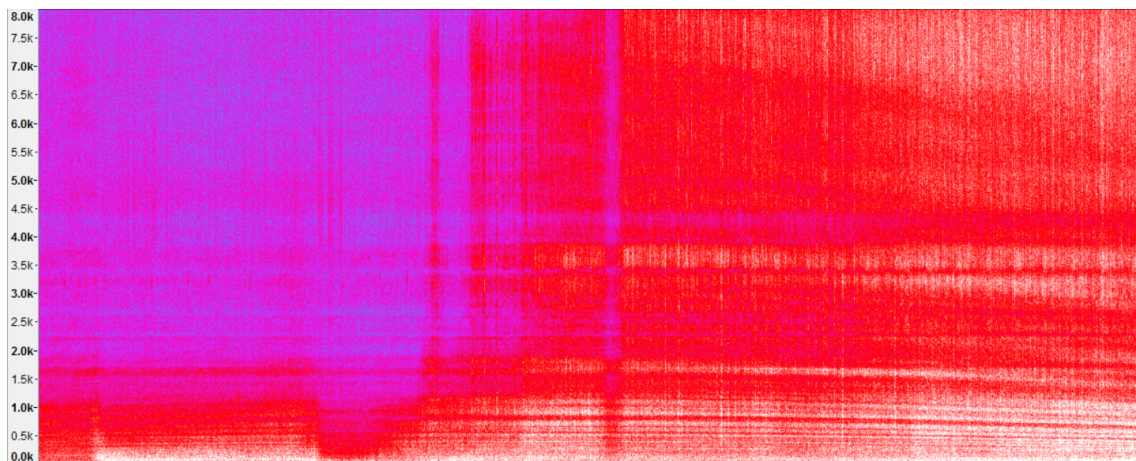


**Figure 2.5:** Spectrogram showing the cavitation of a ship at Trelleborg. X-axis is time, Y-axis is frequency (kHz). SPL is the highest in the white areas. Cavitation starts being dominant at one-third into the spectrogram and is constant after the half-way point.

Cavitation is damaging to the propellers in the long run because the release of acoustic energy by each bubble gradually causes mechanical abrasion of the surface. As with related physical phenomena such as the building up of clouds or the change from water to ice there needs to be an initial nucleation event for the cavitation to start. If there is any unevenness in the propeller it becomes more likely to cause cavitation. The energy content of the cavitation is exponentially proportional to the rotational velocity of the propeller.

### 2.3.5 Active sonar

Navy mid-frequency active sonar for submarine hunting usually sends out pulseforms at 200 to 225 dB re 1  $\mu$ Pa at 1 m. The Swedish Navy generally sends out signals at frequencies higher than 20 kHz and NATO uses active sonar in the interval 1 – 10 kHz [2]. The military are the only ones that use active sonar in these frequency ranges, and this is for the following two reasons: First, equipment for active sonar

in mid frequencies is extremely expensive; in the tens of millions of SEK. This is because for any single transducer, the pressures at the surface of the diaphragm as the sound levels start to reach 205 dB re 1  $\mu\text{Pa}$ , are so high that it leads to cavitation at the diaphragm surface. To reach the sound pressure levels necessary for submarine hunting requires sizeable phased arrays. Secondly, the resolution desired by the Navy is usually in the region of 50 – 100 m, which is enough for the detection of a target. Fishing vessels use frequencies in the hundreds of thousand Hz, which gives very good resolution, at the cost of losing ability to detect at long distances due to high frequency absorption.

For submarine hunting with active sonar it is usually of interest to find both position and speed of the target. One way to fix the position is to use a chirp pulse. The first reflection reveals the distance to the target. Lloyd's mirroring effect can be used to estimate the depth of the target. The speed of the target can be determined using a windowed sine-wave tone. The reflection from the tone is shifted in frequency depending on the relative speed of the target due to the Doppler effect.

### 2.3.6 Sound from precipitation

Underwater noise from rain and other precipitation is caused by several factors. Energy is input to the water when rain drops, of varying sizes and speeds, collide with the sea surface, giving rise to stochastic excitation of the surface. For some rain drops, once they have collided with the surface some air is forced down into the water. These air bubbles end up acting as cavitation and will generate a noise found to be greater than that of the impact [51]. The resulting sound from all of this, sounds almost like white noise, although with a heavier emphasis on the higher frequencies than the lower. Rain drops fall stochastically, leading to a static noise. Most of the sound is in a high frequency range with ray propagation. Two examples are shown in Figures 2.6 and 2.7.

Bubbles in the water strongly decrease the sound speed, meaning that in the layer just beneath the surface, sound will tend to bend upwards, meaning that the sound channel properties can temporarily change dramatically. For those reasons, rain in itself can be assumed to have a spectral signature that is dependent on the rain intensity, but also to affect the rest of the soundscape in various ways; in effect creating different types of channels and temporarily changing the horizontal propagation properties of the sound channel. The bubbles also attenuate the higher frequencies of the noise [19].

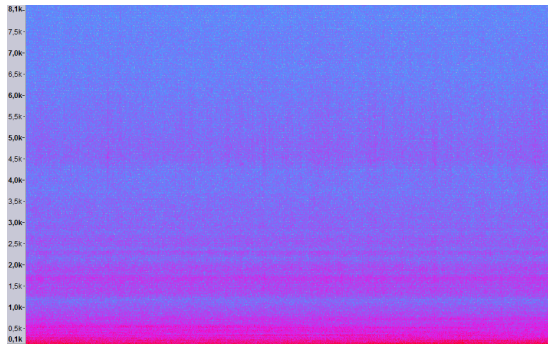


**Figure 2.6:** Spectrogram showing light rain on the surface. X-axis is time. Y-axis is frequency. There are two main bands of sound energy: 1 – 3 kHz and 4 – 6 kHz.

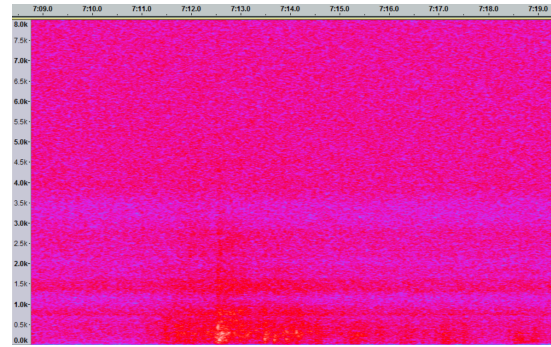


**Figure 2.7:** Spectrogram showing heavy rain with thunder. X-axis is time. Y-axis is frequency. There are the same two main bands of sound energy as in Figure 2.6 but they are amplified. A loud thunderstrike is present at 07:12:05 in the frequency range 0 to 0.5 kHz.

Rain-induced noise was described by Wenz mainly by summarizing results presented by Franz in 1959: *“Franz has measured the sound energy radiated by air bubbles formed when air is entrained in the water following the impact of water droplets on the surface of the water. His results are given in the form of one-half-octave-band sound-energy spectra which exhibit maxima. The decline toward lower frequencies is sharp (8 to 12 dB per octave, in terms of energy-spectrum level) and is attributed to an almost complete absence of bubbles larger than a certain size. A more gradual decline toward higher frequencies (-6 dB to -8 dB per octave) was found and was interpreted as being the result of a decrease in the radiated sound energy per bubble rather than a decrease in the prevalence of bubbles”* [68].

Scrimger presented a spectrum showing some typical properties of various types of precipitation [56], see Figure 2.8.

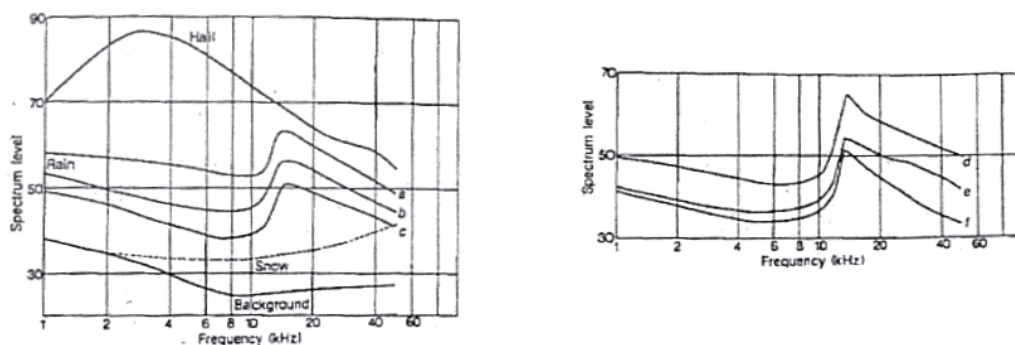


**Figure 2.8:** Rain spectra taken from Scrimger, 1985. Shown in the left panel is underwater noise spectra of rain, hail and snow for wind speeds less than 1.5 m/s. In the right panel is shown underwater noise spectra of rain for wind speeds greater than 1.5 m/s. SPL is expressed in dB re 1  $\mu$ Pa.

The peak at 14 kHz was replicated by several other measurements, for example by Scrimger [56] and Nystuen [42] in both lakes and oceans. Prosperetti et. al [51] replicated it in artificial rain experiments in tanks and found that it was an effect of the resonance frequency of air bubbles caused by rain drops of a size in the range 0.8 mm to 1.1 mm in diameter.

### 2.3.7 Offshore piling

A relatively new noise source in the oceans are off-shore wind farms. The construction of these require pile-driving. Piling during off-shore or harbor construction is an action that introduces a lot of energy into the water, which can translate to sound pressure levels of 230 dB re 1  $\mu\text{Pa}$  [61]. The sounds are approximately impulse sound point sources. In the near field the sounds behave like those from underwater explosions and there is the potential risk of direct damage of nearby aquatic life although a study showed few direct damages on specifically steelhead trouts exposed to up to 188 dB re 1  $\mu\text{Pa}$  peak sound pressure levels [45].

There has been concern in the EU over the appropriate way of modeling, monitoring and regulating the sound that is introduced into the water from piling [36]. Estimations of source level spectra were shown by Ainslie *et al.* [1] to be dependent on the seabed, as shown in Figure 2.9.

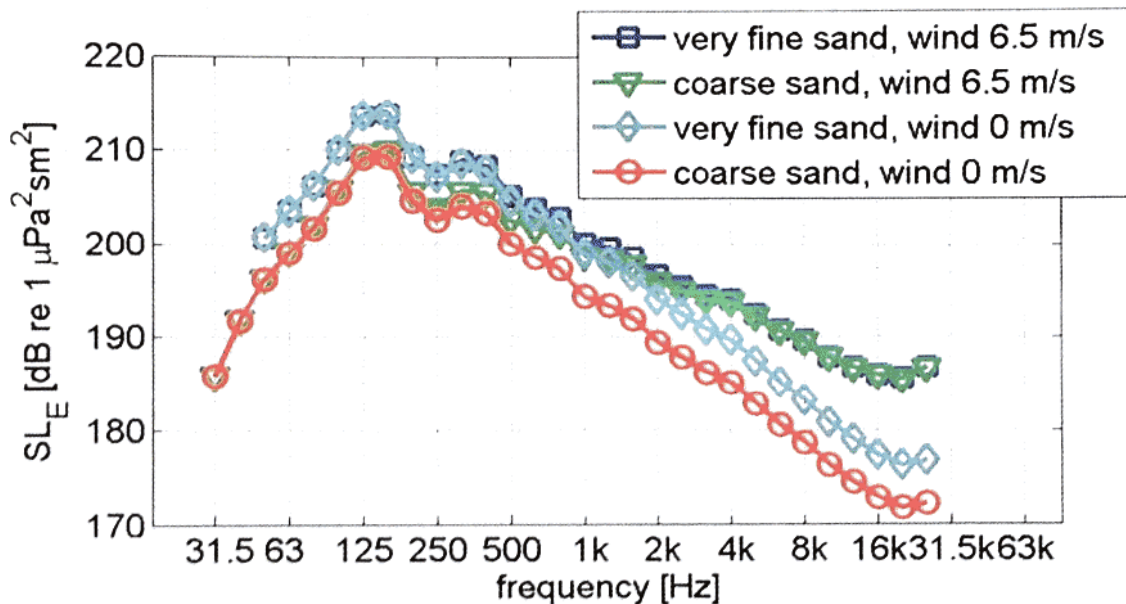


**Figure 2.9:** Sound Pressure Level (denoted  $SL_E$ ) spectra for different seabeds. Estimated for a site in the Netherlands by Ainslie *et al.*, 2012. Pile diameter was 4 m and hammer energy 800 kJ.

During offshore construction of a German wind farm, the effect of piling on harbor porpoise was studied by Dähne *et al.*, who found that the threshold level at which the harbor porpoise fled from the sound was in the range 139 – 152 dB re 1  $\mu\text{Pa}^2\text{s}$  [9]. The porpoise generally returned in around ten days after the noise has stopped. This deterring effect of impulse sounds was studied by Kyhn *et al.* as a potential

way of warning porpoise from fisher boats to avoid having them get caught in nets [33].

### 2.3.8 Wenz curves

The paper *Underwater ambient noise* by Knudsen *et al.* from 1944 was an attempt to gather all the knowledge about underwater ambient sound into a single paper [32]. The paper *Acoustic Ambient Noise in the Ocean: Spectra and Sources* by Wenz from 1962 was an attempt by the author to gather this knowledge into a single diagram [68]. Diagrams of that sort are normally referred to as *Wenz curves* or *Wenz diagrams*.

Figure 2.10 shows the approximate frequency ranges and levels at which certain types of sound sources can be expected to be dominant. The figure is taken from a more modern report but is basically identical to the curves created by Wenz in 1962 [39].

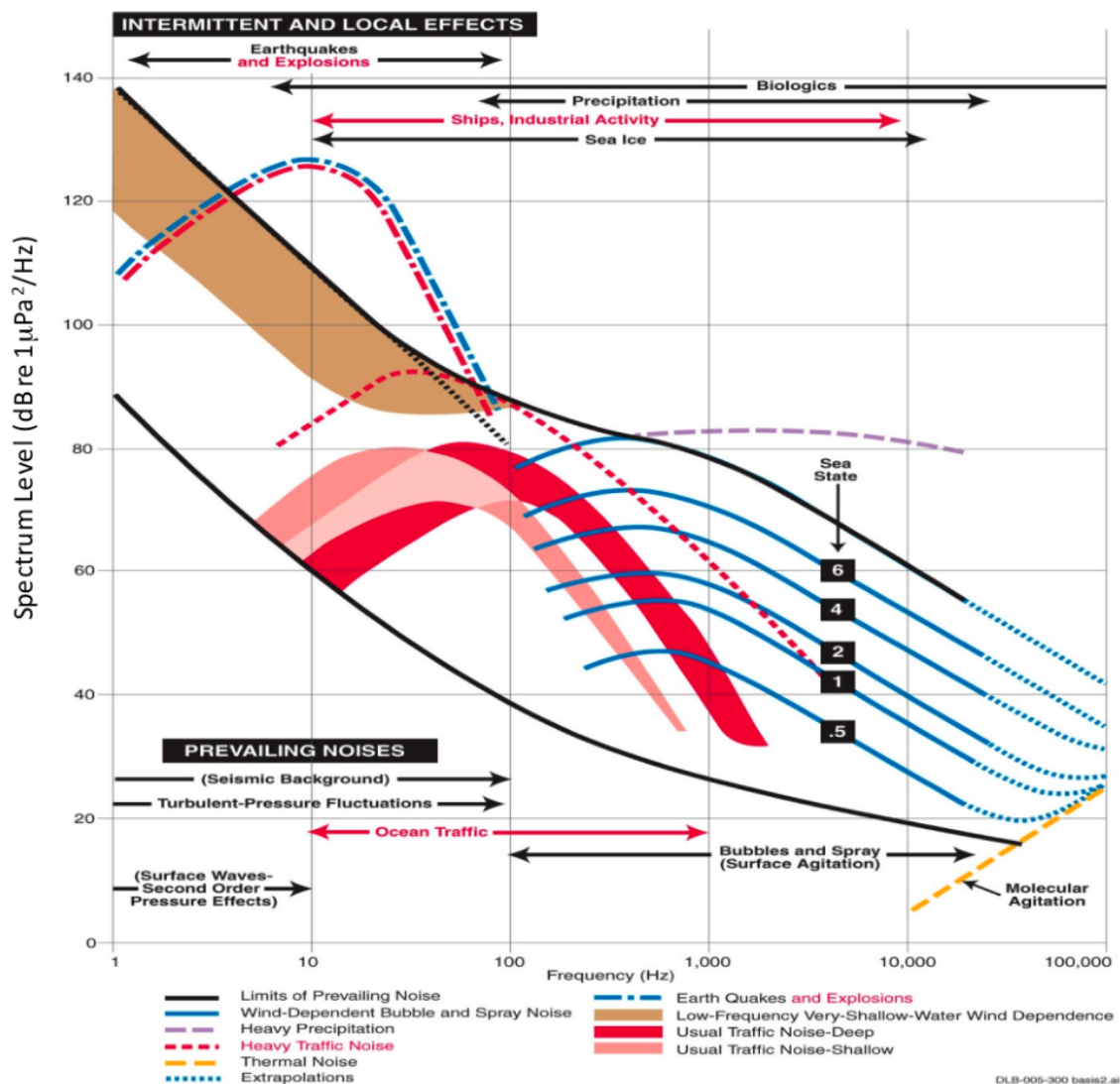


Figure 2.10: The Wenz curves, redrawn by Miller, 2010.

There have been a number of updated versions of the Wenz curves. Ross made an attempt in 1974 to update them with the higher average SPL from shipping that had been observed since 1962 [54]. Ross also incorporated curves of rain and wind that was developed by Bell Labs and that had more spectral structure than the original Wenz curves. Hamson made an attempt at updating the model and making even more detailed curves, quantifying a large number of aspects of shipping and wind noise [21].

The curves will end up being slightly different between different seas and between different parts of the seas. For this reason the higher the level of detail in the curves, the more site specific they become. Knudsen and Wenz came up with rule of thumb that was assumed to be applicable to most sea conditions. The trend since then has been to make detailed site-specific analyses of sound sources related to certain regions [4, 42, 65, 67].

### 2.3.9 Environmental impact of noise and regulation

Noise pollution in the oceans started coming into study in the 1990s, when there was concern as to whether mid-range active sonar directly caused the stranding of whales. In the United States use of military sonar is at present highly regulated under the National Environmental Policy Act, the Marine Mammal Protection Act and the Endangered Species Act [46]. The Swedish Navy is currently investigating the effects of active sonar (submarine hunting and minesweeping) and underwater explosions in the Baltic Sea. Especially the effects on the harbor porpoise is of importance. Although the species is not globally listed as vulnerable it is vulnerable in the Baltic Sea. The forming of Swedish regulation of sonar use is an ongoing process that is not, as of the writing of this thesis, finished [2].

Whereas visible pollution such as plastic waste floating around the oceans or even oil spills is harmful it can somewhat easily be observed and avoided since its effects are direct and obvious. The effects of less noticeable pollutants such as weak toxins can be much more harmful in the long run since the effects can be hard to notice and hard to identify. As for acoustic pollution loud impulse sounds can be thought of as being in the "visible" category and a raised ambient threshold level can be thought of as an "invisible" pollutant. A specific source such as active sonar is comparatively easy to study and regulate because the effect of a single event is easily observed. Piling can generate impulse noises of up to 230 dB re 1  $\mu$ Pa, which can be damaging to nearby aquatic life [61]. The effects of rising ambient levels due to tens of thousands of ships in the oceans are harder to establish and thus harder to regulate [54], see section 2.3.3.

The experimental studies that have been undertaken show no physiological effects on a population-level from offshore piling, explosions or from explosive air guns [27]. There are potentially long term damaging effects on behavior, which are less well-studied: animals that are displaced from their natural habitat by piling over extended periods may lead to unforeseen consequences. Tougaard *et al.* list some of these as exclusion from habitat, reduced time for feeding, fewer mating opportuni-

ties and reduced time for nursing [61]. The first two of these directly cause reduced access to food, which has rather direct consequences. The last two of these cause population effects that take much longer to observe. Studies have shown stress effects and avoidance behavior of cod and sole from playbacks of impulse sounds. In a study by Thomsen, *et al.*, sole started showing significant movement response at 144 – 156 dB re 1  $\mu$ Pa and cod at 140 – 161 dB re 1  $\mu$ Pa [60].

Other more speculative potential consequences can involve e.g. animals erroneously interpreting the sounds of piling as earthquakes, leading to unwillingness to move back. Animals that migrate *en masse* to a new habitat can become invasive species.

In recent years, there has been discussion about EU-wide regulation of the marine environment of which anthropogenic underwater noise is one factor [7]. The EU directive Marine Strategy Framework Directive (2008/56/EC) states as a goal that: "*Anthropogenic inputs of substances and energy, including noise, into the marine environment do not cause pollution effects*" [11]. The impact that anthropogenic noise might have on the aquatic life is an understudied phenomenon. The effects that increased noise levels have may differ between aquatic species. It might be necessary to study individual species separately [49].

Since the aquatic animals to a large extent orient themselves and communicate using sounds there is a concern among researchers that higher levels of ambient noise may cause masking of sound for communication. This might lessen the sphere of vision and communication, possibly impacting the animals' use of sound when mating, giving warning or detection of predators and prey.

All animals have a Critical Ratio (CR), which is the ratio below which individual sounds become imperceptible in ambient noise. CR for fish in general tends to be around 13 dB for the lowest frequencies (20 Hz) and then increasing with 3 dB per octave [12]. Ship noise can potentially displace fish. De Robertis *et al.* [52] found that a noise-reduced vessel will detect between 10 – 30% more fish than a louder vessel. In general, heavy shipping is usually found in densely populated shipping lanes. Shipping lanes cause noise to be concentrated mainly along these lanes and not spread to the entire oceans. If the lanes pass through important habitats of certain animal populations then those populations will either be forced to migrate to less optimal regions or to stay and deal with the increase in SPL.

Curves showing sensitivity of hearing at different animals at different frequencies are shown in Figure 2.11.

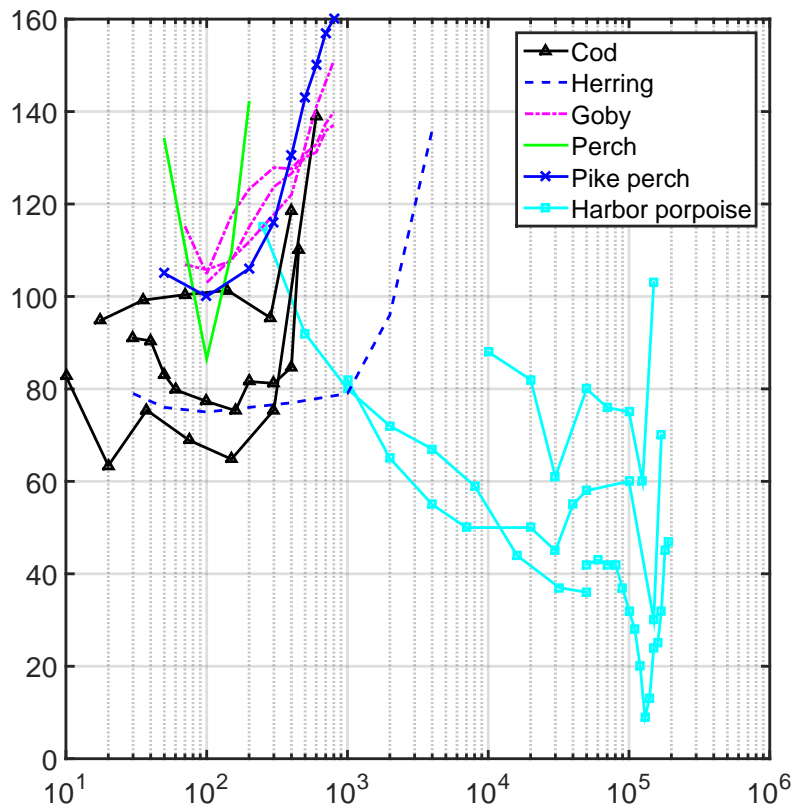


**Figure 2.11:** Curves of hearing thresholds for some common animals in the Baltic Sea, adapted from Nedwell *et al.*, 2004. The curves are gathered from various measurements of animals. Hence the large variations in levels. Note that hearing among fish is in general best at low to mid frequency range, whereas the harbor porpoise has excellent hearing in high frequency range but poorer at the lower frequency ranges.

It is difficult to determine whether any animals are displaced as a consequence of shipping lanes passing through their habitat. If an animal population is observed living and hunting in the ocean far from any shipping lane then it is not obvious whether that is their natural habitat or if the population would have preferred staying at a different habitat that happened to have a shipping lane going through it. Vice versa, if an animal population is observed living close to a shipping lane then it is not obvious whether the population would have fared better, had the lane not been there. It may even be the case that a predatory population is thriving close to a shipping lane simply because the shipping sound masks the sounds of that predator, making it easy for it to hunt down unsustainable amounts of a prey population. The harbor porpoise, for example, uses echolocation clicks at higher than 100 kHz and has poor hearing below 1 kHz. In the Baltic Sea the harbor porpoise is the most common in the parts which also happen to be the noisiest albeit mostly noisy in low- to mid-frequencies [23].

No matter what type of regulation that is eventually inferred it will prove difficult to regulate sound in the oceans. One reason is that the oceans belong to no single nation and they easily fall victim to the "Tragedy of the Commons". This situation is described in economic theory and game theory as a game in which it is in all players' best interest for themselves to act selfishly and for everyone else to act altruistically. If all or most players tend to act selfishly then all players lose. It is in all individual countries' best interest for there to be healthy and thriving life in the oceans but the oceans have historically been easy and rewarding to use as places to dump toxic waste and for fishing up seemingly unlimited amounts of fish. This has led to the oceans being polluted and overfished. Hypothesize a regulation requiring all ships to adhere stricter to standard shipping routes as a way of limiting the spatial extent of the noise impact of shipping and a re-routing of shipping routes according to which areas will be deemed extra sensitive for wildlife. One concern with such a regulation on an EU level is how it would be enforced and if ships registered in EU countries would be treated differently from ships registered in countries outside the EU. Article 87 of the *United Nations convention of the Law of the Sea States* recognizes freedom of navigation as a basic principle of all states [62]. The freedom of navigation is a right that has historically been allowed to override contended territorial claims [13]. Regulation based on a presumed impact on wildlife would therefore likely not be used to strictly forbid ships from free movement but rather to be incorporated as a part of the trade agreements of the EU region with the expectation that most shipping companies honor the agreements.

## 2.4 Statistics and signal processing

Historically underwater acoustics has been a military subject to a large extent focused on the detection of enemy submarines through acoustic means and the silencing of own submarines. For this reason the subject has been treated in standard books as being largely about detection of signals in noise. Signal and anomaly detection is about establishing a normal and undisturbed baseline and detect anything that lays too far outside of the range of the baseline. This thesis deals with defining these values in terms of third-octave sound pressure levels.

A fundamental property of statistics is stationarity. If the statistical values for a number of consecutive time intervals are the same then it can be stated that the time series are stationary.

It should be underlined that outliers should be excluded from the data set or else the data set might be skewed severely and lead to erroneous results.

### 2.4.1 Correlation, cross-correlation and autocorrelation

Correlation is the measures of covariance of two variables. Correlation goes from no correlation to high correlation and it can be negative or positive. High correlation is generally an indication that the two variables are dependent or that both are related to a third variable. Low correlation means that the two variables are not related. Positive correlation means that as one of the variables goes up, the other goes along

with it. Negative correlation means that as one variable goes up, the other goes down.

Cross-correlation between two signals is defined as follows:

$$\rho = \frac{cov(X, Y)}{(\sigma_X^2 \times \sigma_Y^2)^{1/2}}, \quad (2.8)$$

where  $\rho$  is the correlation coefficient,  $\sigma_X$  is the standard deviation of the signal  $X$  and  $\sigma_Y$  is the standard deviation of the signal  $Y$ .  $cov(X, Y)$  is the covariance between the signals  $X$  and  $Y$ . The discrete covariance of two signals is defined:

$$cov(X, Y) = E[(X - \mu_X)(Y - \mu_Y)] \quad (2.9)$$

where  $E$  is the expectation value and  $\mu_X$  and  $\mu_Y$  are the arithmetic means of the respective signals [50].

Auto-correlation is the process of cross-correlating a signal with itself at various time-lags. A strictly stationary signal does not change its properties over time, so it will not matter at what time-lag it is cross-correlated with itself [50].

An infinite array of perfectly random numbers corresponds to a signal that is perfectly stationary and uncorrelated in time. The first step is the zero lag correlation, which is always high. For any other lag, the correlation is zero, meaning that an arbitrary sample chosen at any position in the array is as good a representative as any other of the entire array.

The autocorrelation of a periodic signal such as a simple sinewave is itself periodic. This is because a periodic signal will tend to slide in and out of correlation with itself, sometimes leading to constructive interference and sometimes to negative. If a Fourier transform is performed on the autocorrelation signal the signal will show up as peaks at certain frequencies. The peaks can be studied to study periodic content in the original signal.

Four common types of periodic sound sources that can be observed using autocorrelation are: certain types of defect sounds from ships (periodic in various frequencies), the sound of distant piling (periodic in low frequencies), active sonar (periodic in just one or two third-octave bands at mid-to-high frequencies) and the type of modulation by waves on the sea surface that is visible in Figure 2.1.

### 2.4.2 Stationarity

Averaging over several spectra requires that the ambient noise is stationary, that is, during the ships passings no new features should occur. Furthermore, since each ship is travelling at different angles to the hydrophone, with differing local conditions of bathymetry and seabed properties, the sound will travel in different channels and end up sounding slightly differently at the same distances even for similar ships.

For calculations to be statistically sound and reproducible the signal must generally be stationary. It is possible to draw conclusions from non-stationary data but for the standard statistical variables (e.g. mean value, kurtosis, skewness) to be reliable, the signal should be stationary or else the estimates can be misleading. Absolute stationarity, however, is impossible except in the theoretical realm. Priestley notes that: *"In practical applications the most we could hope for is that, over the observed time interval, the process would not depart "too far" from stationarity for the results of the subsequent analysis to be invalid"* [50].

Stationarity is related to the integration time. For it to be possible to take meaningful  $n$ -second means, the signal needs to be stationary for those  $n$  seconds. In this study, 1 second spectra were established. The reason for this choice was that the sound level of a ship does not change very much over the 1 second integration time. Further, 1 second is short enough to identify individual transient sounds. [34, 50].

The aim of this study is to establish a relation between different environmental variables (e.g. distance, temperature and wind speed) and the resulting SPL. This is done by investigating one variable at a time. It should be stressed that there will always be unknowns that influence the ship noise. In the event of cavitation the noise from the ship will be difficult to predict.

Processes that are not stationary are referred to as non-stationary or evolutionary [50]. In this study there are two main types of non-stationary signals: slow trends of rising and falling levels as well as short transient sounds. The first of these types occurs when ships in the near-field approach or leave the hydrophone. The second type can be divided into two main types: sounds that are audibly present in the environment and sounds internal to or caused by the equipment itself. Sounds such as waves breaking, seals making noise and cavitation from ship propellers are a part of the environment of the Baltic Sea and would be present irrespectively of the hydrophone. Sounds such as creaking or flow noise near the hydrophone itself, or digital glitches are only considered unwanted noise as far as this study is concerned. Several statistical tests have been implemented to quantify them and to remove or avoid them.

Weak stationarity is defined as the mean and the autocorrelation of the signal remaining constant over time. Since audio signals are oscillatory in nature the mean of the signal is zero except if there happens to be a DC component added in by the recording equipment [20]. Autocorrelation, however, can not be assumed to be zero if there are periodic sounds present. Some anthropogenic signals such as piling generate monotonously rhythmic signals which give rise to high autocorrelation but there are also naturally rhythmic processes such as the oscillation of sea surface waves.

A signal is covariant stationary when the covariance is a time-invariant process.

### 2.4.2.1 Ergodicity

For ergodicity to be valid requires that only one transfer function from the input to the output is applicable. If the input is "a ship is present" the output should be "the sound of a boat and nothing but a boat." If the input is "a boat comes and the wind blows at 5 m/s" then the output should reliably be a function of those criteria. This is defined as follows: if  $f(t) \implies g(t)$  then  $f(t + \Delta t) \implies g(t + \Delta t)$

Ergodicity is a strict assumption in that the process can only be stationary in one way but it can be non-stationary in an infinite amount of ways [50]. If a sea under certain conditions of weather, bathymetry, temperature and salinity has a stationary soundscape then that sound can basically be assumed to consist of a sum of pure sinewaves with no beginning or end. Any sudden sound of a creak in the hydrophone or splashing of a wave will ruin that assumption.

### 2.4.2.2 Grubbs' test

Stationarity can be tested using Grubbs' test, which is defined as follows:

$$G = \frac{\max|Y_i - \mu(Y)|}{\sigma}, \quad (2.10)$$

where  $Y$  is a vector,  $\mu(Y)$  is the arithmetic mean of  $Y$  and  $\sigma$  is the standard deviation of  $Y$ .

Specifically,

$$G = \frac{\mu(Y) - Y_i}{\sigma} \quad (2.11)$$

tests whether a value  $Y_i$  which is smaller than  $\mu(Y)$  is an outlier.

$$G = \frac{Y_i - \mu(Y)}{\sigma} \quad (2.12)$$

tests whether a value  $Y_i$  which is larger than  $\mu(Y)$  is an outlier [50].

The test flags for non-stationarity if the following proves to be the case:

$$G > \frac{N-1}{\sqrt{N}} \sqrt{\frac{t^2}{N-2+t^2}}, \quad (2.13)$$

where  $N$  is the length of the vector and  $t$  is the statistical t-distribution (a number which is 1.7459 for 0.95 significance).

The test shows whether  $Y_i$  is an outlier. If equation 2.13 is zero the test does not flag  $Y_i$  as an outlier.

## 2.4.3 The Fourier transform

Most waveforms can be decomposed into linearly independent trigonometric functions. Mathematically this is described by the Fourier transform:

$$f(t) = \sum_{k=-\infty}^{\infty} \frac{1}{T_0} \int_{T_0} f(t) e^{-jk\omega_0 t} dt. \quad (2.14)$$

This is a transformation that is based on the fact that the correlation of trigonometric signals is non-zero only if the signals are linearly dependent. All linearly independent trigonometric signals will sum to zero. A waveform is correlated with all frequencies from negative to positive infinity. The correlation will be non-zero for frequencies that share information with the original signal and zero for all other frequencies. Slow movements in the waveform will correlate with low frequencies and fast movements will correlate to high frequencies. It is possible to establish a table of the frequency content for the given waveform. The table can be used as well to recreate the signal. The invariance is uniquely defined. It is thus possible to decompose and synthesize the waveform without losing any information. The signal in time-domain and the signal in frequency-domain are complimentary ways of describing the same signal.

An infinitesimally short jump with infinite amplitude is known as a Dirac delta function or a Dirac impulse function. It can be shown that such a function involves all frequencies of equal amplitude. Even transients that occur suddenly will consist of many frequencies. An audio recording that starts and stops at different values introduces frequencies that are not present in the original signal. To overcome this deficiency, signals are usually faded in and out. This is referred to as tapering or time windowing. There are many types of windows and each of them alters the frequency and power content different ways. The power content can be corrected for by scaling the signal [22]. One requirement for tapering is that the signal is stationary.

In fact, all signals are windowed in both time and frequency domain. This is because it is impossible to save infinite amounts of time and frequency data.



# 3

## Methods

In this chapter the methodology is outlined for how hydrophone recordings were used to compose spectral curves that quantify the influence of anthropogenic noise mainly from ships in the far-field and the near-field but also from rain, thunder, piling and from Navy sonars. The resulting curves are analogous to Wenz and Knudsen curves but they are not defined the same way. The curves are site-specific, adhering in this study to Trelleborg and Norra Midsjöbanken.

The hypothesis was to test whether such curves could be established from raw data, given that the amount of data is large enough.

### 3.1 Equipment and recording of audio data

Audio data consisted of underwater recordings performed by FOI as part of the BIAS project. The data covered the full year of 2014. The recording equipment consisted of a number of units with a piezoelectric hydrophone connected to an SM2M recorder manufactured by Wildlife. The recorder saved data onto SD cards. The battery power for such a setup lasts for 3-5 months and had to be changed with regular intervals.



**Figure 3.1:** Photograph showing a recording setup being retrieved. The buoy keeps the setup suspended. The yellow part is the recorder. The gray PVC pipe contains the release mechanism that responds to an acoustic signal containing a password by releasing the setup so that it floats up to the surface.

The autonomous hydrophone system is shown and described in Figure 3.1. The units were all calibrated in 2013. They were deployed at their positions in the end of 2013 and beginning of 2014. For both positions some data were lost. One month of audio data was missing for Trelleborg and two months for Norra Midsjöbanken [16, 17]. Every third to fourth month the system had to be retrieved and a new system deployed.

## 3.2 Pre-processing of audio data

Raw sound data for the two hydrophone positions were available in wave format, covering most of the year 2014. In total there were 14235 recorded files. The sampling frequency was 32000 Hz with a Nyquist frequency of 16000 Hz. Each file had a duration of either 1200 s or 1380 s and was recorded from the first minute of each hour of the recording session. 1380 seconds was the most common playtime. The number of files per month varied between 0 and 744 files. 744 is the maximum number of hours in a month and most months have the same number of files as there are hours in the month. For some months, however, some files were corrupted or the batteries of the hydrophone had run out before a new hydrophone could be deployed, bringing down the total number of recorded hours.

### 3.2.1 Third-octave band frequency spectra

All recorded audio data were converted to 1-second spectra using Matlab. This was done by first removing the DC component, i.e. subtracting the means of the audio data. After this the audio data were adjusted for the hydrophone sensitivity  $S$ , which was  $-184$  dB re  $1 \mu\text{Pa}$ . This value of  $S$  was within the error range of all of the hydrophones so the same sensitivity value was used for all months for both positions.

The audio time series were cut into one-second bins. A Hanning window in the time domain was applied to each bin and scaled by 1.633 to compensate for the amplitude loss due to the windowing [22]. Each individual one-second bin was Fourier transformed. The narrowband spectrum was subsequently divided up into 32 third-octave frequency bands ranging from 12 Hz to 16000 Hz. Each band was adjusted to give the RMS mean.

In total this resulted in up to 744 data sets per month and hydrophone position, each with 32 third-octave band columns of 1200 or 1380 second time-length. This resolution was sufficient to provide details in both the frequency and the time domain while also being sufficiently short to not take up too much memory and hard drive space. Specifically, the time resolution was fine enough that individual glitches and other transient sounds could be identified and dealt with in the same domain as stationary sounds.

The major disadvantage with converting to third-octave band spectra, as opposed to staying in narrow-band spectra, is loss of detailed information. Specifically, Wenz curves are only well-defined in narrowband representations. Third-octave band resolution was too coarse to be able to extract the individual spectral components in e.g. ship motors contributing to the noise [3]. The aim of this work was instead to

focus on more general features.

### 3.2.2 RMS averaging frequencies

All of the audio recordings were converted to 32 third-octave bands where the narrowband spectra of 1 second bins were split into third-octave bands and root-mean-squared over the frequency bands. Perhaps a more common method is to take the arithmetic mean of the squared pressures of each band.

Figure 3.2 shows the power content of an arbitrary recording in narrowband as well as frequency-averaged in pressure RMS and in arithmetic mean of pressure squared. For further comparison another method where the median is used is also shown even though this is not a commonly used method. Also featured is a common method where the powers are summed up over the third-octaves. As can be noted the difference between RMS and arithmetic mean is small but prevalent. The maximum difference between the two for this particular file is 2.3178 dB. The RMS curve seems located along the upper part of the narrowband curve and the median curve seems to follow the middle of it. The arithmetic mean curve is found somewhere in between the RMS and the median curve. The three methods show somewhat similar tendencies and the general conclusions drawn by either will likely be the same, although the RMS method is the one showing the largest variation depending on narrowband peaks and mostly resembles the shape of the upper envelope of the narrowband curve. The summation method shows another type of result altogether which has to be interpreted differently from either of the others.

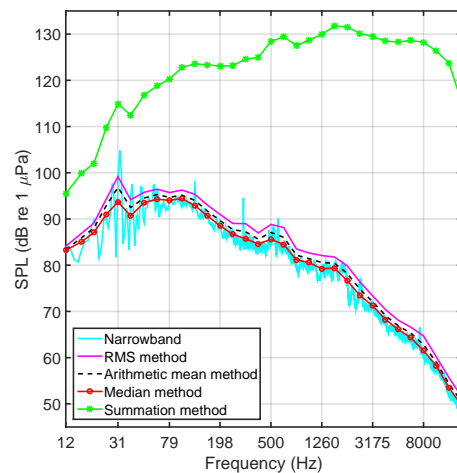


**Figure 3.2:** Example of a single audio file, divided into mean third-octave bands in four different ways

### 3.2.3 Audio errors and abnormalities

Measured data are always prone to errors. Things go wrong and equipment might not be working properly or data gets corrupted. The audio data in this study had several types of errors, which are described in this chapter.

#### 3.2.3.1 High-pass filter

All the recorders high-pass filter the sound with a cut-off frequency of 10 Hz. This is to avoid to record the slow movement of the hydrophone in the water. This amplitude exceeds any harmonic pressure signals and would require a much lower gain, which would make the signal noisier.

Note that shallow waters in itself behaves as a high-pass filter. This is due to the way normal modes are propagated in sound channels, having to do with the fact that low frequencies (i.e. long wavelengths) cannot fit in shallow waters [26]. The cutoff frequency for modal propagation in Trelleborg is:

$$f_0 = (2m - 1) \frac{c}{4D} = \frac{1500}{4 \times 23} = 16 \text{ Hz}, \quad (3.1)$$

where  $m$  is the integer number of modes (the lowest being  $m = 1$ ),  $c$  is the velocity of sound (approximately 1500 m/s and  $D$  is depth (m), which was 23 m. Below 16 Hz the water is already quite a poor channel for sound propagation.

For Norra Midsjöbanken  $D = 40$  m and the cutoff frequency becomes:

$$f_0 = \frac{1500}{4 \times 40} = 9 \text{ Hz}, \quad (3.2)$$

which is close to the cutoff frequency for the equipment itself.

#### 3.2.3.2 Digital glitches

In some files audio glitches were found. Most of them were wideband and of high amplitude, implying that they affect the total levels. It turns out that in most of the equipment the glitches appeared at certain times into the files, specifically 601, 901 and 1201 seconds. They also showed up for about a week each and in about a third of the files in that period. Before and after this period entire months could go by without any glitches. The glitches at 1201 seconds into the files were the most common type.

Figure 3.3 shows an example of a spectrogram of such a glitch. Note the wideband nature of the glitch and the way it stands out against the rest of the sounds.

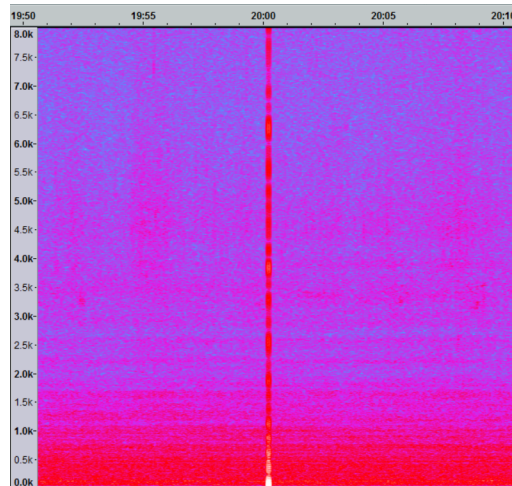


**Figure 3.3:** Spectrogram showing time and frequency composition of a typical glitch. X-axis is time (minutes). Y-axis is frequency (Hz).

It is speculated that this type of glitch is a result of the equipment performing some type of buffer flush 10, 15 and 20 minutes into recording. If the recording times had been longer, there would most likely continued to be a glitch every fifth minute. Other possible explanations include: systematic error in the model of the recorder (Wildlife Acoustics SM2M), individual errors in some of the recorders, possibly resulting from the handling of the recorders, the conditions of use (mainly temperature), the duration of the recording, the quality and brand of SD card and the number of previous rewrites to the SD card.

As a solution the glitches were removed by an insertion of the previous seconds' data in erroneous timeslots. In total, three seconds from each of the 744 files for each month were removed. This added up to almost 15 hours over all the files.

### 3.2.3.3 DC correction

Sound is normally made up of harmonic pressure oscillations around the ambient pressure. The mean of these changes shall, thus, always be zero. Comparatively sudden changes in ambient pressure and unknown artifacts introduced by the recording equipment can sometimes lead to non-zero means. The means of each audio signal was subtracted from the respective signal before any other processing was made to ensure harmonic signals.

### 3.2.3.4 Time windowing over the files

Grubbs' tests were performed on all the files to identify non-stationarity. The results of the tests revealed more non-stationary seconds in the beginnings and ends of the files than in the middle. Taken as an average over the entire month the density of test flaggings appeared like an inverted Hanning window in the time-domain. This pattern was the same for all months and for both positions, pointing to a systematic error in either the recording or the after-processing of the files. The effect appeared to be unimportant so no action was taken.

### 3.2.3.5 Self-noise

The recording equipment was prone to self-noise. In many of the files there was a creaking sound, which intermittently showed up. This was from the knots that tied the floating hydrophones to their weights. In some cases this resulted in a creaking sound. Most of the time the creaks were not very loud and could safely be ignored. In some cases, however, the creaks were very loud and led to non-stationarities that had to be sorted out.

### 3.2.3.6 Time drift

The time base in the recording equipment is temperature dependent. Higher temperatures lead to faster molecular movement which in turn lead to clock speeds that are higher than GPS time. With lower temperatures clock speed lags behind GPS time. In almost all of the hydrophones time drift was manifested as the hydrophone lagging behind GPS time by up to 90 s/month.

The time drift has previously been shown to be linear [18]. The correction chosen for the time-drift was a linear extrapolation of zero to maximum lag over each recording period. Each time-stamp of each recording period was corrected by adding the interpolated lag.

## 3.3 Pre-processing of AIS data

Automatic Identification System (AIS) data is a system used to identify location, type, velocity, draught, size, cargo and size of every large ship at all times. Each ship is identified by an MMSI number. All of this data is open and can be looked up online at any time. Ships transmit their location differently, depending on how fast they move. The fastest ships transmit every third second and the slowest ships transmit every 240 seconds.

The datum of the AIS data used in this study was WGS84 decimal coordinates and it was delivered in raw text format. Each row of the text files consisted of time-stamp, MMSI number, latitude, longitude, number for ship type, number for cargo type, velocity (in knots) and draught as well as distances from the AIS transmitter to the port, starboard, bow and stern of the ship.

All of the text files were cleaned of errors, NaNs and poor formatting using stream editors. To the extent possible, defect individual fields were replaced with zeros to indicate missing values and to avoid having to delete the entire rows. In cases where data corruption affected the formatting of the rows the rows were removed. The files were formatted to be imported to Matlab. All rows with positions farther away than 25 km from the hydrophone were removed.

Entries with zero velocity were sorted out completely. This mostly included functional harbor ships working in and around the harbor as well as a number of pleasure crafts where the owners may have forgotten to turn the transmitters off while the ship was dormant. Some permanent installations such as wind farms and lighthouses also have MMSI numbers and were sorted out in this step.

The AIS system is a one-channel system. Each MMSI signature in a given region is given a specific time slot for the data with GPS time as the common time. This and the fact that ships do not transmit at the same update frequency lead to the data having to be interpolated to be given a uniform time base. A 1 second base was chosen and each ship was interpolated onto this base.

### 3.3.1 Defects with the AIS data set

The raw AIS data contained some errors. In some cases data had been swapped around so that the length of a ship was reported as its width. In a number of cases, data on the ships were missing. There were also glitches and junk data in the AIS files. For every file of AIS data a few thousand rows turned out to contain junk data. These glitches were easily sorted out but at the cost of removing entire data points. It is possible that the existence of some entire ships were erased if their transmitted AIS data was systematically corrupt. This could potentially lead to the occurrence of false negatives. The number of data points removed, however, was so small compared to the full data set that this was considered acceptable.

A disadvantage with sorting out vessels with zero velocity is that some ships that do not move will still make sound. For example tankers may stay still but have the motor running, while waiting to enter the harbor. Fishing boats may have stopped to throw out nets. Again, this is estimated not to lead to erroneous conclusions over the entire dataset but it might contribute to some of the observed deviations, especially at Trelleborg.

A systematic error with AIS data is that most smaller and private vessels lack transponders and are thus not included in the analysis. Especially during summer months, when the number of private vessels increases, large numbers of small ships end up being unaccounted for in the data [24]. This was probably not a big problem in the Norra Midsjöbanken position which lies far from any harbors or coast lines, but it might have influenced the results somewhat for the Trelleborg position where there are several harbors for leisure boats close by.

## 3.4 Quantification of stationarity

All files were tested for stationarity. Since the DC component was removed from the audio data the first criterium for stationarity, which is that the arithmetic mean  $\mu$  is constant, was satisfied for all recordings. Grubbs' test was applied to all data directly on each third-octave band, to determine stationarity of individual seconds. Data that were classified as stationary were used to investigate the influence of wind-speed and of shipping noise.

$$N = \text{length}(X) \quad (3.3)$$

$$\mu = \frac{1}{N} \sum_i \quad (3.4)$$

$$t = 1.7459 \quad (3.5)$$

$$G = \frac{\text{abs}(X_i) - \mu(X)}{\sigma} \quad (3.6)$$

$$G > \left( \frac{N-1}{\sqrt{N}} \sqrt{\frac{t^2}{N-2+t^2}} \right), \quad (3.7)$$

where  $X$  is the time segment to be tested and  $X_i$  is an individual element of the segment,  $t$  is the statistical t-distribution, which was chosen to make the precision  $p < 0.05$ . The test returned a zero for each second that did not differ much to the consecutive second and a one when there was a large difference. A value of one is hereafter referred to as a Grubbs' test flag.

In files with very calm weather and no ships nearby there were generally no flaggings. When a ship passed by there was a high density of flaggings as the ship reached its closest point of approach. This was especially true for ships with cavitating propellers.

The presence of cavitation generally resulted in non-stationary audio data. An example spectrogram of a cavitating ship can be seen in Figure 2.5. Note the sudden starts and stops of loud and sharp sounds as a result of the cavitation. For this reason cavitating ships were sorted out before doing any calculations of transmission loss.

## 3.5 Transient sources

The analyses reveal that there were both periods with single, rare transients and periods with frequently occurring transients. Sources of the first type included thunderstrikes, earthquakes and miscellaneous transient sounds, such as bottom scraping or otters playing with the hydrophone. Sounds of this type were difficult to quantify automatically and had to be judged by ear. Examples of the second type of sounds were wind-induced noise and ships passing. These types of sources were easy to relate to metadata (weather models and AIS data) and existed in quantities that they could be extracted by employing signal processing without any human intervention.

There was a gray-zone in between these types that included: piling sound, active sonar and rain noise. These sources reoccurred frequently enough to be averaged and modelled, but still seemed to require a human element of picking and choosing which exact recordings and parts of recordings that were useful as source material. Once the frequency ranges were known it was easy to find recordings that contained either piling or sonar from their respective strong periodicities and from the fact that both sounds stood out considerably from the normal levels in the respective third-band octaves. Rain was complicated to identify from levels alone but loud levels at high frequencies were an indicator. The presence of rain could then easily be confirmed from a quick glance at the spectrograms.

### 3.5.0.1 Detection of piling

There was distant piling audible in many of the recordings at the Trelleborg site. There was piling done in Trelleborg harbor during January and February. The harbor was reconstructed during which piling was done on the ground near the seashore as well as retaining walls were sheet piled in the water. There was also off-shore piling performed in February and March during the construction of a wind farm

between Trelleborg and Putgart. There were other instances of piling audible, but the origin and nature of these are unknown.

The sound from both piling positions was clearly audible as a monotonous thumping in the low frequency bands. The thumping often dominated the soundscape to the point of being audible even when ships were passing by in the near-field.

Recordings with piling noise were detected using autocorrelation. For each third-octave band in the region 63 – 500 Hz the autocorrelations of the 1-second RMS spectra were calculated. In the third-octave bands with clear non-stationary periodicities (e.g. a monotonous piling sound) this was visible as a periodic content in the autocorrelation function. The autocorrelations were Fourier transformed to frequency domain. Finally, the variance of the absolute values of the non-DC frequencies of the Fourier transform was deduced.

$$f(x) = |fft(autocorr(X))|, \quad (3.8)$$

where  $X$  is the signal in a given third-octave frequency band. If the variance of  $f(x)$  was high there was a periodic content to the signal  $X$ , which typically indicated the presence of piling sound. The actual selection of recordings for closer study was done by ear because it was important to find time segments with few other disturbances.

### 3.6 Correlating factors

There are a number of factors that potentially have an influence on the soundscape. Some of them covary. It is therefore important to establish the relation between variables. There are natural factors, anthropogenic factors and a mixture of both (time-dependent noise).

A simple way of testing the influence is to correlate variations with the recorded SPL. If a factor influences the soundscape it is expected to correlate, positively or negatively, with the SPL in one or more third-octave bands. For there to be a significant correlation the correlation is expected to be above 0.5 or below  $-0.5$ . The correlation of a factor with SPL is not sufficient to establish a direct relation. The lack of correlation might be due to the influence of the factor being masked or dominated by other noise.

For any non-ship-related variable to be significant it can be expected on good ground that no ships are in the near-field. Individual ships in the near-field usually dominate the entire soundscape. For this reason the correlation was established for different minimum distances to the closest ship. This gave a minimum distance at which a factor becomes important to the soundscape.

For ship-related factors to be significant it can be expected that the correlation between the factor and SPL becomes stronger when ships are in the near-field than in the far-field.

A drawback, especially for the Trelleborg position, was that the position was so busy that the number of cases when there were no ships were few. Most of the time there were ships closer than 7 km. It was extremely rare that there were no ships closer than 20 km. Even with one year of recordings the dataset became too small to establish reliable statistical estimates.

## 3.7 Time-related noise sources

The soundscape can be expected to change with time, date, weekday and the seasons. Some of it is natural and some of it is anthropogenic. The division of days into weekdays and weekends is a human invention and any statistically significant difference between weekdays and weekends can be assumed to be due to different patterns in shipping. Months, however, are more indicative of the change in seasons, meaning that changes over months are probably primarily due to different weather conditions.

There are some expected co-variances. It is very likely that the human patterns of ship traffic change considerably depending on the seasons and the weather. Summer and vacations tend to result in a higher number of leisure boats which leads to more variation. Leisure boats do not use AIS, making traffic data not represent the full picture of the soundscape [23]. This change in human behavior also correlates with certain natural sound sources such as wind speeds, storms and rain periods, making it hard to isolate the time-dependency of these factors.

It could be speculated that shipping companies might intensify shipping to meet economical goals before the end of a financial quarter. Over longer periods of time (years and decades) the nature of shipping is bound to change drastically depending on technological development and on global economical trends. In recent years (since 2013) the trend in the Baltic Sea and globally seems to have been towards fewer ships but each ship being bigger and loaded with more cargo [59].

### 3.7.0.2 Dependence on time slot of recordings

All recordings were started at sharp hours and lasted for either 1200 s or 1380 s. An underlying assumption that is implicit in the choice of this time slot is that the soundscape during the first third of a given hour would be representative of the rest of the hour. A necessary condition for this is that the traffic during the hour was time-independent which might very well be the case out on open sea. This assumption is less obvious close to a large harbor. There are ferries going in and out of Trelleborg harbor with fixed time tables. This might give a statistical bias of the estimates.

The mean value in the time-domain of the 20 – 1000 Hz band of all files for each individual month for both positions are shown in Figures 3.4 and 3.5.

Note that the curves for the Trelleborg position tend to slope downwards for the first 800 seconds of almost every month, indicating a systemic pattern throughout the set of recordings. In most months there is a flat or slightly positive slope after that. In July there is a strongly positive slope which indicates a regular ferry arriving to

Trelleborg harbor.

No such pattern was visible for any of the months for Norra Midsjöbanken. Note that there are some digital glitches causing the spikes that are visible in the beginning of some of the months which in later analysis were discarded.

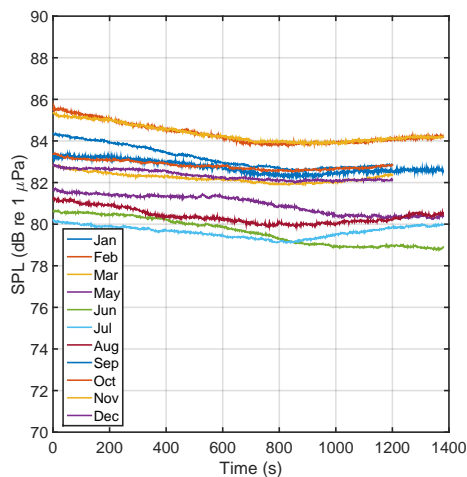


**Figure 3.4:** Broadband mean values of all files of the months for the Trelleborg position. Most months show decreasing levels over the first 13 minutes of the recordings. Recordings in July stand out as having a particularly clear pattern of decreasing levels over the first 13 minutes and then rising levels over the last 10 minutes.

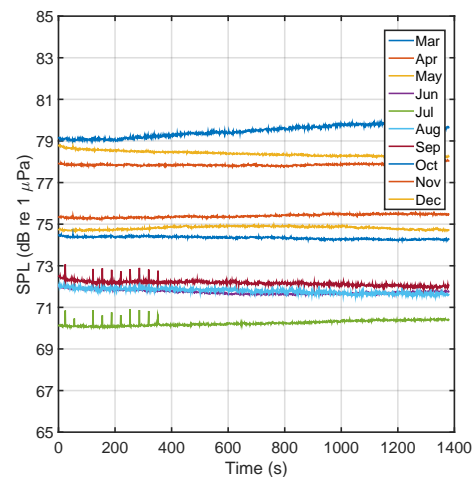


**Figure 3.5:** Broadband mean values of all files of the months for the Norra Midsjöbanken position. The mean recordings are flat. Some months show slow glitches for the first 6 minutes of the recordings but those have subsequently been taken care of.

### 3.7.1 Dependence on time of day

In order to study the dependence of time of day, days were split up into four equal slices. The mean SPL for each slice is shown in Figures 3.6 and 3.7. Only windspeeds between 0 – 10 m/s were used, to avoid having extreme variations that are related to the weather rather than time of day.

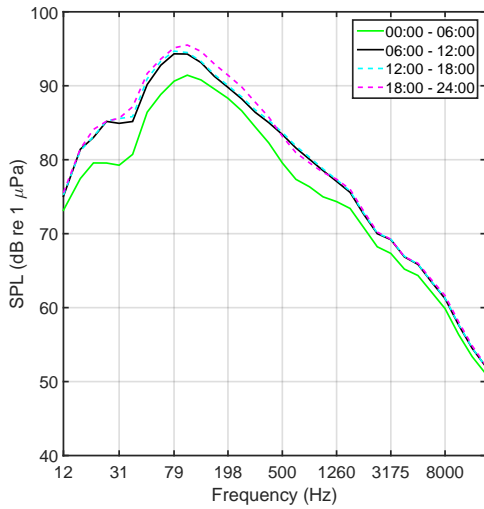


**Figure 3.6:** Mean SPL for different times of the day for Trelleborg. Windspeed was 0-10 m/s.

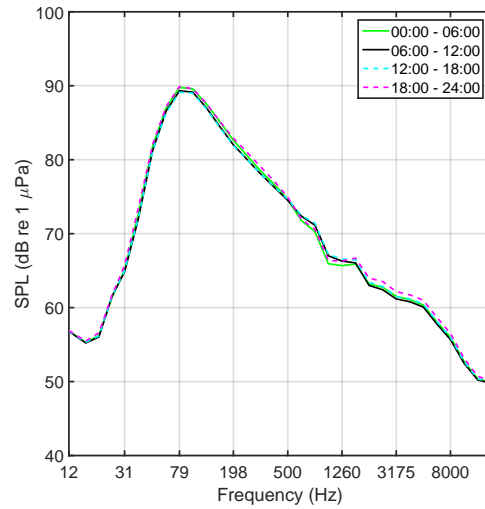


**Figure 3.7:** Mean SPL for different times of the day for Norra Midsjöbanken. Windspeed was 0-10 m/s.

Note that the Trelleborg curves in Figure 3.6 show a large variation compared to the Norra Midsjöbanken curves in Figure 3.7. In Trelleborg the first six hours of the day tended to be the most quiet. This was found to be true for every month although only the total mean is displayed in Figure 3.6. Further, the last six hours of the day were usually the loudest. For Norra Midsjöbanken there seemed to be almost no dependence on time of day for any of the months.

### 3.7.2 Dependence on day of the week

Differences in different days of the week were studied by taking the mean spectra of each of the weekdays and weekends for each of the stations, using the full dataset. The results are displayed in Figures 3.8 and 3.9. Note that because there are more weekdays than weekend days that the standard deviation for weekends is more sensitive to outliers. Overall, the weekday-related differences are minor. For both positions the standard deviations for weekends were a few decibels lower than those for weekdays but the differences were small. The conclusion is that days of the week have no influence on SPL.

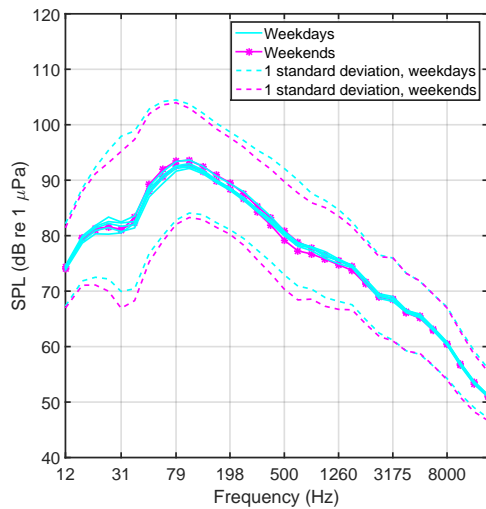


**Figure 3.8:** Mean SPL at Trelleborg for different days of the week. Windspeed was 0-10 m/s

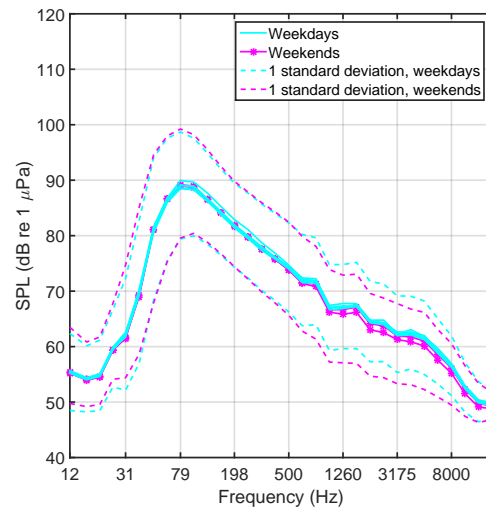


**Figure 3.9:** Mean SPL at Norra Midsjöbanken for different days of the week. Windspeed was 0-10 m/s

### 3.7.3 Dependence on month

Months were studied much the same way as weekdays. Mean spectra of each month are displayed separated by the occurrences of wind speeds in Figures 3.10, 3.11 and 3.11. Windspeeds higher than 10 m/s were not included in the analysis.

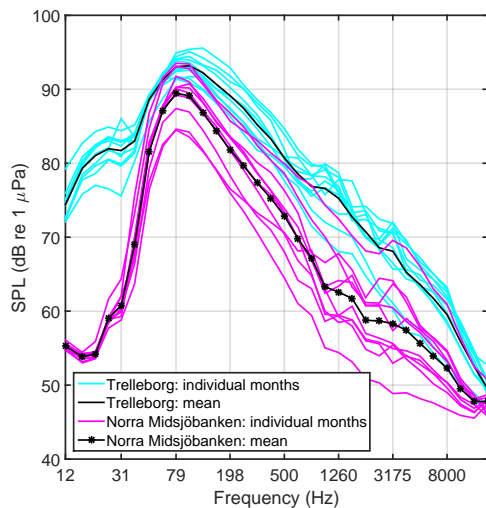


**Figure 3.10:** Mean SPL for different months for both positions as well as the total mean. Windspeed was 0-5 m/s

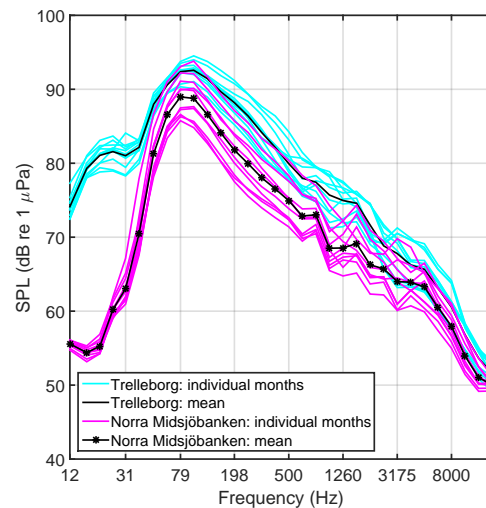


**Figure 3.11:** Mean SPL for different months for both positions as well as the total mean. Windspeed was 5-10 m/s

The largest differences between single months were found when wind speeds were low for Norra Midsjöbanken. In frequencies 1000 – 3000 Hz, the difference was around 20 dB between the loudest and the most quiet month. This can be interpreted as

differences in shipping, throughout the year, being the dominating factor. With the comparatively much lower density of shipping in Norra Midsjöbanken, compared to Trelleborg, there were smaller variations in SPL.

There was much lower variation between months at higher wind speeds, indicating that the predicted weather throughout the month was dominating the soundscape at least in the higher frequency range.

Figures 3.12 to 3.19 show cumulative distribution functions (CDF) for four different third-octave frequency bands for each individual month and for both positions.

It can be seen in the Figures 3.12 and 3.16 that 63 Hz is a frequency highly influenced by shipping. Note that the the CDF for Trelleborg remained rather steady with every single month, having a much higher level difference up to the upper percentiles than down to the lower percentiles. There was also almost no difference between 0.75 and 0.95 whereas the lower three percentiles were almost equidistant. This might be because of a high occurrence of ships passing nearby. Despite the fact that the first three months of the year contained much low-frequent sound of piling this was not discernible in any of the Figures.

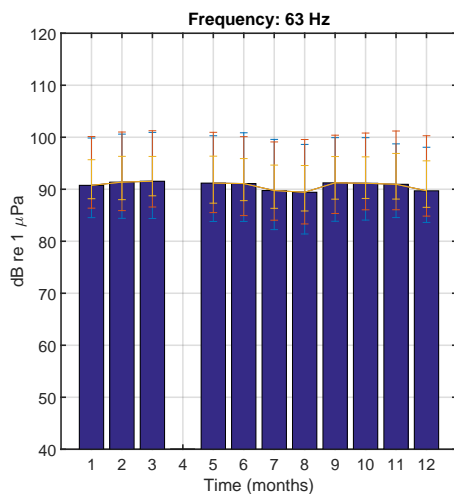


**Figure 3.12:** Trelleborg, CDF plot of all months,  $f_c = 63$  Hz. The bar shows the median. Upper orange is 0.95 exceedance level, upper blue 0.90, upper yellow 0.70, lower yellow 0.25, lower blue 0.10 and lower orange 0.05.

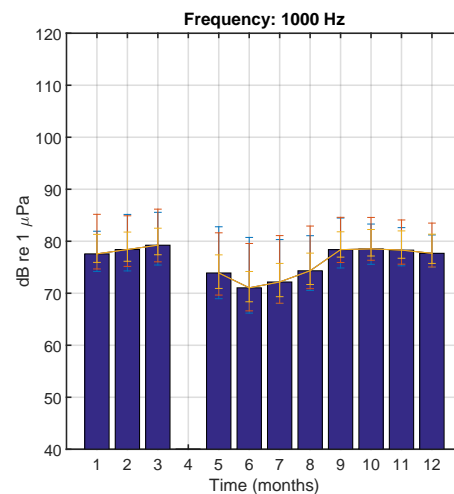


**Figure 3.13:** Trelleborg, CDF plot of all months,  $f_c = 1000$  Hz. The bar shows the median. Upper orange is 0.95 exceedance level, upper blue 0.90, upper yellow 0.70, lower yellow 0.25, lower blue 0.10 and lower orange 0.05.

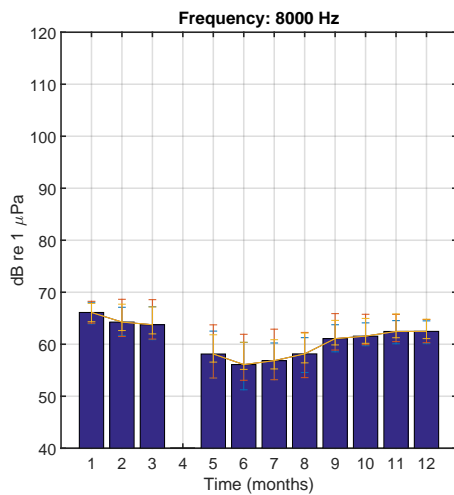


**Figure 3.14:** Trelleborg, CDF plot of all months,  $f_c = 8000$  Hz. The bar shows the median. Upper orange is 0.95 exceedance level, upper blue 0.90, upper yellow 0.70, lower yellow 0.25, lower blue 0.10 and lower orange 0.05.

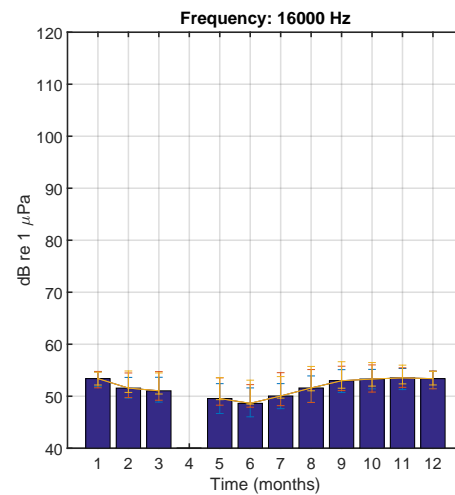


**Figure 3.15:** Trelleborg, CDF plot of all months,  $f_c = 16000$  Hz. The bar shows the median. Upper orange is 0.95 exceedance level, upper blue 0.90, upper yellow 0.70, lower yellow 0.25, lower blue 0.10 and lower orange 0.05.

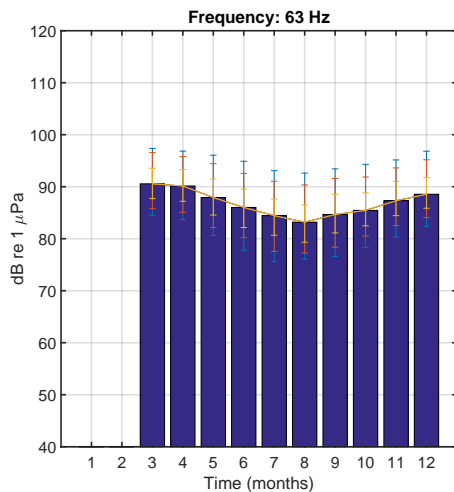


**Figure 3.16:** Norra Midsjöbanken, CDF plot of all months,  $f_c = 63$  Hz. The bar shows the median. Upper orange is 0.95 exceedance level, upper blue 0.90, upper yellow 0.70, lower yellow 0.25, lower blue 0.10 and lower orange 0.05.

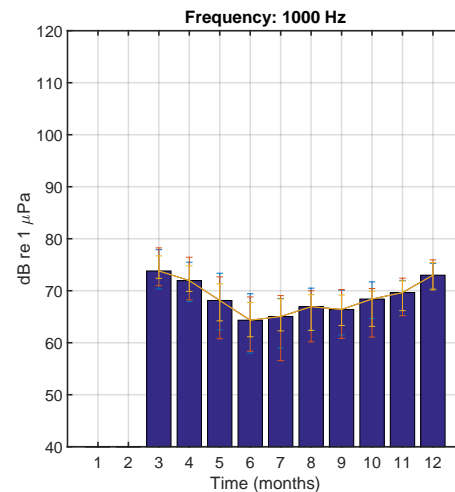


**Figure 3.17:** Norra Midsjöbanken, CDF plot of all months,  $f_c = 1000$  Hz. The bar shows the median. Upper orange is 0.95 exceedance level, upper blue 0.90, upper yellow 0.70, lower yellow 0.25, lower blue 0.10 and lower orange 0.05.

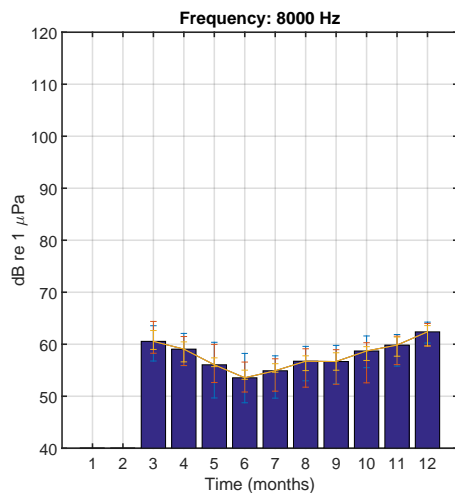


**Figure 3.18:** Norra Midsjöbanken, CDF plot of all months,  $f_c = 8000$  Hz. The bar shows the median. Upper orange is 0.95 exceedance level, upper blue 0.90, upper yellow 0.70, lower yellow 0.25, lower blue 0.10 and lower orange 0.05.

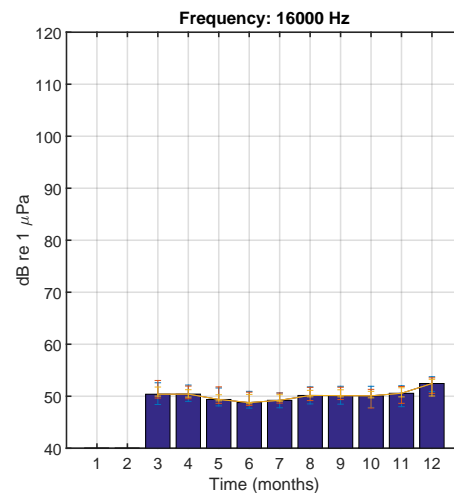


**Figure 3.19:** Norra Midsjöbanken, CDF plot of all months,  $f_c = 16000$  Hz. The bar shows the median. Upper orange is 0.95 exceedance level, upper blue 0.90, upper yellow 0.70, lower yellow 0.25, lower blue 0.10 and lower orange 0.05.

For the Trelleborg position the plots for frequencies 8000 Hz (Figure 3.14) and 16000 Hz (Figure 3.15) also follow the windspeed pattern but the 1000 Hz plot in Figure (3.13) is much more irregular with an increasing median during the first three months and an almost constant level for the last four months. In the quiet summer months there was a much larger difference to the top percentiles than to the bottom percentiles, explained by the relatively low base ambient levels and a continued high density of near-field passes of ships.

The 63 Hz plot for Norra Midsjöbanken (Figure 3.16) shows a linear decline from March to August and then a linear increase in levels. There is also about the same behavior in the percentiles above and below the median level.

The rest of the plots for Norra Midsjöbanken (Figures 3.17, 3.18 and 3.19) also show a linear decrease during the summer and then a steady increase during the winter. In all three plots the lowest SPL was found during June. The curves correlate with the changes in average windspeed during the year.

#### 3.7.4 Summary of time-related noise-sources

Obviously, time effects matter. Time of day and day of the week are not important factors, however, changes over the months matter a lot.

Sometimes the variation within a month was found to be large. The patterns present at the beginning of the month were not the same as those at the end of the month.

In the case of Norra Midsjöbanken the month of March has only the last week's data but this data can not be said to represent the whole month. The behavior throughout a month with missing data can be estimated by looking at weather data and density of shipping throughout the month. This has limited influence on annual estimates.

In general, while time and season dependencies influence various variables and levels, they were not seen as crucial for the estimates of the Wenz curves. Thus, time variations were ignored in this thesis.

## 3.8 Natural noise sources

In this section the noise sources which are not generated by human activity are studied. These include the baseline ambience, wind speed, temperature-dependance, rain, thunder and biological noise.

### 3.8.1 Influence of wind speed

Wind speed has long been known to correlate positively with SPL. Wenz' conclusion was that the influence of wind on the sea surface was the dominant factor influencing SPL at frequencies higher than 500 Hz [68]. Wenz notes, however, that the influence is highly dependent on other factors such as depth, distance to land, direction and duration of the wind. In this test only the wind speed was tested. The wind data were recorded at SMHI weather stations, which are several tens of kilometers away from the hydrophone positions and with a resolution of 1 hour.

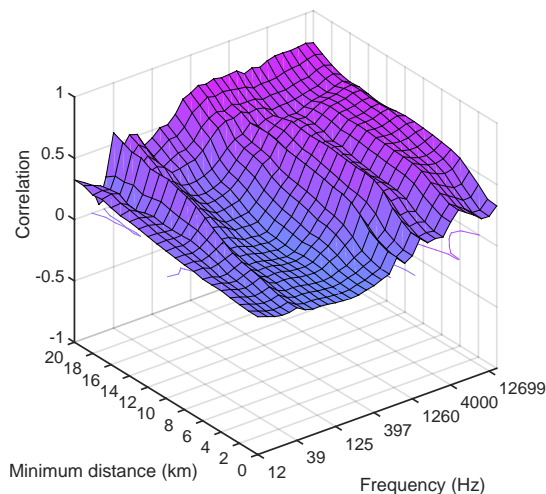


**Figure 3.20:** Correlation between windspeed and SPL at the Trelleborg position for different frequencies and minimum distances to the closest ship.

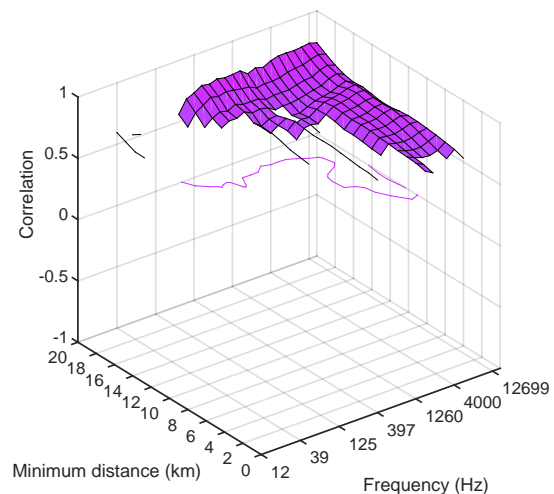


**Figure 3.21:** Correlation between windspeed and SPL at the Trelleborg position for different frequencies and minimum distances to the closest ship. Only correlations with absolute value above 0.5 is shown.

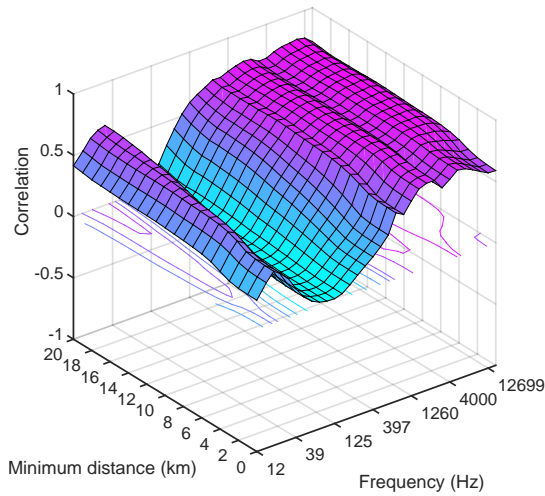


**Figure 3.22:** Correlation between windspeed and SPL at the Norra Midsjöbanken position for different distances to the closest ship

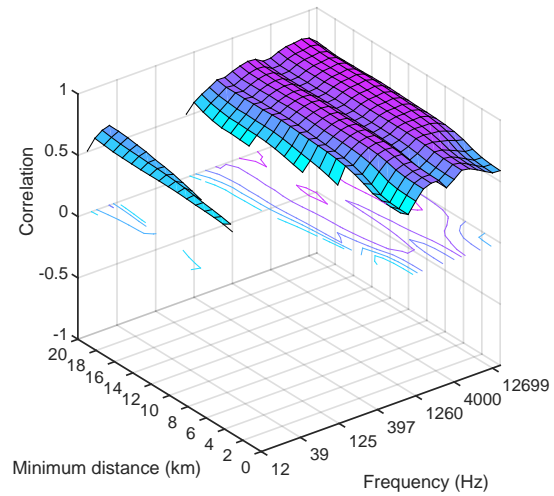


**Figure 3.23:** Correlation between windspeed and SPL at the Norra Midsjöbanken position for different distances to the closest ship. Only correlations with absolute value above 0.5 is shown.

Both positions show increased correlation between windspeed and SPL in the higher frequency range. The correlation increases with frequency. For especially the Trelleborg position the relationships between windspeed and SPL only start being strong, when there are no ships within 5 km for 5040 Hz and within 22 km for 99 Hz, see Figure 3.20.

There is a lower minimum distance to closest ship at which correlation between windspeed and SPL starts being high for the Norra Midsjöbanken position due to the lower density of traffic. For frequencies above 1000 Hz the correlation is above 0.5 even before all near-field ships are excluded.

Both positions show a trough with almost no correlation in between the lowest and the higher frequency regions, i.e. between 63 Hz and 800 Hz. The correlation in the lower frequency region is more pronounced in Trelleborg than in Norra Midsjöbanken, although the general shape of the plots are the same with the lowest frequencies correlating positively with the windspeed. The same pattern was observed by Wenz, who wrote that: *"minima or inflection points appear in the spectra between 100 and 500 cps. This spectrum shape suggests the possibility, at least, of two different wind-dependent sources or mechanisms. In the system used for the measurements from which the data (...) were obtained, the hydrophones were not well isolated from the effects of surface fluctuations, and there is a strong possibility that the low-frequency wind-dependent noise is a form of system self-noise."* [68] The same effect can be expected to be true in this study, suggesting that the lowest frequencies can be ignored.

The correlation between windspeed and SPL was found to change as a function of the month, see Figures 3.24 and 3.25. Note that these are correlations established on the full unordered set of data for each month without ships being sorted out.

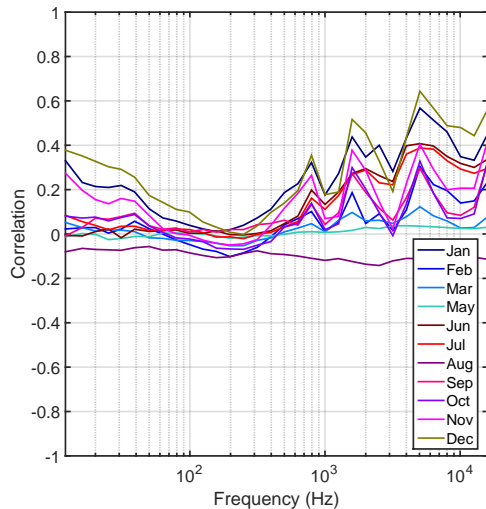


**Figure 3.24:** Correlation between windspeed and SPL for full months at the Trelleborg position.

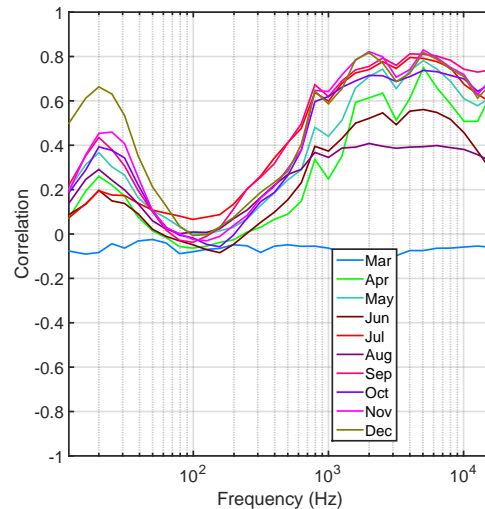


**Figure 3.25:** Correlation between windspeed and SPL for full months at the Norra Midsjöbanken position.

For Trelleborg the correlation was found to be low during most months and most frequencies but there is still a significant positive correlation at low and high frequency regions with a trough in between in most months. May, August and February show close to zero correlation across all frequencies.

For Norra Midsjöbanken March is the only month that shows zero correlation. Note that the full month of March was not recorded so the set of spectra for March is roughly one fourth that of the other months.

In these plots it is also notable that there is a peaks-and-troughs-pattern in the higher frequency range, with higher correlations at frequencies 800, 2000 and 5000 Hz, and lower correlation in frequencies 1000, 3000 and 10000 Hz. It is unclear whether the cause of the pattern is natural or anthropogenic.

### 3.8.1.1 Method and Results for windspeed analysis

It can be established that windspeed causes noise in the frequency range 200 Hz and up.

All months showing zero correlation between and SPL are discarded. That includes February, May and August for the Trelleborg position and the month of March for the Norra Midsjöbanken position.

### 3. Methods

---

For each third-octave frequency band the spectra when there were stationarity and no ships within the assigned distance-criterium are kept. Linear curve-fitting of windspeed and SPL were performed. Various minimum distances to the closest ship were used. It is preferred to have ships as far away as possible to avoid any influence on the soundscape. At the same time a large number of spectra was kept so that enough different windspeeds were represented.

In the end a minimum distance of 19 km was chosen. With this distance 13 different windspeeds (m/s) were represented at the Trelleborg position and 20 at the Norra Midsjöbanken position. Overall, a lower variance of windspeeds was found at Trelleborg, compared to Norra Midsjöbanken as can be seen in the CDF plot in Figure 3.26.

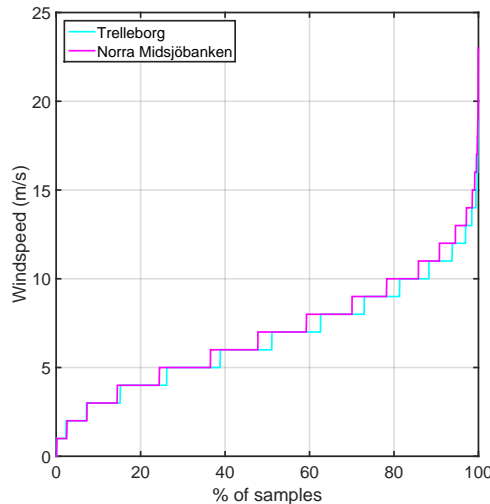


**Figure 3.26:** CDF of windspeed distributions at the two positions.

Curves were established by linear fits of windspeed against SPL for all the third-octave bands. The curves that resulted from this were equidistant spectra. The curves for higher windspeeds lined up quite well with mean spectra. For lower windspeeds (10 m/s and lower), however, a second linear interpolation was done for the curves to match. This was done by lowering the curve for 1 m/s down to the level of the mean spectrum of files where the closest ship was more than 15 km away and the windspeed was less than 2 m/s. The curves up to 11 m/s were then linearly weighted between the 1 m/s curve and the 10 m/s curve. The resulting curve showed a good match. The curves also showed a closer resemblance to the curves found by Hamson [21]. The result is shown in Figures 3.27 and 3.28.

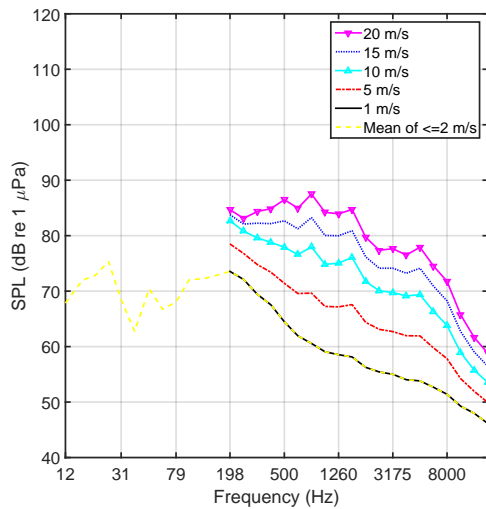


**Figure 3.27:** Curvifitted windspeed spectrum for 1 – 20 m/s at the Trelleborg position.

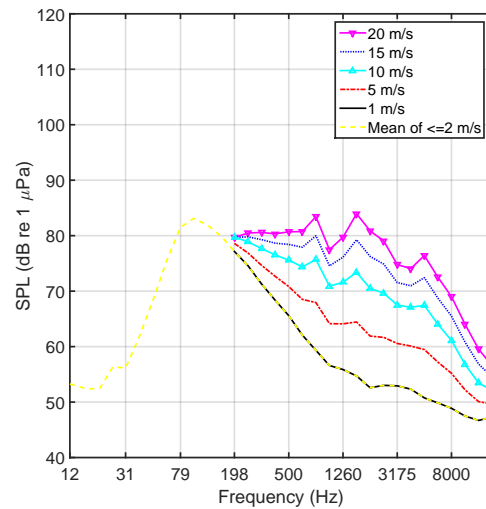


**Figure 3.28:** Curvifitted windspeed spectrum for 1 – 20 m/s at the Norra Midsjöbanken position.

These finally were used as the spectra describing the influence of windspeed on SPL for the two positions.

### 3.8.2 Influence of rain

Correlations between the reported rain intensities (mm/h) and SPL were established. The second-to-second or hour-to-hour correlations were essentially flat. This is likely due to the erroneous nature of the rain data. The nearest SMHI weather stations was several tens of km away from the hydrophones. The correlation between windspeed (m/s) and rain intensity (mm/h) was only 0.0125 for the Trelleborg site. Correlation between windspeed (m/s) and the existence of rain was only 0.0374. For Norra Midsjöbanken the correlations were 0.0194 and 0.0836, respectively. Without any spatial and temporal accuracy the rain intensity correlations would be too low. The correlations between mean rain intensity for each month and mean SPL for each month were investigated, see Figures 3.29 and 3.30.

The correlations for both positions tend to be negative except for low frequencies and for very long distances to the closest ship. The initial assumption was that rainy months would be louder than other months since they have an added sound source that can be remarkably loud. A strong negative correlation was found, contrary to what was expected. There was significant negative correlation in the low-frequency band centered at 100 Hz for Trelleborg and centered at 200 Hz for Norra Midsjöbanken. This is in frequencies where ship noise was dominating, indicating a decrease in shipping during rainy months.

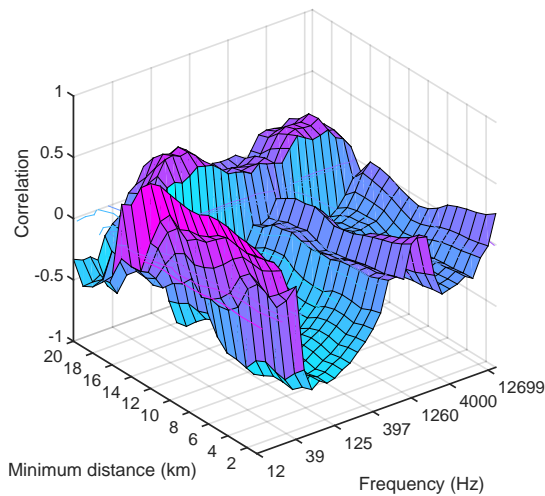


**Figure 3.29:** Correlation between monthly rain and monthly SPL for the Trelleborg position for different frequencies and minimum distances to the closest ship. The sudden rise in correlation when ships are at above 15 km distance is likely due to a low number of data points.

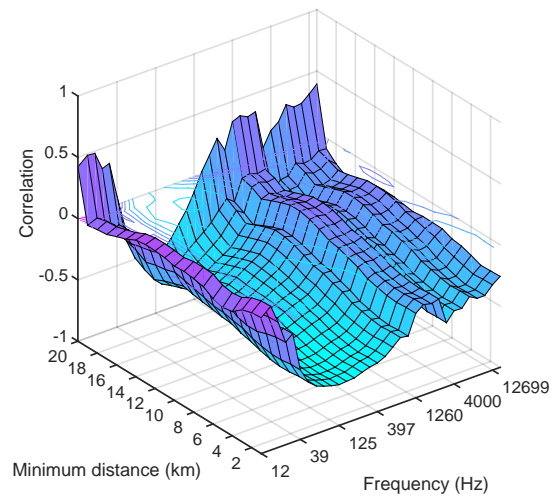


**Figure 3.30:** Correlation between monthly rain and monthly SPL for the Norra Midsjöbanken position for different frequencies and minimum distances to the closest ship. The sudden rise in correlation when ships are at above 19 km distance is likely due to a low number of data points.

The sudden rise in correlation at 15 km distance in Figure 3.29 and the slightly less sudden rise at 19 km in Figure 3.30 can be explained as an artifact of the low number of data points. An alternative approach was needed to determine the influence of rain on the soundscape.

Heavy rainfall stands out as the loudest stationary sound source present in the dataset. The rainfall shown in Figure 3.31 generated one of the loudest recordings for the entire year for the Norra Midsjöbanken position. Furthermore there were two clearly audible thunderstrikes. The rain data at the time did not indicate any rain. Vice versa, there was often indications of intense rain in the rain data but no audible sound of rain in the audio data. This misfit between data was to be expected since the weather station records water falling at the station, whereas what is audible under the water is generated in the vicinity of the hydrophone position.

For Trelleborg the rain sequence from August shown in Figure 3.32 was of the heaviest rainfall in which ship noise was negligible. Furthermore, intense rain gradually started and stopped centered around 13 minutes into the recording. The rain-induced differences in levels could thus be deduced. There were also several audible thunderstrikes in the recording. The loudest was found at 16 : 30 minutes. It was a recording that stood out as one of the few where there was intense rainfall, no ships nearby and there were no other sound sources present.

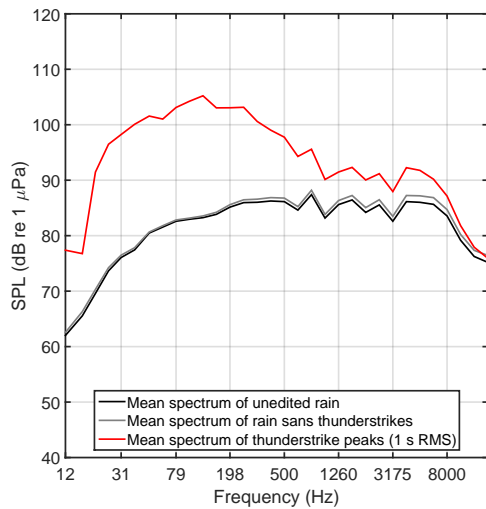


**Figure 3.31:** Spectrum of heavy rainfall with thunderstrikes at Norra Midsjöbanken.

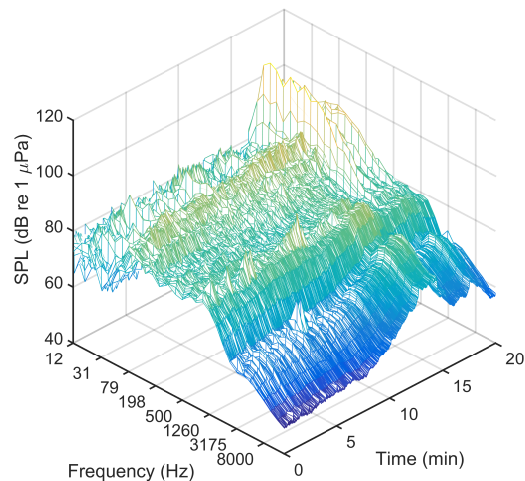


**Figure 3.32:** Sequence of heavy rain in Trelleborg in August. Note the flat levels in bands lower than 1000 Hz. At ten minutes a heavy rainfall starts sweeping by and the levels in the frequency range above 1000 Hz rise smoothly, with a peak at 15 min. The spectra that stand out the most in low frequencies are of clearly audible thunderstrikes at 17 min.

Note how the rising intensity of rain is visible as a smooth increase in the higher frequencies, with a plateau at minutes 13 to 14 in Figure 3.32. This smooth rise can be assumed to be completely related to the rain. The spectra from the start of the rise to the peak are displayed in Figure 3.33. The smoothly rising region seems to be at and above 1000 Hz. Figure 3.34 shows this region which seems to be frequency range in which heavy rain is dominant and it was chosen to represent the rain curve for Trelleborg. For Norra Midsjöbanken the same frequency range from the recording with the loudest rain of the year was chosen.

The frequency range of rain seems to be above 1000 Hz and thunderstrikes below 1000 Hz. This means that although the two sound sources often occur together, rain noise propagates only by ray propagation and thunderstrike noise only propagates as normal modes.

### 3. Methods

---

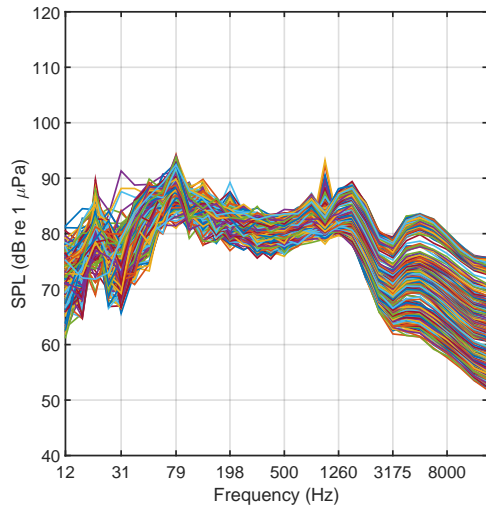


**Figure 3.33:** All spectra during the increasing rain that was recorded at Trelleborg. Note the smooth increase of the frequency range above 1000 Hz.

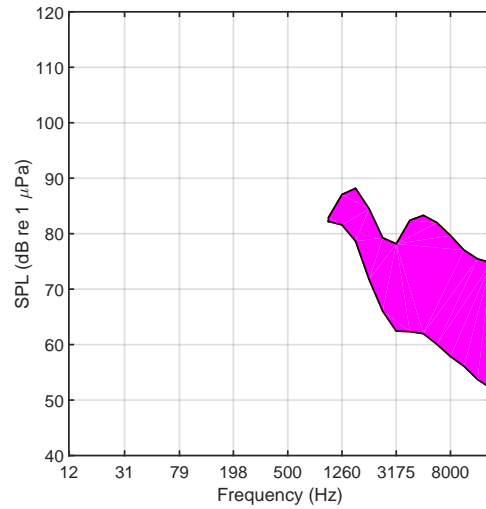


**Figure 3.34:** The region in which rain noise was dominant at Trelleborg.

Figure 3.35 shows the spectra from the start of the loudest thunderstrike to the peak spectrum. Figure 3.36 shows the active region of the thunderstrike.

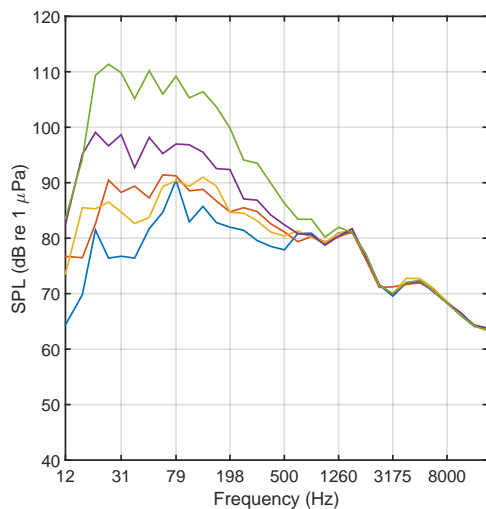


**Figure 3.35:** The spectra for the loudest thunderstrike of the year at Trelleborg is shown. Note that the frequency range is almost opposite that of rain noise.

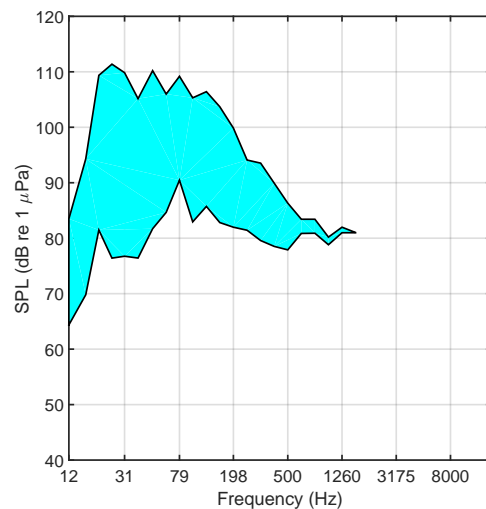


**Figure 3.36:** The region in which thunderstrike noise is dominant at Trelleborg.

### 3.8.3 Influence of temperature

Temperature is not a direct sound source but it affects sound propagation in that it changes the sound speed profile. There is also the possibility that temperature changes the behavioral patterns of ship traffic.

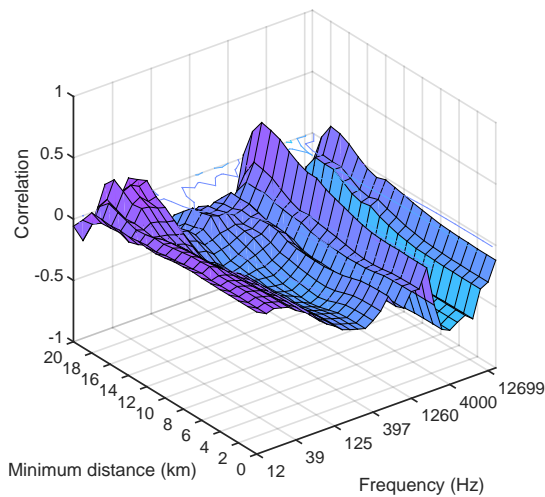


**Figure 3.37:** Correlation between SPL and temperature for the Trelleborg position for different frequencies and minimum distances to the closest ship.

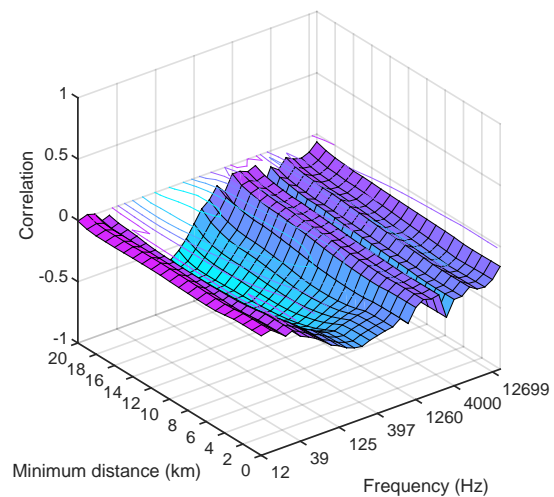


**Figure 3.38:** Correlation between SPL and temperature for the Norra Midsjöbanken position for different frequencies and distances to the closest ship.

Temperature correlated weakly with SPL in both positions. The correlation was both negative and positive but only significant (negative correlation) in mid-frequency range, 2000 – 6000 Hz, at 5 km distance. For Norra Midsjöbanken, the correlation was close to zero for all frequencies except for a valley ranging from the lowest frequencies to around 500 Hz. Significant correlation was found in the frequency range 40 – 200 Hz at 5 km distance to the closest ship.

Mean temperature was strongly related to the sound speed gradient of the water. Soundspeed gradient is a function of the temperature and salinity gradients. In cold seasons the sound speed gradient in the Baltic Sea tends to be negative (sound speed decreases with depth) and in warm seasons it tends to be flat [15]. In the data temperature varied between 0 °C and 22 °C in Trelleborg and between 3 °C and 17 °C in Norra Midsjöbanken. Sound speed gradient varied between  $-0.5 \frac{m}{s} \frac{1}{m}$  and  $0 \frac{m}{s} \frac{1}{m}$  in Trelleborg and between  $-0.9 \frac{m}{s} \frac{1}{m}$  and  $0 \frac{m}{s} \frac{1}{m}$  in Norra Midsjöbanken. The correlation between temperature and sound speed gradient in the data were  $-0.46$ .

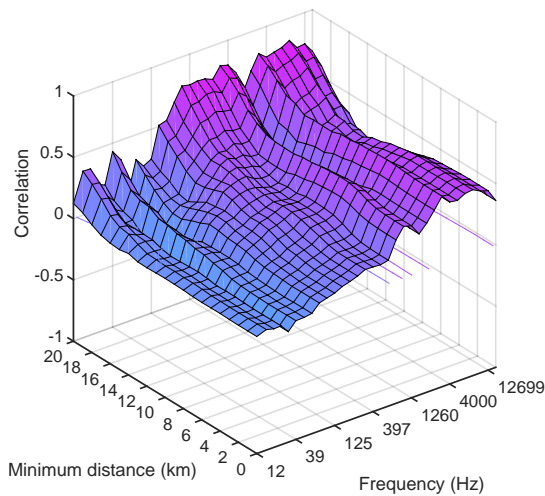


**Figure 3.39:** Correlation between sound speed gradient and SPL for the Trelleborg position for different frequencies and minimum distances to the closest ship.

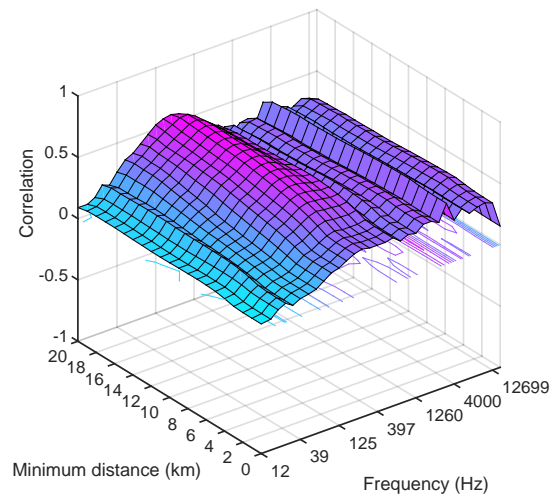


**Figure 3.40:** Correlation between sound speed gradient and SPL for the Norra Midsjöbanken position for different frequencies and minimum distances to the closest ship.

### 3.8.4 Influence of biological noise

Noise from aquatic animals is a major part of the soundscape in many seas in the world. Especially in seas with snapping shrimp. In the Baltic Sea, however, biological noise is much rarer. No animal sounds were found in the data set.

### 3.8.5 Summary of natural noise sources

Natural noise sources have large influence on the soundscape, often dominating anthropogenic sources. Especially noise from the wind is a factor that affects levels at the higher frequencies. When this occurs the shipping noise gets overpowered by wind noise at longer distances. For this reason higher wind speeds will not be included in the distance versus SPL analysis.

Wind itself turned out to be easy to isolate as a sound source. It was much easier to do at the Norra Midsjöbanken position than at Trelleborg due to the influence of shipping at Trelleborg.

Rain was found to be a strong sound source. With rain data of a higher quality it would have been possible to extract and analyse the effect of rain intensity on SPL and increase the significance of the results.

## 3.9 Anthropogenic noise sources

In this section the noise sources which are directly due to human activity are studied. The most prominent of these is ship noise.

### 3.9.1 Influence of shipping

Individual ships make noise when they pass both at close and long range to the recording equipment. The full set of ships that are active at long range generate a near constant ambient hum. At both the Trelleborg and Norra Midsjöbanken positions there were ships present at audible range most of the time, see Figures 3.41 and 3.42. This made it difficult to extract the influence of individual ships from shipping ambience in general.

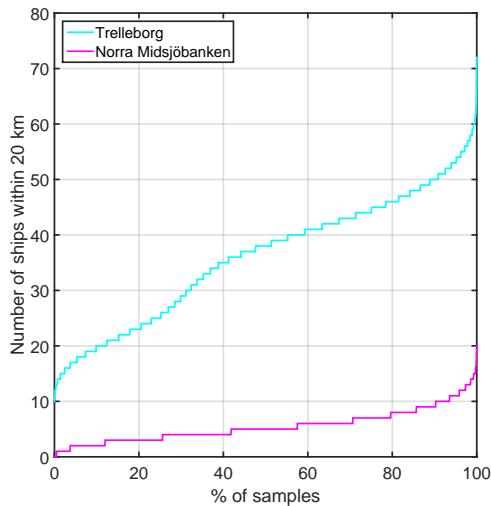


**Figure 3.41:** CDF of the number of ships within 20 km distance to the hydrophones. Especially at the Trelleborg position there were at all times several ships within 20 km distance. At Norra Midsjöbanken the density was considerably lower but there were a few ships present most of the time.

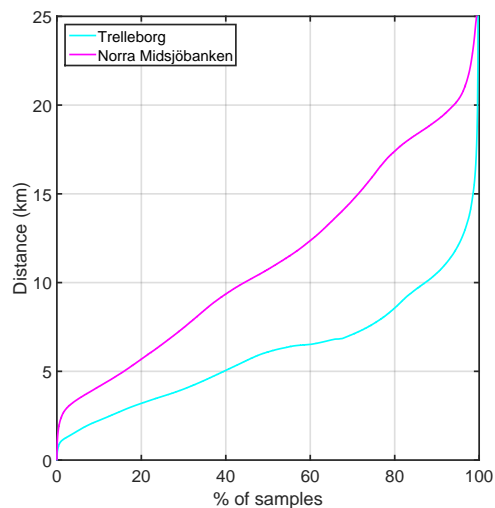


**Figure 3.42:** CDF of the distance to the nearest ship from the hydrophones. At Trelleborg there was almost 90% of the time a ship within 10 km distance. At Norra Midsjöbanken there were 3% of the time no ships within a 25 km distance.

There are a number of factors that are known from previous studies to influence noise from ships.

First, velocity of the ship. Because velocity is dependent on how much energy the ship injects into the water a higher velocity means more sound. A higher velocity also raises the probability of cavitation.

Secondly, the heavier and bigger the ship the more energy will be required to propel it forward resulting in more sound and a higher probability of cavitation. A large but empty ship can also behave as a resonance box, greatly increasing the levels of certain low-to-mid-frequent tones.

Thirdly, ship noise has directivity. Ships might sound different as they are approaching compared to when they are heading away from the hydrophone.

Fourthly, defects in the machinery can cause very sharp tonal and loud noises. These types of sounds generally indicate that some aspects of the machinery are slowly breaking down and should be repaired. It should be underlined that the sounds are not necessarily audible above the surface. Two examples of spectrograms of tonal ship signatures are shown in Figures 3.43 and 3.44.

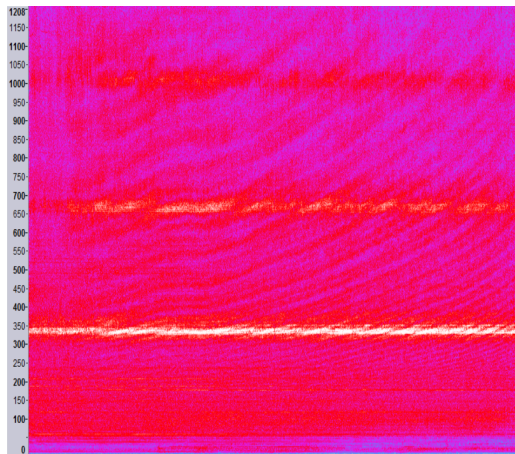


**Figure 3.43:** Spectrogram example of the sound of defect machinery. X axis is time and Y axis is frequency (Hz).

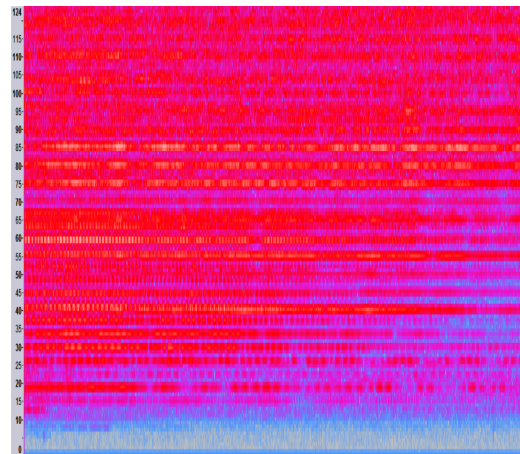


**Figure 3.44:** Spectrogram example of the sound of low tonals, as a cause of (possibly) an empty ship functioning as a resonance box. X axis is time and Y axis is frequency (Hz).

It was found that third-octave frequency band resolution was too coarse to accurately present the characteristics of ship noise with strong tonal components. Fortunately, such cases were rare and they did not alter the mean spectra of shipping in general.

All ships had more or less narrow peaks in the spectral signatures (as a consequence of e.g. motor speeds) which was obscured by using third-octave bands [3]. A large number of ship signatures in the data set showed a near constant tonal component at around 30 Hz. This signature was the most distance-independent part of the sound and was sometimes clearly present in the spectrogram even when the closest ship was at 15 km distance. The tonal component was found between 18 – 40 Hz and was not present in all ship signatures.

#### 3.9.1.1 Influence of velocity of nearest ship

It is previously known that the velocity of the closest ship has a significant influence on the recorded SPL [53]. As an isolated factor in this study, however, it did not correlate at all with increased SPL in any of the third-octave frequency bands for either of the positions. The correlation curves were almost flat. This lack of velocity dependence made velocity an irrelevant variable in this study.

### 3.9.1.2 Influence of the number of ships near to the hydrophone positions

Increased density of shipping was hypothesized to correlate positively with SPL in low frequencies. This preassumption was based on the fact that low frequencies travel long distances without being absorbed. Furthermore, this correlation was hypothesized to be stronger in oceans than in shallow waters due to presence of sound channels [26]. Correlation between the number of ships within 20 km and SPL was established for both positions.

In Trelleborg no significant correlations were found. In most third-octave bands the correlation was slightly on the negative side. For the Norra Midsjöbanken position the correlation was essentially flat and close to zero.

### 3.9.1.3 Influence of type of ship

Types of ship are categorized by classes in the AIS system. In theory it is likely that ships of the same class generate similar SPL. An attempt was made to study noise from different class, lengths, sizes and weights. It turned out to be too complex due to large variations between ships of the same class. There was even considerable variations in SPL from the same ships passing at different times.

Some patterns could be found between ships of certain categories but in general there was a large variation in SPL, varying between 15 – 60 dB for most individual ships and more so between ship categories and sizes. It would require careful study to draw any conclusions about entire categories of ships. The Wittkind model for ship noise requires input data in the form of number of propeller blades, details about the mass and mounting of the diesel engine [70]. Such details were not known about more than a handful of the ships in the data set.

Due to the complexity in studying differences between classes of ships this aspect was not dealt with in this study. The same applies for other ship parameters such as length, width, weight, displacement or age of the ship, country of origin and cargo type.

### 3.9.1.4 Spectrum of ship noise

Ship noise was chosen to be represented by mean spectra independent of ship class, *c.f.* section 3.9.1.3. It would have been preferable to establish the mean spectra from the subset of spectra with one ship at 1 km distance, with no wind and no other ships audible. This distance is likely long enough that ships can be regarded to be point sources while still dominating the soundscape and any other ship sources. The best compromise that could be found was the following:

- For Trelleborg: All spectra with a ship at a distance of 1 km with wind speed less 5 m/s and no other ships within at least 10 km.
- For Norra Midsjöbanken: All spectra at a distance of 3 km with wind speed less 5 m/s and no other ships within at least 10 km. The spectrum was scaled up by two times the difference between the 3 km and the 4 km spectrum,

### 3. Methods

creating a 1 km-equivalent spectrum. This was done because the spectra for 1 and 2 km distances were erratic and in fact had lower SPL than at 3 km distance.

The resulting spectra are shown in Figure 3.45.

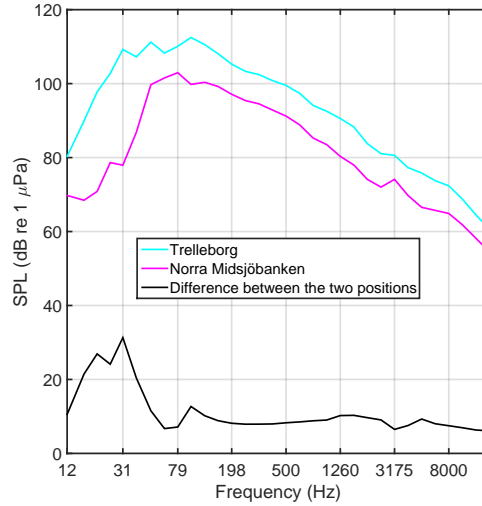


**Figure 3.45:** Mean spectra of ships at 1 km distance

Noise from shipping tended to peak at 50 – 200 Hz with the bulk of the energy found in the range 30 – 1000 Hz and sometimes up to 2000 Hz. Overall, the levels were in the range of 6 – 10 dB higher in Trelleborg than in Norra Midsjöbanken. The difference was strikingly high in the lowest frequency range, which may be explained by lower density of ships around Norra Midsjöbanken.

In order to separate the spectrum of a given ship from the noise caused by wind it is possible to subtract the estimated wind noise, *c.f.* section 3.8.1. The total SPL can be modelled:

$$L_{total} = 10 \log \left( 10^{L_{ship}/10} + 10^{L_{wind}/10} \right). \quad (3.9)$$

Given that  $L_{wind} > L_{total}$  for all frequencies, this can be rewritten as follows:

$$L_{ship} = 10 \log \left( 10^{L_{\Sigma}/10} - 10^{L_{wind}/10} \right). \quad (3.10)$$

Decomposed wind and ship noise are shown in Figures 3.46 and 3.47.

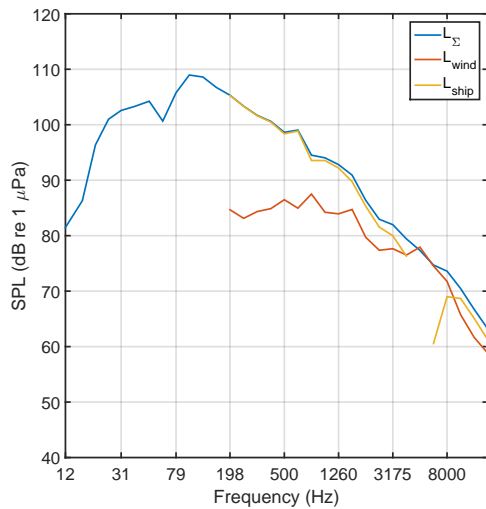


**Figure 3.46:** Decomposed wind and ship noise for a spectrum with a wind-speed of 2 m/s at the Trelleborg position.  $L_{\Sigma}$  is raw data,  $L_{wind}$  is modelled and  $L_{ship}$  is the result using Equation 3.10.

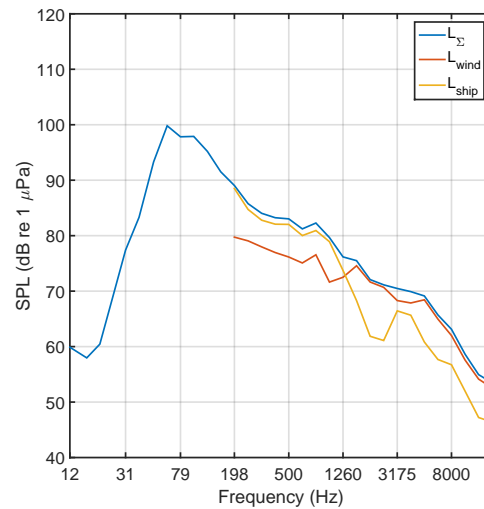


**Figure 3.47:** Decomposed wind and ship noise for a spectrum with a wind-speed of 10 m/s at the Norra Midsjöbanken position.  $L_{\Sigma}$  is raw data,  $L_{wind}$  is modelled and  $L_{ship}$  is the result using Equation 3.10.

Figures 3.46 and 3.47 show that the method does justice for higher windspeeds. For lower windspeeds the method breaks down.

### 3.9.2 Influence of piling

During January to March, several piling events were found that were audible at the Trelleborg position [37, 58]. Several hundred individual recordings were found to contain piling noise. The following specific events were found:

1. Piling performed on land at Trelleborg harbor (6.2 km distance to Trelleborg hydrophone)
2. Piling performed in the water just outside the harbor (6.2 km distance to Trelleborg hydrophone)
3. Piling performed in the open sea during the construction of off-shore wind farms (36 km distance to Trelleborg hydrophone)

The three different events provided opportunity to study different sound sources. The standard methods of studying and quantifying piling noise usually involve broadband analysis aimed at quantifying the maximum levels and the time-equivalent levels over longer periods [28]. In this study an attempt was instead made to quantify all sound sources using the same methodology. Because the curves for ship noise and for windspeed stem from averages of 1-second spectra, the same granularity was used for piling noise as well. Only the audio data with piling noise that clearly stood out from otherwise stationary soundscapes were used. Individual recordings of piling events are shown in Figures 3.48 to 3.50.

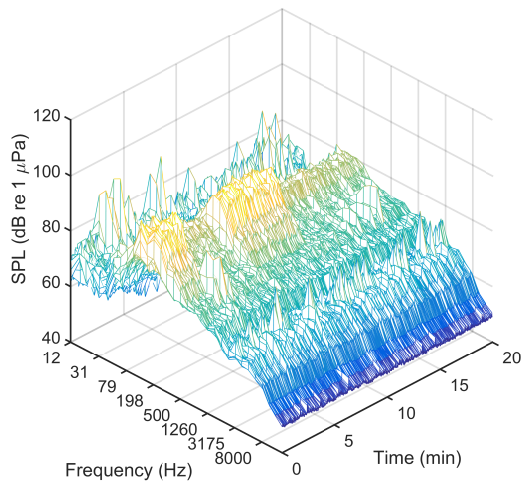


**Figure 3.48:** Piling performed on land, at Trelleborg harbor (6.2 km distance) plotted in frequency, time and SPL.

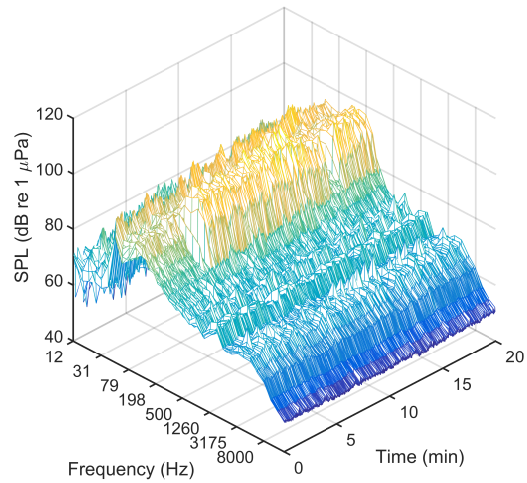


**Figure 3.49:** Piling performed in the water, just outside the harbor (6.2 km distance) plotted in frequency, time and SPL.

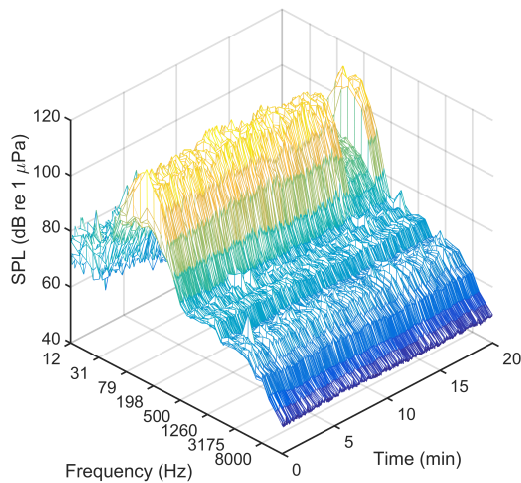


**Figure 3.50:** Piling performed in the open sea, during the construction of offshore wind farms (36 km distance) plotted in frequency, time and SPL.

The relevant frequency range was found to be 31 Hz to 500 Hz. The loudest individual spectra from the loudest individual recordings are overlaid and unsorted in Figure 3.51. Most of the time the sound of piling was found to be loudest in the frequency range between 100 and 200 Hz. The resulting zone-spectrum of piling in Trelleborg is shown in Figure 3.52.

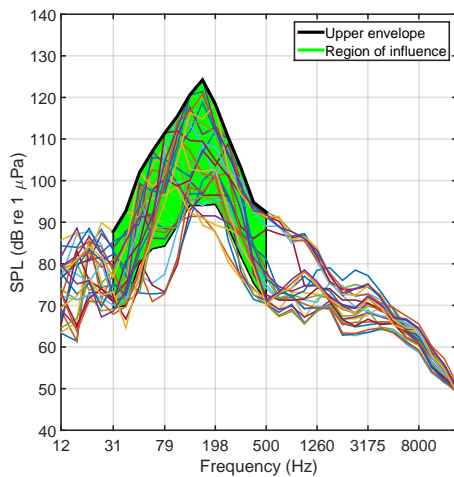


**Figure 3.51:** An aggregation of the loudest individual spectra from the loudest recordings of piling observed at the Trelleborg position. The upper envelope is shown in a thick black line. The shaded area shows the approximate region that is influenced by piling.

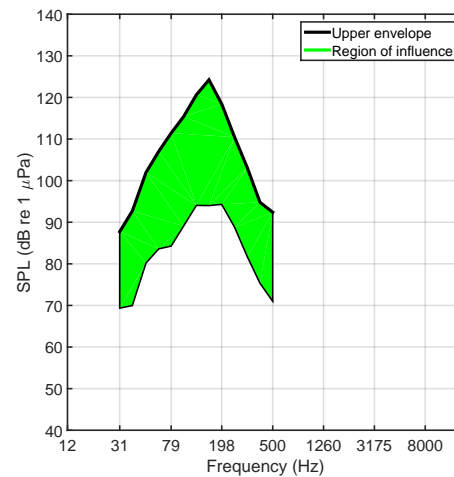


**Figure 3.52:** The zone-spectrum of piling captured by the hydrophone at the Trelleborg position. The upper envelope is shown in a thick black line. The shaded area shows the approximate region that is influenced by piling.

An attempt was made to determine the relationship between distance and SPL by comparing the data from two of the Danish hydrophones that also observed the piling instances. This, however, proved to be difficult because the geological properties in the directions from the piling position differed. No relationship between distance and SPL could be drawn from the difference between the piling in Trelleborg harbor and the one off-shore because the piling intensities were unknown.

### 3.9.3 Influence of active sonar

Several Navy exercises using active sonar were observed. At least six different occasions were clearly audible in the dataset. Some of them lasted for several hours. The transmitted frequencies were found to be centered around 3000, 7000 and 9000 Hz.

Sonar operators, in order to get the highest possible signal to noise ratio, transmit at the highest levels possible. Sonar pings are generally transmitted at 225 dB re 1  $\mu$ Pa, which is at the limit when water starts cavitating at the surface of the transmitter. Note that this is referring to narrowband levels and is not comparable to the third-octave band levels used in the rest of this thesis. Sonar is a very loud source and periodic transient just like piling. It can be identified using similar techniques as was used to identify piling.

Sonar pulses in a single recording from Trelleborg are shown in Figure 3.53. It is noted that the sonar signals stand out from the background considerably, have a

narrow frequency range, strict periodicity and somewhat constant SPL.

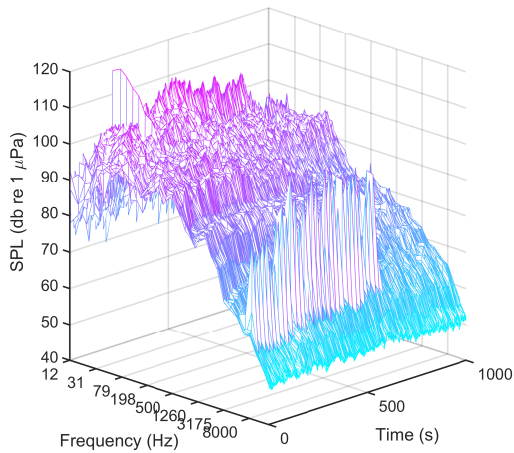


**Figure 3.53:** Example of a recording with sonar pings obtained at Trelleborg. The pings are notable in the frequency range 6350 to 8000 Hz. Note the limited frequency range as well as the periodicity of the pings.

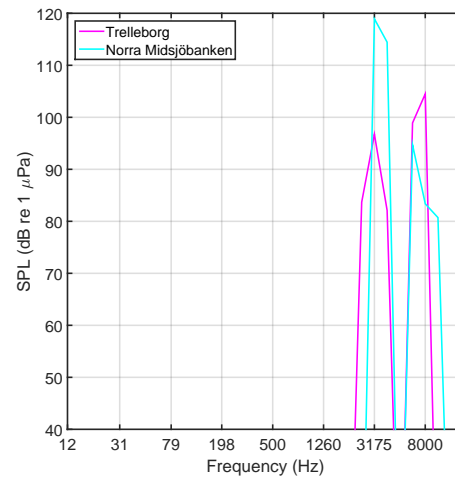


**Figure 3.54:** SPL of active sonar at the two positions. The peaks correspond to three main frequency ranges of transmitters. The lowest and most common consists mainly of sweeps centered around 3000 Hz. The higher frequency ranges are centered around 7000 and 9000 Hz.

Comparable with rain noise it is impossible to know the relationship between the source and the resulting SPL. In rain this was due to the lack of detailed information about intensities of rain. In the case of active sonar it is because the exact location, SPL and type of transmitter were unknown. Instead the loudest occurring examples for each of the two positions during the recorded year of 2014 were studied. These define the one-year maxima and are shown in Figure 3.54. Only the recordings where the sounds of the active sonar are clearly distinguishable from other sounds were used.

### 3.9.4 Summary of anthropogenic noise sources

Anthropogenic noise sources can roughly be categorized into transient sounds (e.g. piling, sonar and propeller cavitation) and continuous sounds (e.g. ships and operational wind farms).

Cavitation is a non-deterministic sound source. It occurs more frequently at higher propeller velocities. The exact propeller velocities are not logged by the AIS data, making it difficult to predict. The ground-borne part of piling noise can be predicted but for the prediction to be accurate to model numerical models have to be employed. Detailed knowledge about the geology is necessary as input to these.

Strong transients such as piling noise and active sonar were removed by Grubbs' test. Both piling and active sonar was detected using autocorrelation methods. The

detected events were then auditorially examined to determine the quality of data. Maximal SPL were determined. However, it was not possible to deduce source information due to lack of spatial knowledge of the active sonar and knowledge about intensity levels of the piling events.

The frequency ranges in question for anthropogenic noise sources are, for the most part, below 1000 Hz.

### 3.10 Baseline levels of ambience

At each site there can be assumed to exist a characteristic minimum noise level, referred to here as the baseline level of ambience. Theoretically, this level is reached when the wind is calm and there is as no shipping or other sound sources around. It is indicative of the normal levels that are always present at the site. The characteristics of the baseline ambience are noted by sorting the 100 000 lowest levels of each third-octave frequency for the full year. The sets of the 100 000 most quiet seconds for the year (referred to as the *quiet sets*) are shown in Figures 3.55 and 3.56, in bins of 1000.

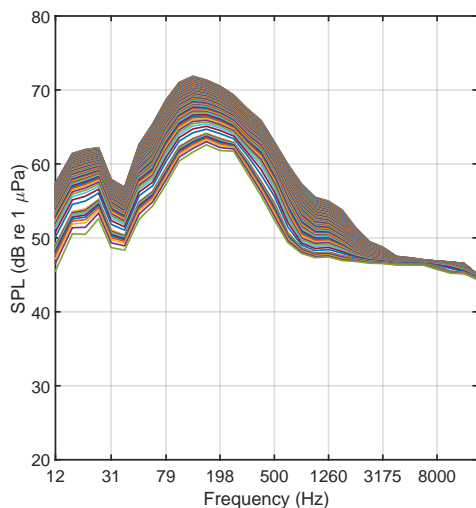


**Figure 3.55:** Lowest 100000 seconds for Trelleborg for each third-octave frequency band.

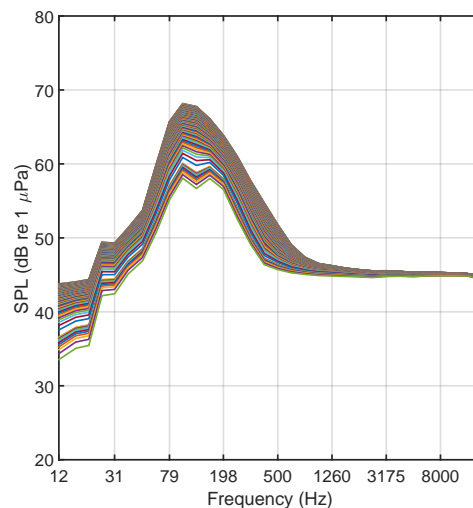


**Figure 3.56:** Lowest 100000 seconds for Norra Midsjöbanken for each third-octave frequency band.

It can be noted that the *quiet sets* of both positions have low variations in frequency bands higher than 3174 Hz, indicating that these levels were not all that rare at those frequencies. Norra Midsjöbanken was found to have low variations in frequencies above 1000 Hz. In frequencies below 1000 Hz for Trelleborg and below 500 Hz for Norra Midsjöbanken, the variation was large, indicating that baseline ambience is rare. Note, specifically, that neither *quiet set* converges to a lowest value in low frequencies. Overall, the variation was lower for Norra Midsjöbanken, which was expected, given that the position was overall more quiet.

Note in Figure 3.55 that there is a terrace for the *quiet set* of Trelleborg at the frequency 1600 Hz which has no analogy in the Norra Midsjöbanken *quiet set*.

For both positions, the mean of the lowest 100 samples, for each third-octave frequency band, are presented in Figure 3.57.

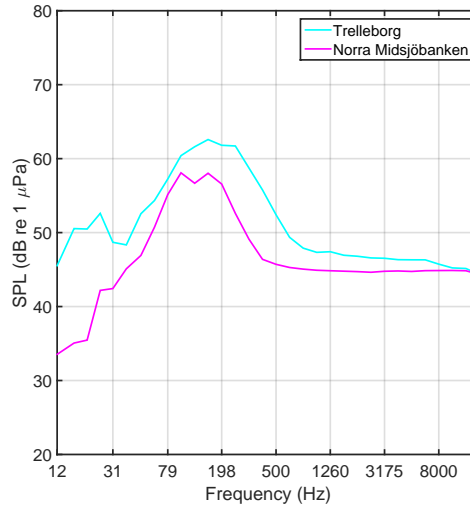


**Figure 3.57:** Baseline silence for both positions.

For Trelleborg, a local peak was observed at 25 Hz. These types of peaks are common in shallow waters and are possibly caused by standing modes in the water due to the shallow depth. Further, in the highest frequencies the two curves intersect completely, meaning that at those frequencies there seems to be no influence of either bathymetry or far-field shipping on the soundscape. An important observation is that the global peaks of the curves are likely due to distant shipping. This will be expanded on in Section 4.0.13.

### 3.11 Distance dependence

The previous analysis sets the base for investigating the measured sound from individual ships. There are assumed to be three distinct ranges: Ships in the near-field where SPL is expected to decrease steeply with distance, ships in the far-field where SPL decrease less steeply and a near constant lower level of shipping noise caused by the presence of ships in the sea.

There is a gradual transition between the near-field and far-field behavior. A previous study done in the Bay of Bothnia showed this distance to be at around 5 km, although the distance is site-specific and can vary quite a lot depending on depth, sound speed profile, and sediment properties [18]. It can even be expected to be directionally dependent as the bathymetry is different in different directions. Direction, however, is not considered in this thesis.

In reality, there is a continuous change from near-field to far-field. Further, there is high variation when ships enter into the near field region. Note also that Wenz estimated a 20 dB spread of a typical ship source [68]. This variation is as big as a standard deviation of the mean spectrum of the entire year.

### 3.11.1 Methodology for determining transmission loss

Transmission loss is different depending on position and frequency. For the two positions studied, TL surfaces with frequency in one axis and distance in the other axis were established.

From the sets of all individual recordings of ships passing by, the ones where the closest ship to the hydrophone could be expected to dominate the soundscape were kept. This meant that the second closest ship had to be at least a further 5 km distance away from the hydrophone. Linear curve fits of distance to SPL were performed for all recordings for all third-octave frequency bands.

For each curve-fitted recording: if there was more than 3 km between the closest and the farthest distance it gets considered potentially well-ordered. Any ships that remained more stationary than that were likely to lead to ill-conditioned curves. The resulting curves were only defined at the distances where the closest ship in the recording itself was present. That is: a curve fit from a ship that moved between e.g. 7 and 13 km distances would only contribute to the average at those distances.

For each third-octave frequency band and each integer km distance, the slopes that were deemed to be outliers by the Grubbs' test at 95% confidence interval were discarded. After that: positive slopes were discarded as defective. Finally, the mean of the remaining slopes were kept as the true value at each distance.

The point of the TL surface is that a single spectrum, herein called the seed spectrum, of a ship at a single distance can be used to estimate the SPL spectrum at different distances. With a single spectrum defined at distance  $D$  km (rounded off as an integer), each third-octave band of the TL matrix is subtracted the value at the row that corresponds to distance  $D$ , making that row/distance the neutral distance. To each row, the ship SPL spectrum is then added with the result being that distance  $D$  km remains the same and the SPL spectra at distances closer to and farther away from  $D$  km are approximated.

For a visual example of the way this method works, see section 3.11.2.

### 3.11.2 Example of the method

In this section, a calculated example of the way the TL surface is applied is shown, step by step.

A recording is arbitrarily chosen. This recording is from a ship passing by at the Trelleborg position. The SPL goes up in most third-octave bands, as the ship comes nearer to the hydrophone.

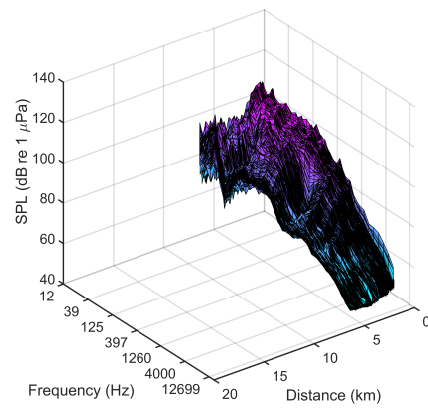


**Figure 3.58:** Example usage of the TL surface, part (1/8)

A single random spectrum is picked from the recording. This particular spectrum is taken when the ship is at distance  $\approx 4$  km.

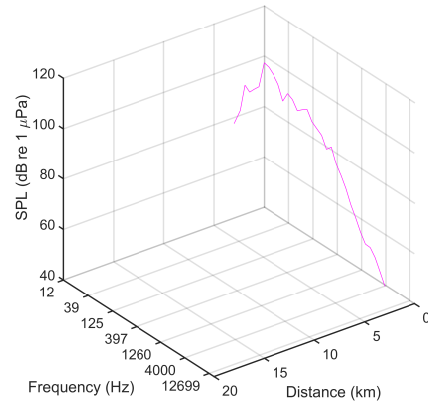


**Figure 3.59:** Example usage of the TL surface, part (2/8)

The spectrum gets stretched out to cover the entire distance. The distance of the seed spectrum is shown in black.

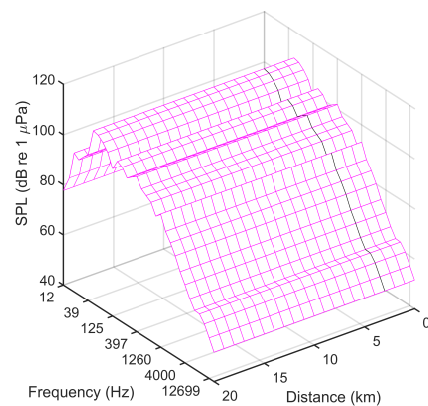


**Figure 3.60:** Example usage of the TL surface, part (3/8)

The TL surface from the model is shown here. The relevant distance is shown in black.

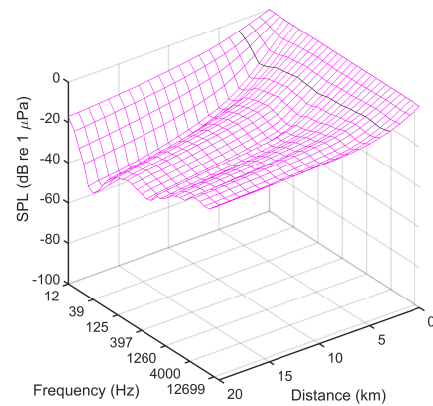


**Figure 3.61:** Example usage of the TL surface, part (4/8)

The value of the TL surface at the relevant distance is subtracted from the entire surface. This shifts the surface up so that the TL at the distance where the seed spectrum was taken becomes zero.

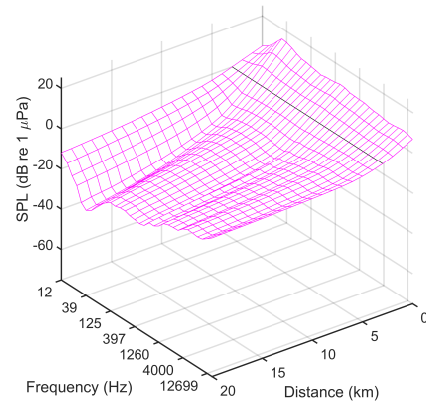


**Figure 3.62:** Example usage of the TL surface, part (5/8)

The surface in 3.60 and the surface in 3.62 are added together, resulting in the final result. This is the probable SPL generated by the ship at various distances.

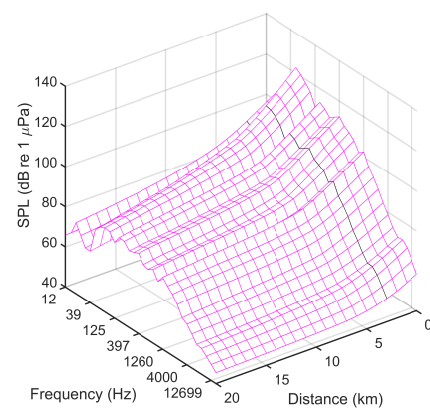


**Figure 3.63:** Example usage of the TL surface, part (6/8)

The model and the original recording are overlaid here, which reveals where the model over- and underestimates what the SPL is going to be.

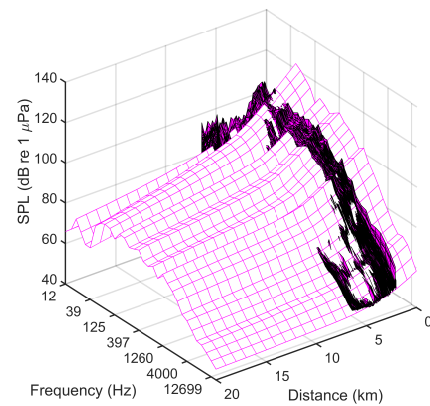


**Figure 3.64:** Example usage of the TL surface, part (7/8)

The result is shown again in 2d, together with the seed spectrum.

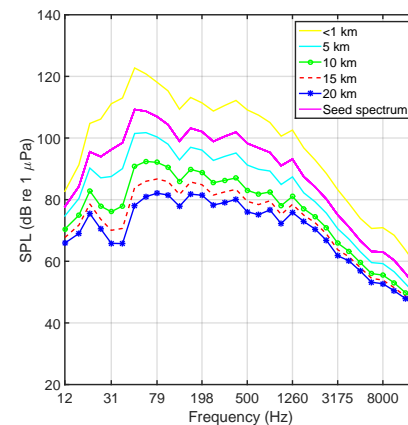


**Figure 3.65:** Example usage of the TL surface, part (8/8)

### 3.11.3 Error estimation

For a given spectrum, the error is going to be different depending on the characteristics of the soundscape at that time. It is also going to be different depending on what distance the spectrum was chosen at and how representative the spectrum at that particular distance was of the whole set. Even for a normally behaving recording, the prediction is going to be less reliable at distances differing from the distance at which the seed spectrum was defined.

For this reason, the error was estimated by going through each file and taking a random spectrum to base the method on and then comparing the difference between the two. This was done over the whole set of files and mean errors for each distance for each third-octave frequency band. Because the calculated distance relationship can end up radically different depending on which exact spectrum at which exact distance is chosen as the seed, the process was repeated over all the recordings 100

times. The results were 100 mean errors over all the recordings. Although most of the error plots looked very similar for most of the distances, especially the closest and the farthest distances tended to show large variations. The mean of all mean errors was taken, giving the mean mean errors for each position. These are plotted in Figures 3.66 to 3.67.

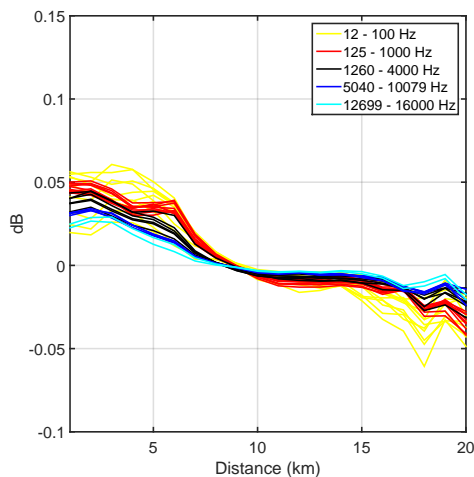


**Figure 3.66:** Mean mean errors of TL for individual third-octave bands at Trelleborg, calculated using Monte Carlo method.

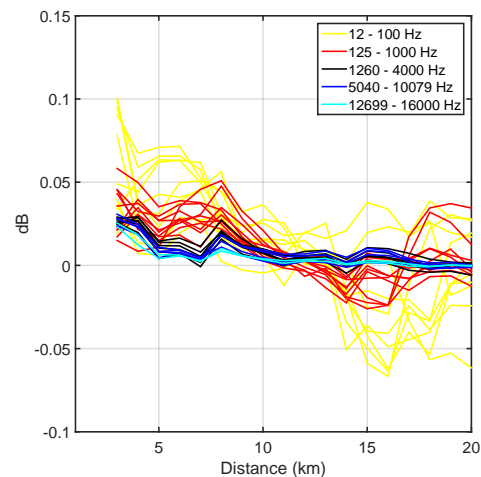


**Figure 3.67:** Mean mean errors of TL for individual third-octave bands at Norra Midsjöbanken, calculated using Monte Carlo method.

The mean mean errors were subtracted from the respective TL matrices, hopefully giving a better approximation. As can be seen from the Figures, however, the mean mean errors were small, meaning that this step was not strictly necessary. The errors were, however, systematic, in that it was mostly a positive error and the positive error was greatest in the nearest few kilometres. Note that the errors tend to be an overestimation in the nearest near-field and an underestimation in the furthest far-field. Both of these distances were extra hard to estimate. In the near-field, this was because the ships stopped behaving like point sources. At the farthest distances, there was a bigger likelihood that some other disturbances were influencing the soundscape. At either extreme, there was also the case that there were fewer sample points available for the curve fitting.

### 3.11.4 Comparison with FOI's empirical TL

Spherical TL is described by  $20\log(r)$  and cylindrical TL by  $10\log(r)$ , where  $r$  is distance. In a shallow sea the TL is going to be found somewhere in between. In earlier work done by the Swedish Defence Research Agency (FOI), TL in the Baltic Sea was found to generally be between  $14\log(r)$  and  $17\log(r)$  [47]. It varies a bit depending on depth and seabed material.

Comparisons between those empirical transmission losses and the ones found in this study are shown in Figures Figures 3.68 and 3.69.

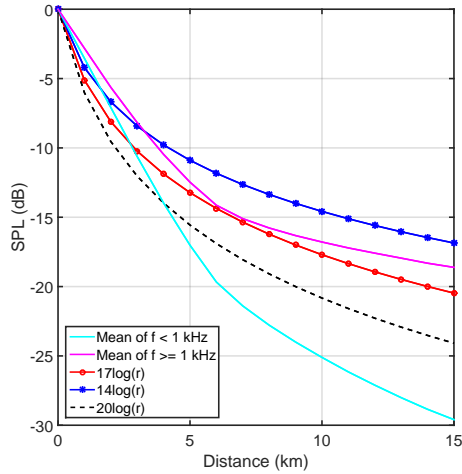


**Figure 3.68:** Comparison between FOA’s empirical TL and the ones found for the Trelleborg position. The results are shown as the mean of TL at the frequency range of modal propagation (below 1 kHz) and the one of ray propagation (above 1 kHz)

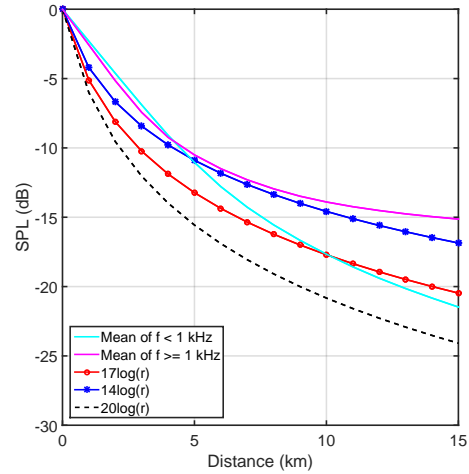


**Figure 3.69:** Comparison between FOA’s empirical TL and the ones found for the Norra Midsjöbanken position. The results are shown as the mean of TL at the frequency range of modal propagation (below 1 kHz) and the one of ray propagation (above 1 kHz)

For Trelleborg, in Figure 3.68, the slope of the TL in the higher frequency range was steep for the first 6 km and then levelled out for the rest of the distance, ending up right between  $14\log(r)$  and  $17\log(r)$  at the 15 km distance. The TL was considerably greater at the lower frequency range. It was larger than what cylindrical spreading would predict, ending up approximately being  $25\log(r)$ .

For Norra Midsjöbanken, in Figure 3.69, the TL for the higher frequency range was smaller than  $14\log(r)$ . It was approximately  $13\log(r)$ . The TL for the lower frequency range looked almost linear for the first 6 km and ended up slightly overshooting the  $17\log(r)$  estimation.

### 3.11.5 Comments on the method

The method generated reliable estimations of frequency-dependent TL. It was predicted that TL would be higher at the Trelleborg position than at Norra Midsjöbanken due to the shallower waters at Trelleborg. There was possibly a difference in seabed material as well. There was a large a variation between recordings in the reliability but over the whole dataset the error was small.

Temperature-dependant TL surfaces can be generated by separating the recordings by temperature range. Depending on the length of the temperature ranges, a larger set of recordings may be necessary for this. Overall, the method for generating the TL surfaces can be improved by increasing the set of recordings.

# 4

## Results and Conclusions

The previous analyses this thesis was dealing with include the following: windspeed, rain, thunderstrikes, shipping, baseline ambience, piling and active sonar. In this chapter these results are synthesized into a single diagram for each position respectively. Trelleborg is shown in Figure 4.1 and Norra Midsjöbanken is shown in Figure 4.2. The diagrams are analogous to Wenz diagrams.

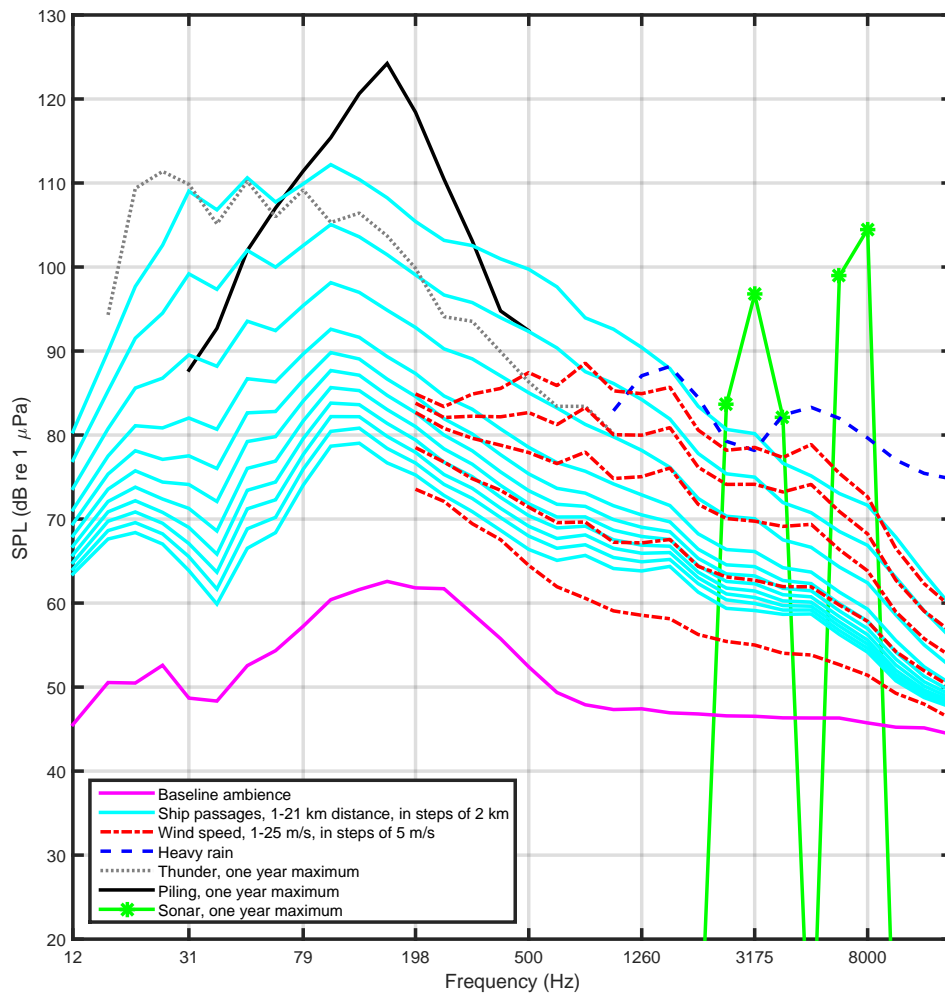
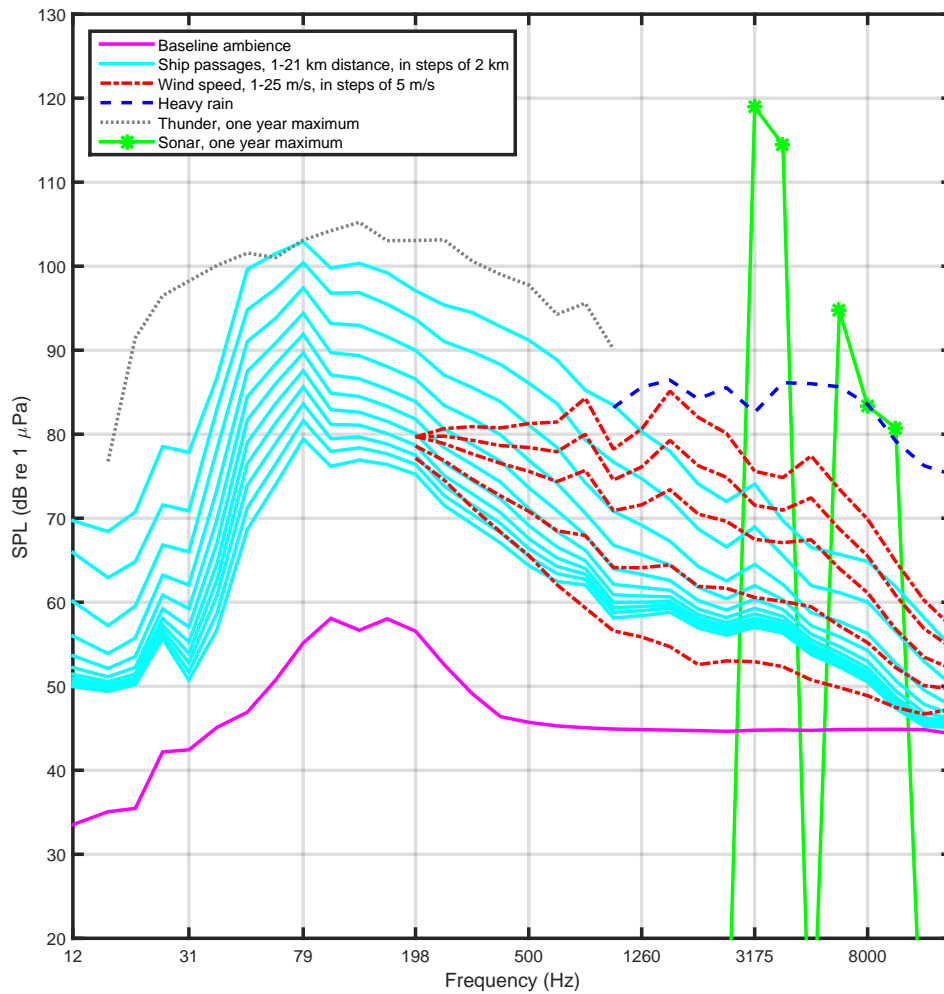


Figure 4.1: Wenz diagram for Trelleborg



**Figure 4.2:** Wenz diagram for Norra Midsjöbanken

#### 4.0.6 Comparisons between Wenz diagrams

The diagrams are site-specific and based on the raw data recorded by each hydrophone. Comparing Figures 4.1 and 4.2 it can be noted that the main features are similar at both sites. Levels and frequencies vary. The differences are due to both differences in ship traffic and in acoustical properties at the two positions.

The original Wenz diagram was defined in narrowband and the diagrams for Trelleborg and Norra Midsjöbanken in third-octave band so the levels are not directly comparable. Neither are the equivalent time-averages. Therefore, the level differences are to be taken with caution. They are compared here, even though the underlying analyses differ.

### 4.0.7 Shipping

**Original Wenz diagram:** Noise from shipping dominates in the frequency range 10 – 1000 Hz. The heavy traffic curve contributes up to a few thousand Hz. The loudest level is in the range 30 – 100 Hz. Highest SPL from heavy shipping is about 90 dB re 1  $\mu$  Pa, at 30 Hz. Shallow waters are correlated with peaks in lower frequency than deep waters.

**Trelleborg:** The curves span the entire frequency range. The loudest level is found to be at 100 Hz. The 7 km distance curve SPL corresponds best to the heavy traffic curve in original diagram. The overall shape of the curves is the presence of a major hill with a maximum at 100 Hz generated by ships in the near-field. The shape consists of two hills when ships are in the far-field, with one maximum at 20 Hz and the other at 100 Hz. The trough between those two is found at 40 Hz. The maximum at 20 Hz is often observed in shallow waters and is likely caused by a standing modal pattern.

**Norra Midsjöbanken:** The curves span the entire frequency range. The loudest SPL is found at 80 Hz, despite deeper waters than Trelleborg. The 9 km distance SPL corresponds to heavy traffic in the original Wenz diagram. The shape of the curves resemble a hill, with a peak at 80 Hz for all distances, a concave left side and a convex right side. There is, however, a small local peak at 25 Hz.

### 4.0.8 Wind

**Original Wenz diagram:** The effect of wind is represented as a function of Sea State, that is defined in terms of the waves that resulted from wind. The curve is a smooth parabola. The loudest levels are found at 250 – 600 Hz. Notable frequency range is 100 Hz for the highest Sea States and 200 Hz for the lowest Sea States.

**Trelleborg:** Wind is represented as m/s and not Sea State. There are discrete peaks at 800, 1600 and 5000 Hz. The loudest of these is found at 800 Hz. Levels from windspeed can not be directly compared to levels from Sea State, but in general, in the Sea State scale: SS0.5 corresponds to an average windspeed of 2 knots (1 m/s) and SS7 corresponds to 37 knots (20 m/s). Therefore, the first four steps of the windspeed scale corresponds to the entire SS scale. The levels of the windspeed 20 m/s curve correspond well to the SS7 curve. The SS0.5 curve, however, ends up being below even the baseline ambience level. The 1 m/s curve corresponds best to the SS2 curve. The curves at low windspeeds do not converge towards the lower frequencies.

**Norra Midsjöbanken:** As with Trelleborg, there are discrete peaks and they are found at 800, 1600 and 5000 Hz. The loudest is found at 1600 Hz. The wind curve for Norra Midsjöbanken is 1 – 4 dB lower than for Trelleborg, which may have to do with the distance from the surface to the hydrophone being twice as long. As for the levels, 20 m/s corresponds to SS7 and 1 m/s to SS1. All the curves converge towards the lower frequencies.

### 4.0.9 Rain

**Original Wenz diagram:** Heavy precipitation has a notable influence on the soundscape in roughly the frequency range 100 – 30000 Hz. The shape of the spectrum curve is a wide parabola with the highest SPL in the frequency range 800–5000 Hz. Highest SPL was 85 dB re 1  $\mu$ Pa.

**Trelleborg:** The curve has two hills, with peaks at 1600 and 5000 Hz. It is established in frequencies 1000 Hz and up. The levels are roughly similar to the ones found in the original Wenz diagram.

**Norra Midsjöbanken:** The curve has the same two hills as Trelleborg, but with an extra hill peak at 2500 Hz. The levels are similar to Trelleborg.

### 4.0.10 Thunder

**Original Wenz diagram:** Not present.

**Trelleborg:** The curve appears strangely similar to the 1 km ship distance curve in the range 30 – 80 Hz because both curves overlap in that frequency range with three consecutive hills and troughs at the same levels. This is most likely a coincidence, as the thunderstrike spectrum is taken from a single second's spectrum when there were no ships present. That is, unless both sources are influenced by a third factor, having to do with the bathymetry of the position. The levels, in general, correspond to a ship at 1 km distance. Alternatively, the levels of near-field shipping correspond to a pulse-train of thunderstrikes.

**Norra Midsjöbanken:** The spectrum looks like a parabola compared to Trelleborg. The levels are lower in the low frequencies but higher in frequencies above 125 Hz, suggesting that the thunderstrike for Norra Midsjöbanken likely occurred at a closer distance. Overall, they are comparable.

### 4.0.11 Active sonar

**Original Wenz diagram:** Not present.

**Trelleborg and Norra Midsjöbanken:** Both positions experience similar types and levels of active sonar. They are divided by sonartypes with a lower region centered around 3000 Hz and a higher region centered around either 7000 or 9000 Hz with only a low variation around those frequencies. The active sonar activity seems to be about the same in both positions.

### 4.0.12 Piling

**Original Wenz diagram:** Not present. Perhaps the closest analogy would be "*earthquakes and explosions*" but that is notable only up to 100 Hz.

**Trelleborg:** It is by far the loudest of any of the sound sources in the diagram. It is notable up to 500 Hz with the loudest frequency at 160 Hz.

**Norra Midsjöbanken:** Not present.

#### 4.0.13 Baseline ambience

**Original Wenz diagram:** The "*limits of prevailing noise*" curve is monotonously decreasing, starting from 1 Hz. Around this and lower frequencies the level generally tends to be the same all around the world.

**Trelleborg:** Instead of a monotonously decreasing curve, Trelleborg has an almost flat level slightly below 50 dB re 1  $\mu\text{Pa}$  at both low and high frequencies, broken off by a hill of around 15 dB height centered at 160 Hz and that stretches from 40 to 800 Hz. The increase is most likely caused by distant shipping.

At most frequencies the baseline ambience is higher than the curve in the original Wenz diagram. The exception to this is in the lowest frequencies, where the Trelleborg levels reach 46 dB re 1  $\mu\text{Pa}$ , whereas the original Wenz curve is instead 60 dB re 1  $\mu\text{Pa}$ . This has to do with the fact that the level curves simply do not behave in the monotonously decreasing way that Wenz's curve does.

There is also something of a smaller peak of just a few dB in the frequencies below the big one.

**Norra Midsjöbanken:** For Norra Midsjöbanken, too, the curve is flat in high frequencies and there is a hill centered around 125 Hz and in the interval which is from 50 to 500 Hz. The hill is 12 – 13 dB louder than the flat level. With lower frequencies, below 50 Hz, there is a monotonous decrease, down to 34 dB re 1  $\mu\text{Pa}$ .

The hill seems to be the permanent influence on the soundscape that shipping has at that particular position. The 3 dB difference and the difference in frequency of both the center and the interval of the hill may be due to the differences in average density and distance of the shipping. Distant high-density shipping has previously been expected to be dominant in frequencies below 200 Hz [65]. In shallow waters the limit might be a few hundred Hz higher.

#### 4.0.14 Overall comparison between Trelleborg and Norra Midsjöbanken

The shapes of the curves for the two positions generally resemble one another. Some differences can be noted.

The ship levels differ especially at close distances. The TL is considerably steeper for Trelleborg than for Norra Midsjöbanken. It might be due to bathymetry and sediment. The seabed may be sloping in such a way as to shield off some of the sound or the sediment may be soft so that the sound impinging on the seabed gets efficiently absorbed.

Overall, it was observed that Trelleborg had a higher SPL in the low frequency range than Norra Midsjöbanken. This is true for the three curves that are located

#### 4. Results and Conclusions

---

below 100 Hz frequencies, i.e. ship distance curve, thunder and baseline ambience. The consistently higher levels in low frequencies may be due to influence from the constantly higher numbers of distant ships. All three curves, therefore, may be influenced by the same factor.

# 5

## Conclusion

The hypothesis in the beginning of this thesis was that Wenz curves could be made from raw data from unsorted underwater recordings in the Baltic Sea. The aggregated results strongly suggest that this is the case. The goal of constructing Wenz-like curves from the recorded raw data has been achieved. The results provide an overview on the common sound sources and their respective normal frequency ranges and SPL.

### 5.1 Evaluation of the methodology

The model predicts the SPL in relation to environmental variables. The uncertainty of the prediction is high. The soundscape is at all times influenced by unforeseeable factors. Furthermore the transmission loss varies depending on temperature and can sometimes change drastically in the span of just a few minutes. Knudsen and Wenz, in their time, had far less data to scrutinize and far fewer signal processing capabilities than what are available today. Most likely, those two gentlemen hand-picked data and improved their curves to make them fit their hypotheses.

Some of the results, such as active sonar, thunder and rain, inevitably end up being weak due to a large variation and a small set of data available. There was also no reliable information on intensity of the rain and the distance to the thunderstrike. The method of taking the one year maxima of these may be expanded to taking means of a number of maxima. If more years of data were to be recorded it would be relevant to take means of several one year maxima. Preferably, a detector of those types of sources should be developed so that more events could be detected and more reliable curves could be created. In order to develop a detector it is first necessary to extract good examples to test the detector on.

Overall, the method is feasible to use, for a full year of data, for an arbitrary position. With some effort it would be possible to automate many of the steps, given that most assumptions hold true. It might be necessary to change some of the assumptions depending on the position. Also, when applying anything on a large-scale basis, there will always be unforeseen aspects that will require *ad hoc* solutions. There may show up new types of surprises.

#### 5.1.1 Future research

There are some improvements to make, for future research of a similar nature or even on the same dataset.

A better selection of recordings could be made. Many of the recordings have misleading information, e.g. transient sounds starting when a ship is leaving, which ruins the relationship between distance and SPL. There is a lot of work that can be done to sort or tag recordings. It will be useful to continue work on detectors and automatic processing to identify data that are erroneous while at the same time not deleting too many false positives. During the work in this thesis attempts to develop detectors for piling, active sonar, cavitation, creaking of knots and rain have been attempted but it was found to be difficult and outside the scope of this thesis.

It can be assumed that ships have to work hard when they travel orthogonally to the direction of the waves. This is because the waves hit a greater surface than when the ship is going against or with the waves. It would be possible to study if this has an effect on the noise from the ship. This thesis was done without taking angle directions into consideration. It would be interesting to use the dataset to see if and how the direction of wind in respect to the ship and the hydrophone affects the TL.

Studies using AIS data to identify and predict ship behavior could be done. The aim would be to find out which variables are independent, e.g., density of ships might be correlated with velocity in that the greater the density of ships is on the sea highways the greater the risk of queues. Further, the risk of ships being in the way of each other and having to slow down the velocity might be dependant on the size and type of the ships. Velocity might be correlated with the Sea State. Shipping density might also be related to the season. Many scenarios are possible to study.

Above all it would be interesting to redo the entire study using narrowband. During the work done a database file with the entire dataset has been used where arrays as long as the entire number of spectra have been used to tag each spectrum with all the metadata (e.g. time, date, number of ships in the area, identity and distance to the closest ship). And-gates have then been used to sort out spectra from an SPL matrix with 32 columns (for the 32 third-octave bands) fulfilling any combination of tags. A narrowband version of such a matrix would be 500 times bigger, requiring considerably more RAM. It is possible to keep the same database for indexing of spectra but instead do workarounds to read only parts of the SPL matrix at a time and process the spectra in smaller sets at a time. A narrowband study would make it possible to more accurately identify the source of any given sound from the shape of the spectra. It would also be possible to create the diagrams in the same bandwidth as the original Wenz curves.

# Bibliography

- [1] Michael A. Ainslie, Christ A.F. de Jong, Stephen P. Robinson and Paul A. Lepper (2012) *What is the source level of pile-driving noise in water?*, published in: *The Effects of Noise on Aquatic Life*, ISBN 978-1-4419-7310-8
- [2] Mathias H. Andersson and Andreas Nöjd (2016) *Påverkan av aktiv sonar på marina däggdjur - Uppdaterat kunskapsunderlag sedan 2013*, FOI-R—4234—SE, ISSN 1650-1942
- [3] Paul T. Arveson and David J. Vendittis (2000) *Radiated noise characteristics of a modern cargo ship*, The Acoustical Society of America, 1063-7834
- [4] Christopher Bassett, Jim Thomson and Brian Polagye (2010) *Characteristics of underwater ambient noise at a proposed tidal energy site in Puget sound*, University of Washington
- [5] BIAS project website, [<https://biasproject.wordpress.com/>], 2016-08-24
- [6] William M. Carey (2006) *Sound sources and levels in the ocean*, 10.1109/JOE.2006.872214, published in: *IEEE Journal of Oceanic Engineering vol. 31, 2006*
- [7] Julia Carlström and Jakob Tougaard (2016) *GES for the Baltic Sea*, Presentation at BIAS project End-of-Project Workshop, Gothenburg, Sweden, Jun 1, 2016
- [8] Conover, W. J. 1999 *Practical nonparametric statistics - 3rd edition*, Wiley, ISBN-13 978-0471160687
- [9] Michael Dähne, Anita Gilles, Klaus Lucke, Verena Peschko1, Sven Adler, Kathrin Krüge, Janne Sundermeyer and Ursula Siebert (2013) *Effects of pile-driving on harbour porpoises (Phocoena phocoena) at the first offshore wind farm in Germany*, Environmental Research Letters, 2013, 8, 025002, 1748-9326-8-2-025002
- [10] Eva Dalberg, Ron Lennartson, Mika Levonen and Leif Persson (2005) *Properties of acoustic ambient noise in the Baltic sea*, published in: *Proceedings of the International Conference "Underwater Acoustic Measurements: Technologies and Results", Heraklion, Crete, Greece, 28th June - 1st July 2005*
- [11] European Parliament and Council (2008) *Directive 2008/56/EC of the European Parliament and of the Council of 17 June 2008 establishing a framework for community action in the field of marine environmental policy*
- [12] Richard R. Fay (2012) *Listening in Noise*, published in: *The Effects of Noise on Aquatic Life*, ISBN 978-1-4419-7310-8
- [13] Federation of American Scientists (2014) *Freedom of Navigation*, [[http://fas.org/man/docs/adr\\_00/apdx\\_i.htm](http://fas.org/man/docs/adr_00/apdx_i.htm)], 2016-08-25

- [14] Försvarets Materielverk (2009) *Hydroakustik och sonarteknik för marinen V. 2.0*
- [15] Försvarets Materielverk (2013) *Hydroakustik och sonarteknik för marinen V. 2.2*
- [16] FOI, Calibration protocols, 2013
- [17] FOI, deployment protocols, 2014
- [18] Johan Fridström (2015) *Some statistical properties of the ambient noise in the Baltic Sea and its relation to passive sonar*, Royal Institute of Technology, Sweden
- [19] Charles C. McGlothlin Jr. (1991) *Ambient sound in the ocean induced by heavy precipitation and the subsequent predictability of rainfall rate*, T256328, Naval Postgraduate School
- [20] Geoffrey Grimmet and David Stirzaker (2001) *Probability and random processes*, Oxford University Press, ISBN 978-0-19-857222-0
- [21] R. M. Hamson (1997) *The modelling of ambient noise due to shipping and wind sources in complex environments*, Elsevier Science Ltd., published in: *Applied Acoustics vol. 51, 1997*, PII: S0003-682X(97)00003-0
- [22] Fredric J. Harris (1978) *On the use of windows for harmonic analysis with the discrete Fourier transform*, published in: *Proceedings of the IEEE vol. 66, 1978*
- [23] Line Hermannsen, Kristian Beedholm, Jakob Tougaard and Peter T. Madsen (2014) *High frequency components of ship noise in shallow water with a discussion of implications for harbor porpoises (*Phocoena phocoena*)*, 0001-4966, published in: *Journal of the Acoustical Society of America, 2014*
- [24] Line Hermannsen (2016) Data analysis and novel results on soundscape, Presentation at BIAS project End-of-Project Workshop, Gothenburg, Sweden, Jun 1, 2016
- [25] Dorian Houser, Laura Yeates, Daniel Crocker, Stephen W. Martin and James J. Finneran (2012) *Controlled exposure study of dolphins and sea lions to mid-frequency sonarlike signals*, ISBN 978-1-4419-7310-8, published in: *The Effects of Noise on Aquatic Life*
- [26] Jens M. Hovem (2010) *Marine acoustics - The physics of sound in underwater environments*, Peninsula Publishing,
- [27] Robert D. McCauley and Chandra Salgado Kent (2012) *A lack of correlation between air gun signal pressure waveforms and fish hearing damage*, ISBN 978-1-4419-7310-8, published in: *The Effects of Noise on Aquatic Life*
- [28] ISO/CD 18406 (2015)
- [29] Darlene Ketten (2002) *Marine mammal auditory systems - A summary of audiometric and anatomical data and implications for underwater acoustic impacts*, published in: *Polarforschung 72(2/3), 79-92*
- [30] Wieslaw Kicinski (1997) *A statistical model for classifying ambient noise in the sea*, Institute of Oceanology PAS, published in: *Oceanologia, vol. 39, 1997*
- [31] Mendel Kleiner (2010) *Acoustics and audio technology - Third edition*, J.Ross Publishing, ISBN 978-1-60427-052-5
- [32] Vern O. Knudsen, R. S. Alford, and J. W. Emling (1944) *Underwater ambient noise*, Yale University, V:7/Y:1948:410-429

- 
- [33] Line A. Kyhn, Poul B. Jørgensen, Jacob Carstensen, Nikolaj I. Bech, Jakob Tougaard, Torben Dabelsteen and Jonas Teilmann (2015) *Pingers cause temporary habitat displacement in the harbour porpoise *Phocoena phocoena**, *Mar Ecol Prog Ser* 526:253-265
- [34] Mika Levonen (2005) *Sonar data characterisation and analysis*, The University of Edinburgh
- [35] M.J. Levonen, R.K. Lennartsson, L. Persson and S. McLaughlin (2006) *Stationarity analysis of ambient noise in the Baltic sea*, IEEE 1-4244-0413-4
- [36] P.T. Madsen (2005) *Marine mammals and noise: Problems with root mean square sound pressure levels for transients*, published in: *The Journal of the Acoustical Society of America*, vol. 117, 2005, 0001-4966
- [37] E-mail correspondence with Rainer Matuschek, mar. 7, 2016
- [38] Nathan D. Merchant, Philippe Blondel, D. Tom Dakin and John Dorocicz (2012) *Averaging underwater noise levels for environmental assessment of shipping*, [<http://dx.doi.org/10.1121/1.4764429>], published in: *The Journal of the Acoustical Society of America* vol. 134, 2012
- [39] James H. Miller, Gopu R. Potty, Kathleen Vigness-Raposa, David Casagrande, Lisa A. Miller, Jeffrey Nystuen, and Peter M. Scheifele (2010) *Acoustic Noise and Electromagnetic Study in Support of the Rhode Island Ocean SAMP*
- [40] J.R. Nedwell, B. Edwards, A.W.H. Turnpenny and J. Gordon (2004) *Fish and Marine Mammal Audiograms: A summary of available information*, published in *Subacoustech Report Reference 534R0214*, September 2004
- [41] Jeffrey A. Nystuen (1985) *Rainfall measurements using underwater ambient noise*, Scripps Institution of Oceanography Published in: *Journal of the Acoustical Society of America* vol. 79 april 1986
- [42] Jeffrey A. Nystuen, Micheal J. McPhaden and H. Paul Freitag (2000) *Surface measurements of precipitation from an ocean mooring: The underwater acoustic log from the south china sea*, published in: *Journal of Applied Meteorology* vol. 39 2000
- [43] Jeffrey A. Nystuen (2008) *Monitoring the ocean using high frequency ambient sound*, University of Washington, N00014-04-1-099
- [44] Lars Odegaard (2015) *Ocean soundscape measurements at the LoVe ocean observatory*, FFI (Norwegian Defence Research Establishment Published in: *UACE2015 - 3rd Underwater Acoustics Conference and Exhibition*
- [45] Richard Oestman and Christopher J. Earle (2012) *Effects of pile-driving noise on *Onchorhynchus mykiss* (Steelhead trout)*, published in: *The Effects of Noise on Aquatic Life*, ISBN 978-1-4419-7310-8
- [46] Office of the General Counsel (2012) *The Marine Mammal Protection Act and the Endangered Species Act in the National Environmental Policy Act*
- [47] Jörgen Pihl, Jan-Olof Hegethorn, Sven Ivansson, Per Morén, Eva Norrbrand, Bernt Nilsson, Gunnar Sundin, Anders Wester and Viggo Westerlin (1998) *Underwater Acoustics in the Baltic* FOA Defence Research Establishment, FOA-R-98-00727-409-SE, ISSN 1104-9154
- [48] Charles L. Phillips, John M. Parr and Eve A. Riskin (2003) *Signals, systems and transforms - Third edition*, Prentice Hall, ISBN 0-13-111500-6

- [49] John F. Polglaze (2012) *"So am I correct in my understanding that a decibel is the same as a Hertz?": The quest for informed, objective environmental impact analysis of marine anthropogenic noise*, published in: *The Effects of Noise on Aquatic Life*, ISBN 978-1-4419-7310-8
- [50] Priestley, M. B. (1996) *Spectral analysis and time series*, Academic Press, ISBN 0-12-564922-3
- [51] A. Prosperetti, L.A. Crum and H.C. Pumphrey (1989) *The underwater noise of rain*, published in: *The Journal of Geophysical Research vol. 94, 1989*, Paper number: 88JC04284
- [52] Alex De Robertis, Christopher D. Wilson and Neal J. Williamson (2012) *Do silent ships see more fish? Comparison of a noise-reduced and a conventional research vessel in Alaska*, published in: *The Effects of Noise on Aquatic Life*, ISBN 978-1-4419-7310-8
- [53] Ross, Donald, 1987 *Mechanics of underwater noise*, Peninsula Publishing, ISBN 0-932146-16-3
- [54] Donald Ross (1974) *Ship sources of ambient noise*, published in: *Proceedings of the international workshop on low-frequency propagation and noise, 1974*
- [55] E. Sairanen (2014) *Baltic Sea underwater soundscape - Weather and ship induces sounds and the effect of shipping on harbour porpoise (*Phocoena phocoena*) activity*, University of Helsinki
- [56] Joseph A. Scrimger (1985) *Underwater noise caused by precipitation*, published in: *Nature, vol. 318, 1985*
- [57] SHEBA project website, [<https://sheba-project.eu/>], 2016-08-24
- [58] Skanska (2013) FL10 Huvudtidplan, Trelleborgs Hamn AB, revised 2013-05-06
- [59] Alexander Klauson, Janek Laaneru and Mirko Mustonen (2016) *Ship source level*, Presentation at BIAS project End-of-Project Workshop, Gothenburg, Sweden, Jun 1, 2016
- [60] Frank Thomsen, Christina Mueller-Blenkle, Andrew Gill, Julian Metcalfe, Peter K. McGregor, Victoria Bendall, Mathias H. Andersson, Peter Sigray and Daniel Wood (2012) *Effects of pile driving on the behavior of cod and sole*, published in: *The Effects of Noise on Aquatic Life*, ISBN 978-1-4419-7310-8
- [61] Jakob Tougaard, Line A. Kyhn, Mats Amundin, Daniel Wennerberg and Carolina Bordin (2012) *Behavioral reactions of harbor porpoise to pile-driving noise*, published in: *The Effects of Noise on Aquatic Life*, ISBN 978-1-4419-7310-8
- [62] United Nations (1958-2013) *United Nations Convention on the Law of the Sea*, [[http://www.un.org/depts/los/convention\\_agreements/texts/unclos/unclos\\_e.pdf](http://www.un.org/depts/los/convention_agreements/texts/unclos/unclos_e.pdf)], 2016-08-25
- [63] Urick, Robert J. (1982) *Sound propagation in the sea*, Peninsula Publishing, ISBN 0-932146-08-2
- [64] Robert J. Urick (1983) *Principles of underwater sound*, Peninsula Publishing
- [65] R.A. Wagstaff (2005) *An ambient noise model for the Northeast pacific ocean basin*, published in: *IEEE Journal of Oceanic Engineering vol. 30, no. 2, april 2005*
- [66] Stephen C. Wales and Richard M. Heitmeyer (2001) *An ensemble source spectra model for merchant ship-radiated noise*, published in: *Journal of the Acoustical Society of America vol. 111, 2002*

- [67] Helen M. Walkinshaw (2005) *Measurements of ambient noise spectra in the south Norwegian sea*, published in: *IEEE Journal of Oceanic Engineering* vol. 30, no. 2, april 2005
- [68] Gordon M. Wenz (1962) *Acoustic ambient noise in the ocean: spectra and sources*, published in: *The journal of the acoustical society of America* vol. 34, no. 12, 1962
- [69] Peter C. Wille and Detlef Geyer (1983) *Measurements on the origin of the wind-dependent ambient noise variability in shallow water*, published in: *The Journal of the Acoustical Society of America* vol. 75, 1984
- [70] Dietrich Wittekind (2009) *The increasing noise level in the sea - a challenge for ship technology*, DW-ShipConsult Published in: *The 104th congress of the German Society for Maritime Technology, 2009*
- [71] Dietrich Wittekind (2014) *A simple model for the underwater noise source level of ships*, DW-ShipConsult GmbH Published in: *Journal of Ship Production and Design, 2014*
- [72] Eberhard Zwicker and Hugo Fastl (2007) *Psychoacoustics - Facts and models*, Springer-Verlag, ISBN 978-3-540-68888-4

